Research Square

Preprints are preliminary reports that have not undergone peer review.
They should not be considered conclusive, used to inform clinical practice,
or referenced by the media as validated information.

Fertilization Mitigates Polyethylene Microplastic-Induced Disruptions in Plant Growth and Soil Microbial Processes in Agricultural Soil

Yibo LI

liyibo@xaut.edu.cn

Xi'an University of Technology Institute of Water Resources and Hydro-electric Engineering https://orcid.org/0000-0002-6225-2372

Shenglong Sun
Ge Li
Weibo Nie
Xiaoyi Ma

Research Article

Keywords: Polyethylene microplastics, Fertilizer, Pisum sativum L., Microbial community, Biomarkers

Posted Date: September 13th, 2026

DOI: https://doi.org/10.21203/rs.3.rs-10852683/v1

License: This work is licensed under a Creative Commons Attribution 4.0 International License. Read Full License

Abstract

Background

Microplastics have emerged as an important environmental concern in agricultural soils; however, their ecological impacts under common management practices remain insufficiently understood. In particular, whether fertilization can mitigate microplastic-induced disturbances in plant–soil–microbe systems is still unclear.

Scope

In this study, we investigated the interactive effects of polyethylene microplastics (PE-MPs) and fertilization on a Pisum sativum L.–soil system. Plant growth traits, soil physical and chemical properties, microbial biomass, extracellular enzyme activities related to carbon, nitrogen, and phosphorus cycling, and microbial community composition were jointly analyzed.

Key findings

The results revealed that PE-MPs significantly inhibited plant growth and altered soil structure and nutrient availability in a particle size- and concentration-dependent manner, accompanied by reductions in microbial biomass and enzyme activities. Fertilization substantially alleviated the negative effects of PE-MPs on plant performance and soil quality. This mitigation effect was closely associated with enhanced microbial biomass and increased activities of nutrient-cycling enzymes, suggesting that soil microbial processes played a key mediating role. Correlation analyses further revealed consistent linkages between microbial variables and plant growth parameters, supporting an indirect pathway through soil–microbe interactions rather than direct phytotoxic effects.

Conclusions and perspectives

Overall, our findings demonstrate that fertilization can effectively modulate the impacts of microplastics on agricultural soil systems by regulating soil microbial functioning. This study highlights the importance of incorporating agricultural management practices into assessments of microplastic pollution and provides practical insights for mitigating microplastic stress in cropland ecosystems.

1. Introduction

Microplastics (MPs), characterized as polymeric particulates less than 5 mm in diameter (Casella et al., 2024; Li et al., 2025; Zeb et al., 2022), present persistent environmental contaminants due to their recalcitrance to degradation in terrestrial systems. Due to their slow degradation in terrestrial environments, MPs can accumulate and eventually enter marine systems via runoff, posing a significant global environmental challenge (Norling et al., 2024). In recent years, increasing attention has been directed toward the impact of MP pollution within agricultural ecosystems, particularly given their ecosystem-level implications (Bethanis and Golia, 2024; Meng et al., 2022). Agricultural soils serve as major sinks for MPs, with primary sources including plastic mulch (Li et al., 2025), greenhouse materials (Ng et al., 2018), irrigation (Nizzetto et al., 2016), soil conditioners (Ng et al., 2018), sludge (Zhou et al., 2024), and atmospheric deposition (J. Wang et al., 2025). In China, the average concentration of MPs in soil is estimated at 18,760 particles per kilogram (Li et al., 2025). This contamination not only alters soil structure and physicochemical properties (de Souza Machado et al., 2018; Zhang et al., 2022), but also is easily absorbed or adsorbed by plants, thereby posing potential risks to crop growth and agricultural sustainability (Sun et al., 2020). Among the agricultural soils contaminated by MPs, polyethylene microplastics (PE-MPs) are the most prevalent type in Chinese farmland, primarily resulting from the degradation of plastic mulch film (Liu et al., 2018). Due to their non-biodegradable nature, PE-MPs accumulate in large quantities within the soil, posing significant threats to both crop health and soil microbial ecosystems (Li et al., 2025).

Consequently, as persistent pollutants, PE-MPs are likely to continue accumulating in farmland, thereby posing a long-term risk to the soil environment.

Recent investigations demonstrate that persistent polyethylene microplastic residues in edaphic environments significantly alter key soil physical characteristics such as bulk density, hydraulic properties, and aggregation stability, while simultaneously modifying chemical parameters including pH balance and essential nutrient cycles (carbon, nitrogen, and phosphorus) (Inubushi et al., 2022; Li et al., 2025; J. Wang et al., 2025; Zhang et al., 2023; M. Zhao et al., 2022). For example, once introduced into the soil, PE-MPs may alter pore structure and modulate the assembly processes of soil structural units. (de Souza Machado et al., 2018; Steinmetz et al., 2016). Empirical evidence demonstrates that large particle size (643 μm) and high concentration (2% w/w) of PE-MP effectively lower soil bulk density while enhancing the proportion of water-stable aggregates, though exhibiting negligible alterations in water holding capacity (de Souza Machado et al., 2019, 2018). Contrastingly, 5-mm PE-MP fractions at subcritical concentrations (0.5% and 1% w/w) can induce soil surface cracking, whereas 2-mm variants predominantly cause soil boundary shrinkage (Wan et al., 2019). The adsorptive capacity of PE-MPs, attributable to their extensive surface-area-to-volume ratio, mediates nutrient-pollutant co-adsorption dynamics within edaphic system (Hodson et al., 2017). In addition, PE-MP at mass fractions of 0.1%, 1%, and 10% decrease pH (W. Yang et al., 2021). Specifically, 100-μm particulates at 1% w/w induced the available potassium (AK) and available nitrogen (AN), while increasing soil organic carbon (SOC), total nitrogen (TN), and available phosphorus (AP) (J. Wang et al., 2025). In contrast, PE-MPs at 100-μm particulates with 5% w/w elevated the levels of nitrate nitrogen (NO_3^--N) and ammonium nitrogen (NH_4^+-N) (Li et al., 2025). Although fertilization practices may help mitigate the negative impacts of PE-MPs on soil ecosystems by enhancing soil structure, nutrient cycling, and microbial activity (Judy et al., 2019; Shah et al., 2023; Wang et al., 2019; Xu et al., 2020), critical knowledge gaps persist regarding fertilizer-PE-MPs interactions in modified pedo-environments.

The biogeochemical cycling of soil carbon (C), nitrogen (N), and phosphorus (P) constitutes a cornerstone of terrestrial ecosystem functionality,, critically regulating fertility preservation, phytogenic development, and planetary ecological equilibrium. (Hu et al., 2025). Microbial biomass carbon (MBC), nitrogen (MBN), and phosphorus (MBP) serve as labile organic reservoirs, functioning as sensitive indicators of microbial metabolic vigor and nutrient transformation efficacy within pedospheric systems (Yan et al., 2022). Specialized microbial consortia and their enzymatic outputs orchestrate C-N-P cycling dynamics[29]. Several studies have demonstrates that PE-MPs can alter the content of MBC, MBN, and MBP, as well as modulate key enzymes involved in the carbon (β-glucosidase), nitrogen (leucine aminopeptidase), and phosphorus (alkaline phosphatase) cycles, thereby influencing the transformation of C, N, and P in the soil (Feng et al., 2021; Yan et al., 2021). The impact of PE-MPs on soil enzyme activity may vary depending on particle size, concentration, and the presence or absence of fertilization (Feng et al., 2021; Iqbal et al., 2025; Liang et al., 2024; S. Zhao et al., 2022). For instance, smaller-sized microplastics may adsorb phosphate in the soil, reducing the substrate availability for phosphatases and inhibiting their activity. High concentrations of microplastics can alter the soil pore structure, restrict microbial activity, and inhibit the activity of enzymes such as sucrase (Liang et al., 2024). Additionally, PE-MPs influence the structure of soil microbial communities. PE-MPs can loosen the soil structure, increasing the surface area available for microbial attachment, which may enable microorganisms to form biofilms on the plastic surface (Zhang et al., 2019). This can lead to changes in the microbial community structure, including increased differences in bacterial community succession (Huang et al., 2019). Furthermore, endocrine-disrupting compounds such as bisphenol A and phthalates, which are often associated with PE-MPs, can leach into the soil and inhibit microbial activity (Wang et al., 2016). Current research extensively documents PE-MPs capacity to modify edaphic enzymatic systems,, yet few studies have specifically investigated their effects on enzymes involved in the C, N, and P cycles and their interactions with soil microorganisms, especially with different fertilizer applications.

It is evident that PE-MPs exert indirect effects on the complex system comprising plants, soil, and microorganisms.. For instance, they have been demonstrated to exert influence on plant growth by various environmental factors, including

soil bulk density, pH, nutrient content, enzyme activity, bacterial and fungal communities, soil contaminants, and other environmental and biological factors (de Souza Machado et al., 2018; Feng et al., 2021; Li et al., 2025; Rillig, 2018; Zhuang et al., 2024). Research has demonstrated that submicron and micron-sized MPs are capable of traversing the xylem of plants such as wheat and lettuce through cracks at the lateral root germination site, subsequently being transported from the roots to the stems, transpiration pull is the primary driving force for this movement (Li et al., 2020). In *Lepidium sativum*, MPs accumulate in the root hairs, blocking channels, inhibiting root development, and disrupting water and nutrient uptake (Bosker et al., 2019). In pumpkin systems, Colzi et al. (2022) documented concentration-dependent reductions in leaf expansion chlorophyll content, photosynthetic efficiency, and root biomass parameters under PE-MP contamination. Subsequent mechanistic studies suggest these phytotoxic effects may be due to PE-MPs interfering with metabolic pathways involved in material accumulation and energy consumption (Wu et al., 2022). Conversely, another study indicated that PE-MPs increased soil nitrogen content by enhancing the activity of nitrogen cycle-related enzymes and the abundance of microbial communities in rhizosphere soil, which promoted soybean growth (Li et al., 2025). Current research thus presents on the effects of PE-MPs on plant growth suggests both inhibitory and promoting influences. Therefore, the impact of PE-MPs on plant growth is not universally negative, and further research and comprehensive evaluations are prioritize needed.

Pisum sativum L. a globally cultivated leguminous crop, serves as both a vital protein source and a cost-effective nutritional supplement in agroecosystems (Xiong et al., 2024;). (Sapre et al., 2022). With its extensive root system and modest plant height, *Pisum sativum L.* is especially susceptible to MPs present in the soil (Xiong et al., 2024). However, research on the impact of PE-MPs on the plant-soil-microbe interactions remains fragmented. Therefore, this study used *Pisum sativum L.* as the test plant and conducted a pot experiment to investigate how PE-MPs with different particle sizes and concentrations, along with unfertilized and fertilized affected (1) *Pisum sativum L*. growth characteristics; (2) soil physical and chemical properties; (3) soil C, N, and P content, along with microbial biomass C, N, and P; (4) soil enzyme activity and microbial community. By integrating fertilization regimes, this multiscale analysis advances predictive frameworks for microplastic fate in legume-based food systems, providing critical data for ecological risk assessment.

2. Materials and methods

2.1 Soil and PE-MPs

Soil samples were taken from the 0–20 cm cultivated layer of agricultural fields in the Yangling Agricultural High-Tech Industrial Demonstration Zone, Shaanxi, China, which have never been covered with mulch (108°06'41"E, 34°15'15"N). Following air-drying and homogenization, soils were sieved (< 2 mm) to remove debris and analyzed for texture via laser diffraction (Mastersizer 2000, Malvern Panalytical). Texture classification confirmed a sandy loam composition (USDA system): 87.10% sand, 11.68% silt, and 1.22% clay. Baseline physicochemical properties (Table 1) were quantified prior to experimentation. Polyethylene microplastics (PE-MPs) used for the microplastic pollution treatment were obtained from Guangdong Hengfa Plastic Technology Co., Ltd., China.

Table 1
Basic properties of experimental soil.

Soil texture	Sand (%)	Silt (%)	Clay (%)	FC (g g^{-1})	pH	Organic carbon (g kg^{-1})	Total nitrogen (g kg^{-1})	Total phosphorus (g kg^{-1})	NH_4^+-N (mg kg^{-1})	NO_3^--N (mg kg^{-1})	AP (mg kg^{-1})
Sandy loam	87.10	11.68	1.22	15.7%	7.58	5.28	0.28	0.57	2.79	10.67	10.59

Note: FC represent field capacity, NO_3^-, NH_4^+, and AP represent nitrate nitrogen, ammonium nitrogen, and available Phosphorus, respectively.

2.2 Pot experiment

Particle size and concentration parameters were selected based on field surveys of Chinese agroecosystems, where PE-MP contamination ranges from 0.05–1.00% (w/w) with 50–1000 μm dominant particle sizes (95%) (Li et al., 2025). Given the accumulation of PE-MPs in agricultural soils, this study selected three PE-MP particle sizes: D1 (550 μm), D2 (50 μm), and D3 (6.5 μm), and three concentrations (w/w): C1 (0.5%), C2 (1%), and C3 (2%). The experimental treatments also included unfertilized and fertilized conditions, with urea (0.15 g kg^{-1}), superphosphate (0.1 g kg^{-1}), and potassium sulfate (0.2 g kg^{-1}) added to the fertilized treatments (Fig. 1). Control group (CK1 and CK2) without PE-MP addition was included in unfertilized and fertilized conditions. In total, 20 treatments were designed, with three replicates for each treatment.

The pot experiment was carried out from September to October 2024 in a climate-regulated greenhouse (25 ± 1°C day/18 ± 1°C night, 65% RH, 14-h photoperiod) at Xi'an University of Technology using cylindrical polyethylene pots (upper diameter 25.5 cm, base 22 cm, height 50 cm) filled with 100 kg of homogenized soil amended with polyethylene microplastics (PE-MPs) across defined gradients of particle size (50–100 μm [micron-scale] vs. 0.1-1 μm [nano-scale]) and concentration (0.1%, 1%, and 5% w/w dry soil)Soil moisture content was controlled using the weighing method, maintaining 60% to 70% of the field capacity to ensure optimal crop growth conditions. Crop disease and pest control were managed according to standard field practices. *Pisum sativum L*. seeds (85% germination rate, Sichuan Kexi Seed Co.) were surface-sterilized (30% H_2O_2, 15 min), rinsed, imbibed (deionized H_2O, 6 h), and sown (8 seeds pot^{-1}; 2 cm depth). Seedlings were thinned to 6 uniform plants pot^{-1} at 7 days post-emergence.

2.3 Plant index determination

Plant height (PPH) was quantified using a graduated meter stick (± 0.1 cm precision), on the 60th day after sowing. Root systems underwent three-stage deionized water rinsing to remove rhizosphere particulates before parallel desiccation processing—initial enzyme deactivation at 105°C (30 min) and subsequent drying at 85°C until mass stabilization (± 0.01 g), yielding aboveground dry weight (ADW) and root dry weight (RDW) measurements. Root architectural analysis employed a calibrated scanner (Epson Perfection 4870 Photo, 600 dpi resolution) to capture grayscale images, with WinRHIZO Pro 2023 software performing automated quantification of four key traits: total root length (RL, cm), average diameter (RAD, mm), surface area (RFA, cm^2), and volume (RV, cm^3) through vector-based edge detection algorithms.

2.4 Soil index determination

This study quantified three soil physicochemical property indices, namely soil bulk density, pH, and water-stable aggregate content (SAA); soil nutrient indices, namely SOC, TN, NO_3^--N and NH_4^+-N, total phosphorus (TP) and AP; C, N,

and P microbial biomass, namely MBC, MBN and MBP, respectively; and four enzymes activities, including β-1,4-glucosidase (BG) related to the C cycle; β-1,4-N-acetylglucosamine glycosidase (NAG) and leucine aminopeptidase (LAP) related to the N cycle; and alkaline phosphatase (ALP) related to the P cycle. The methods for determining soil indices are described in more detail in the supplementary material (Method S1).

2.5 Soil DNA extraction and high-throughput sequencing

The community diversity and structure of soil microorganisms (including fungi and bacteria) were characterized through 16S/ITS rRNA amplicon sequencing. The targeted regions for amplification were the V3-V4 fragment of bacterial 16S rDNA and fungal ITS1-5F. The primer sequences for the 16S rDNA V3-V4 region were: Forward (F) CCTAYGGGRBGCASCAG and Reverse (R) GGACTACNNGGGTATCTAAT, and the primer sequences for the ITS1-5F region were: Forward (F) GGAAGTAAAAGTCGTAACAAGG and Reverse (R) GCTGCGTTCTTCATCGATGC. The above was completed by Beijing Novogene Bioinformatics Technology Co., Ltd. Detailed soil DNA extraction and high-throughput sequencing are described in Methods S2.

2.6 Statistical analysis

Data visualization was performed using Origin Pro 2022b for statistical graphics and Microsoft PowerPoint 2021 for schematic diagrams. Statistical analyses were conducted in R (v4.4.2), including one-way ANOVA, Pearson/Spearman correlation matrices, microbial co-occurrence network construction, LDA effect size analysis (Lefse), Mantel test analysis, and partial least squares structural equation modeling (PLS-SEM) to assess variable interactions. Gephi (0.10.1) was used for visualisation of the network after calculation using R software (v. 4.4.2). Biomarkers at the genus level were chosen to build correlation networks in rhizosphere soils, based on Spearman correlations, using the software packages “phyloseq” (v. 2.0), “ggClusterNet” (v. 2.0), “tidyverse” (v. 2.0.0), “Biostrings” (v. 2.74.1), “SpiecEasi” (v. 1.1.3), “igraph” (v. 2.1.4) and “tidyfst” (v. 1.8.1).

3. Results

3.1 Effects of PE-MPs on *Pisum sativum L.* growth characteristics

Under unfertilized conditions, compared to the control group (CK1), both PPH and ADW exhibited a downward trend as the concentration of PE-MPs increased for the same particle size. When comparing different particle sizes at the same concentration, PPH and ADW also decreased as the particle size of PE-MPs decreased. The most significant reductions in PPH (70.8%) and ADW (88.4%) were observed under the D3C3 treatment (Fig. 2). The results showed that the addition of PE-MPs to the soil inhibited the aboveground growth of *Pisum sativum L.*, and this inhibitory effect became more obvious as the PE-MPs particle size decreased and the concentration increased. The main reason for this inhibition is that PE-MPs can be adsorbed on the surface of plant root hairs, hindering the plant's ability to absorb water and essential nutrients such as nitrogen, phosphorus, and potassium, ultimately inhibiting plant growth (Bosker et al., 2019). As the PE-MPs particle size decreased and the concentration increased, its specific surface area and coverage increased, thereby enhancing the inhibitory effect (Li et al., 2020). Under fertilization alone (CK2), PPH and ADW increased by 48.9% and 48.3%, respectively, compared to the CK1. Furthermore, under fertilized conditions with the addition of PE-MPs, PPH and ADW increased by 7.7%-74.9% and 180.8%-1061.6%, respectively, compared to the unfertilized conditions with PE-MPs (Fig. 2). These results demonstrate that fertilization promotes the aboveground growth of *Pisum sativum L.* and alleviates the negative impact of PE-MPs. The main reason for this alleviation is that fertilization promotes root growth, enhancing the plant's ability to absorb water and nutrients more effectively from the soil (S. Wang et al., 2025). Fertilization also boosts the plant’s stress resistance, allowing it to maintain normal physiological functions under PE-MPs stress, thereby mitigating the inhibitory effects of PE-MPs on aboveground growth (Sulaman et al., 2025).

Under both fertilized and unfertilized conditions, the effects of PE-MPs with different particle sizes and concentrations on *Pisum sativum L*. RDW and ADW were generally similar. Specifically, under unfertilized conditions, compared to the CK1, the RL, RAD, RFA, RV, and RDW of *Pisum sativum L*. under PE-MP treatments changed by − 25.0%-41.8%, − 31.5%-0%, − 43.1%-46.3%, − 71.7%-9.85%, and − 72.7%-−18.7%, respectively. Among these, the RL and RFA were largest under the D1C1 treatment, measuring 81.75 cm and 23.0 cm^2, respectively. In contrast, the RAD, RV, and RDW were greatest under the CK1 treatment, with values of 0.51 mm, 0.39 cm^3, and 2.9 g, respectively (Fig. 2). The results showed that PE-MPs significantly reduced the RAD and RDW of *Pisum sativum L*., while the effects on RL, RFA and RV showed a complex duality, with both promotion and inhibition. This specific effect was closely related to the particle size and concentration of PE-MPs. The main reason is that PE-MPs can indirectly affect the root growth of *Pisum sativum L*. by changing the soil physical and chemical properties, nutrient cycle, related enzyme activity and microbial community (Colzi et al., 2022; de Souza Machado et al., 2019, 2018; J. Wang et al., 2025). Compared to CK1, the RL, RAD, RFA, RV, and RDW under CK2 increased by 116.7%, 4.0%, 110.1%, 30.7%, and 7.6%, respectively. Additionally, compared to the addition of PE-MPs under unfertilized conditions, RL, RAD, RFA, RV, and RDW under fertilized conditions increased by 19.3%-205.5%, 25.8%-88.3%, 30.8%-323.6%, 56.4%-443.7%, and 0.6%-144.3%, respectively (Fig. 2). These results indicate that fertilization promotes the growth of the *Pisum sativum L*. root system and effectively mitigates the negative effects of PE-MPs on root growth. The primary reason for this alleviation is that nitrogen fertilization stimulates root development, while phosphorus and potassium fertilization contribute to root growth and enhance the stress resistance of the root system. This enables the roots to better maintain normal physiological functions when subjected to PE-MPs stress (Sulaman et al., 2025). These findings further support the conclusion that fertilization helps to counteract the detrimental effects of PE-MPs on the *Pisum sativum L*. growth characteristics.

3.2 Effects of PE-MPs on soil physical and chemical properties

The particle size, concentration, and fertilization of PE-MPs had noticeable effects on soil bulk density, SAA, pH, SOC, TP, AP, TN, NO_3^--N, and NH_4^+-N (Figs. 3–4). Under unfertilized conditions, compared to the CK1, soil bulk density decreased by 3.3%-12.3%, while SAA and pH increased by 7.7%-26.9% and 1.6%-6.5%, respectively. Under fertilized conditions, compared to CK2, soil bulk density decreased by 1.6%-8.2%, and SAA and pH increased by 6.7%-26.5% and 0.3%-8.0%, respectively (Fig. 3). These results indicate that the addition of PE-MPs to the soil led to a reduction in soil bulk density, an increase in SAA, and a rise in soil pH. The soil bulk density was negatively correlated with the particle size and concentration of PE-MPs, while SAA and pH were negatively correlated with particle size and positively correlated with PE-MP concentration (Fig.S2a-f). The primary reason for these effects is that PE-MPs have a lower density than the soil, which causes them to occupy soil pores and increase the total volume of the soil, thus reducing the soil bulk density (de Souza Machado et al., 2018). Furthermore, PE-MPs can act as aggregate core, adsorbing surrounding soil particles and promoting the formation of aggregates (de Souza Machado et al., 2019). The smaller the PE-MP particle size or the higher the concentration, the larger the specific surface area, enabling them to adsorb more soil particles and more effectively promote aggregate formation. Additionally, PE-MPs may release some alkaline metabolites during degradation, which increases soil pH (Liu et al., 2024). Fertilization also increased soil bulk density, SAA, and pH compared to the unfertilized treatment. This is primarily due to the fact that fertilization can enhance the organic matter content in the soil, which improves aggregate stability, thereby increasing both soil bulk density and SAA (Tian et al., 2022). However, superphosphate, used in the fertilization treatment, contains acidic compounds that can lower soil pH.

Under unfertilized conditions, PE-MPs increased SOC, AP, and NO_3^--N contents by 46.7%–280.0%, 4.3%–17.8%, and 16.7%–137.5%, respectively (except for AP in the D3C3 treatment and NO_3^--N in the D1C3 treatment). In contrast, PE-MPs generally reduced TN and NH_4^+-N contents by 0–10.7% and 8.0%–21.4%, respectively (except for NH_4^+-N in the D1C1 and D2C2 treatments) (Fig. 4). These results indicate that PE-MPs had minimal effects on soil TP and TN but

exerted more pronounced effects on SOC, NO_3^--N, and NH_4^+-N. This is likely because soil TP and TN primarily originate from the decomposition of organic matter, fertilization, and atmospheric deposition, and PE-MPs do not directly supply P or N (X. Wang et al., 2024). Therefore, their impact on TP and TN is relatively limited. In contrast, PE-MPs contain approximately 80% carbon, which can enhance SOC storage and influence soil nitrogen dynamics, particularly nitrification and denitrification processes (Li et al., 2025; J. Wang et al., 2025). Additionally, fertilization significantly increased soil TP, AP, TN, NO_3^--N, and NH_4^+-N contents (Fig. 4), attributable to the application of urea and superphosphate.

To investigate the relationship between the particle size and concentration of PE-MPs and soil properties (SOC, TP, AP, TN, NO_3^--N, and NH_4^+-N), linear regression analysis was performed. The results revealed that the particle size of PE-MPs was negatively correlated with SOC, while positively correlated with TP, AP, NO_3^--N, and NH_4^+-N. In contrast, the concentration of PE-MPs showed a positive correlation with SOC but a negative correlation with TP, NO_3^--N, and NH_4^+-N (Fig.S2g–r).

3.3 Effects of PE-MPs on soil enzyme activities and microbial biomass

Following a 60-day soil incubation, PE-MPs amendment in unfertilized soils elevated MBC (57.2–117.3 mg kg^{-1}), MBN (5.5–8.2 mg kg^{-1}), and MBP (4.7–7.1 mg kg^{-1}), representing 18.5%–96.3% (MBC), 0.9%–52.1% (MBN), and 9.1%–65.6% (MBP), increases relative to CK1(except for D1C1 and D1C2 in MBC). Under fertilized conditions, MBC, MBN, and MBP in the CK2 increased by 24.1 mg kg^{-1}, 7.0 mg kg^{-1}, and 0.94 mg kg^{-1}, respectively. For PE-MPs treatments combined with fertilization, MBC, MBN, and MBP contents ranged from 37.1–68.1 mg kg^{-1}, 5.8–9.0 mg kg^{-1}, and 4.7–7.6 mg kg^{-1}, respectively (Table 2). These patterns indicate that both PE-MPs and fertilization enhanced soil MBC, MBN, and MBP. However, fertilization reduced MBC under PE-MPs treatments, while MBN and MBP remained relatively stable. This may be attributed to PE-MPs serving as an additional carbon source for soil microorganisms, thereby stimulating microbial activity related to organic carbon decomposition and increasing MBC (J. Wang et al., 2025). Furthermore, PE-MPs may enhance microbial C, N, and P cycling by promoting enzyme activities and increasing the abundance of functional microbes and related genes (X. Wang et al., 2022), ultimately leading to elevated levels of MBC, MBN, and MBP.

Table 2

The effects of different particle sizes and concentrations of PE-MPs on soil MBC, MBN, MBP, NAG, BG, LAP, and ALP contents under unfertilized and fertilized conditions.

Treatment		MBC (mg kg^{-1})	MBN (mg kg^{-1})	MBP (mg kg^{-1})	NAG (nmol g^{-1} h^{-1})	BG (nmol g^{-1} h^{-1})	LAP (nmol g^{-1} h^{-1})	ALP (nmol g^{-1} h^{-1})
Unfertilized	CK1	59.8 ± 3.2c	5.4 ± 0.4c	4.3 ± 0.5b	4.5 ± 0.2b	4.0 ± 0.1d	58.5 ± 5.9d	150.2 ± 4.3d
	D1C1	57.2 ± 3.3c	5.5 ± 0.3c	5.4 ± 0.7a	5.9 ± 0.3a	5.4 ± 0.1c	66.1 ± 3.3d	162.8 ± 3.8d
	D1C2	58.2 ± 2.8c	5.6 ± 0.2c	4.8 ± 0.9b	5.3 ± 0.2a	6.4 ± 0.1b	79.8 ± 2.3d	171.3 ± 5.9d
	D1C3	70.8 ± 2.0b	7.0 ± 0.6b	4.7 ± 0.6b	4.2 ± 0.4b	7.5 ± 0.2a	67.0 ± 3.2d	153.3 ± 6.5d
	D2C1	117.3 ± 6.6a	6.6 ± 0.1b	5.7 ± 0.3a	4.7 ± 0.3b	4.1 ± 0.1d	53.0 ± 2.8d	165.7 ± 6.3d
	D2C2	75.8 ± 5.2b	6.3 ± 0.4b	5.5 ± 0.3a	4.9 ± 0.3b	3.1 ± 0.2e	56.5 ± 1.4d	175.5 ± 3.7d
	D2C3	85.5 ± 3.3b	7.7 ± 0.2a	5.9 ± 0.3a	5.6 ± 0.2a	5.2 ± 0.1c	54.2 ± 1.2d	155.9 ± 4.3d
	D3C1	115.0 ± 4.2a	8.2 ± 0.2a	5.3 ± 0.4b	4.3 ± 0.6b	5.1 ± 0.1c	58.3 ± 1.9d	185.3 ± 5.5d
	D3C2	82.9 ± 2.4b	6.0 ± 0.1b	7.1 ± 0.6a	2.8 ± 0.5c	3.5 ± 0.1e	56.7 ± 3.0d	177.1 ± 4.6d
	D3C3	109.3 ± 2.9a	6.5 ± 0.4b	5.0 ± 0.7b	2.5 ± 0.3c	4.5 ± 0.1d	61.2 ± 1.0d	145.0 ± 3.6d
Fertilized	CK2	83.8 ± 2.5a	12.4 ± 0.5a	5.2 ± 0.2b	5.0 ± 0.2cd	3.1 ± 0.2d	55.9 ± 4.3d	192.8 ± 6.5d
	D1C1	62.4 ± 2.3a	6.8 ± 0.4c	5.2 ± 0.1b	5.9 ± 0.2c	5.0 ± 0.1b	78.0 ± 2.9d	205.4 ± 3.7d
	D1C2	57.3 ± 2.8a	5.8 ± 0.1c	5.2 ± 0.6b	6.9 ± 0.3b	4.6 ± 0.2b	65.6 ± 1.5d	224.8 ± 6.9d
	D1C3	55.4 ± 1.9a	7.1 ± 0.3c	4.7 ± 0.4b	7.3 ± 0.4a	4.1 ± 0.1c	65.6 ± 3.3d	194.7 ± 7.6d
	D2C1	68.1 ± 1.7a	9.0 ± 0.7b	7.0 ± 0.3a	6.9 ± 0.7b	6.6 ± 0.1a	70.2 ± 1.5d	215.7 ± 6.3d
	D2C2	60.2 ± 4.2a	7.3 ± 0.5c	5.5 ± 0.2b	7.5 ± 0.5a	6.1 ± 0.1a	89.9 ± 1.9d	205.5 ± 4.7d

Note: The MBC, MBN, and MBP represent microbial biomass carbon, nitrogen, and phosphorus, respectively. The NGA, BG, LAP, and ALP represent N-acety-β-D-glucosidase, β-1, 4-glucosidase, leucine aminopeptidase, and alkaline phosphatase, respectively. “CK1, CK2” represent the unfertilized and fertilized treatments without the intervention of PE-MPs, respectively. “D1, D2, D3” represent the PE-MPs treatments with particle sizes of 550 μm, 50 μm, and 6.5 μm, respectively. “C1, C2, C3” represent the concentrations of 0.5%, 1.0%, and 2.0% PE-MPs (w/w) relative to the soil weight. Different letters above the bar represent statistically significant difference among all the treatments at $P < 0.05$.

Treatment		MBC (mg kg^{-1})	MBN (mg kg^{-1})	MBP (mg kg^{-1})	NAG (nmol g^{-1} h^{-1})	BG (nmol g^{-1} h^{-1})	LAP (nmol g^{-1} h^{-1})	ALP (nmol g^{-1} h^{-1})
	D2C3	65.4 ± 3.3a	7.3 ± 0.6c	5.7 ± 0.2b	5.5 ± 0.3c	4.7 ± 0.2b	91.7 ± 4.0d	255.9 ± 4.3d
	D3C1	71.9 ± 3.3a	6.7 ± 0.2c	7.6 ± 0.4a	3.5 ± 0.2d	4.8 ± 0.1b	72.8 ± 2.5d	236.3 ± 5.4d
	D3C2	37.1 ± 2.4b	7.6 ± 0.2c	6.2 ± 0.4ab	3.3 ± 0.4d	6.0 ± 0.1a	62.7 ± 3.2d	207.1 ± 3.6d
	D3C3	39.7 ± 1.9b	8.1 ± 0.1bc	5.3 ± 0.1b	4.3 ± 0.3d	4.1 ± 0.1c	63.5 ± 2.1d	195.0 ± 5.7d

Note: The MBC, MBN, and MBP represent microbial biomass carbon, nitrogen, and phosphorus, respectively. The NGA, BG, LAP, and ALP represent N-acety-β-D-glucosidase, β-1, 4-glucosidase, leucine aminopeptidase, and alkaline phosphatase, respectively. “CK1, CK2” represent the unfertilized and fertilized treatments without the intervention of PE-MPs, respectively. “D1, D2, D3” represent the PE-MPs treatments with particle sizes of 550 μm, 50 μm, and 6.5 μm, respectively. “C1, C2, C3” represent the concentrations of 0.5%, 1.0%, and 2.0% PE-MPs (w/w) relative to the soil weight. Different letters above the bar represent statistically significant difference among all the treatments at $P < 0.05$.

The activities of NAG, BG, LAP, and ALP were significantly influenced by PE-MPs particle size, concentration, and fertilization (Table 2). Under unfertilized conditions, compared to the CK1, the activities of BG, NAG + LAP, and ALP in soils treated with 550 μm PE-MPs (D1) at various concentrations increased by 34.0%–85.1%, 13.0%–35.0%, and 2.0%–14.0%, respectively. At a constant PE-MPs concentration of 0.5% (C1), BG and ALP activities increased by 1.7%–34.0% and 8.4%–23.4%, respectively, across different particle sizes. Notably, NAG + LAP activity under D1 increased by 14.2%, while activities under 50 μm (D2) and 6.5 μm (D3) PE-MPs decreased by 8.3% and 0.6%, respectively. Under fertilized conditions, PE-MPs treatments resulted in increases in BG, NAG + LAP, and ALP activities by 31.3%–113.9%, 4.8%–54.6%, and 1.0%–32.8%, respectively, compared to CK2 (Table 2). These findings establish that fertilization as a critical modulator of PE-MP impacts on soil functionality, transitioning from size/concentration-dependent effects in nutrient-poor systems to synergistic stimulation under nutrient-replete conditions. Linear regression analyses revealed distinct size- and concentration-dependent patterns in PE-MP impacts on microbial biomass and extracellular enzyme activities (Fig. S3). Particle size exhibited inverse relationships with MBC, MBN, MBP, and ALP, but positively correlations with NAG, BG, and LAP. Conversely, PE-MPs concentration positively influenced BG and LAP, while negatively correlated with MBC, MBN, MBP, NAG, and ALP (Fig.S3). These antagonistic size-concentration interactions suggest larger PE-MPs preferentially stimulate enzymatic N/P acquisition through enhanced surface biofilm formation, whereas higher concentrations induce metabolic stress that prioritizes C-cycling enzymes over microbial biomass accumulation.

3.4 Effects of PE-MPs on soil microbial communities

Based on the above results, we further analyzed changes in the bacterial and fungal communities in the rhizosphere soil of *Pisum sativum L*. in response to PE-MPs particle size, concentration, and fertilization treatments. Under unfertilized conditions, the bacterial Shannon index under PE-MPs treatments changed by − 50.3% to 5.1%, while the fungal Shannon index changed by − 59.1% to 6.7%, relative to the CK1. Under fertilization, the bacterial Shannon index in CK2 decreased by 4.5%, whereas the fungal Shannon index increased by 19.4% (Fig. 5a). Principal coordinate analysis (PCoA) of functional diversity showed that PC1 and PC2 explained 33.5% of the variation in bacterial communities and 31.8% in fungal communities between PE-MPs and fertilization treatments in rhizosphere soil (Fig. 5b). At the phylum level, PE-MPs treatments increased the relative abundance of Ascomycota and Proteobacteria, while decreasing Crenarchaeota and Basidiomycota, compared with CK1. In fertilized soils, the relative abundance of Acidobacteriota

and Mortierellomycota decreased significantly, whereas Firmicutes and Ascomycota increased, compared with CK2 (Fig. 5c).

Additionally, both bacterial and fungal microbial communities were distinctly separated by the addition of PE-MPs under both unfertilized and fertilized conditions. To further explore these relationships, we performed a co-occurrence network analysis based on the OTU matrix (Fig. 6). The results showed that the number of microbial nodes and edges decreased in both bacterial and fungal communities under fertilization compared to unfertilized treatments. Notably, the number of nodes in the Proteobacteria bacterial phylum increased under fertilization, while the number of nodes in the Chytridiomycota, Blastocladiomycota, and Aphelidiomycota fungal phyla decreased. This shift can be attributed to the role of Proteobacteria in the N and P cycles, which are critical for soil fertility and ecological balance (Mohammed and Dakora, 2024). Fertilization, which supplied N, P, and potassium (K), likely enhanced the growth and proliferation of Proteobacterita. In contrast, Chytridiomycota, Blast, and Aphelidiomycota are important decomposers of complex organic matter and can also cause plant diseases (Wang and Kuzyakov, 2024). The increase in readily available nutrients from fertilization may have supported plant growth, thus inhibiting the growth of these fungal phyla. Furthermore, the bacterial symbiotic network under the fertilization treatment with PE-MPs exhibited more negative correlations, while fewer negative correlations were observed in the fungal network. This suggests that the addition of PE-MPs under fertilized conditions had a more complex effect on the bacterial community, leading to enhanced competition and antagonism among bacterial taxa. This increase in negative correlations may be linked to changes in soil nutrient dynamics induced by fertilization.

We then conducted Lefse analysis to identify key bacterial and fungal taxa as biomarkers of *Pisum sativum L*. plants affected by PE-MPs and fertilization in the rhizosphere soil. A total of 18 bacterial and 36 fungal taxa were identified as biomarkers (Fig. 7a-b). Specifically, bacterial and fungal genera such as Allorhizobium-Neorhizobium-Pararhizobium-Rhizobium and Pseudomonas were identified as biomarkers of PE-MPs involvement under fertilization. In contrast, CENA518 and Pseudopithomyces were identified as biomarkers under unfertilized conditions. Other bacterial and fungal genera, including Paenibacillus, Ceratobasidium, Microdiplodia, Siepmannia, Tulostoma, Myrothecium, Acrocalymma, and Filobasidium, were associated with the fertilized rhizosphere soil, while genera such as Ligilactobacillus, Ochrobactrum, Solicoccozyma, Geastrum, Kohlmeyeriopsis, Cylindrocarpon, Capronia, Cephalotrichum, and Amesia were identified under unfertilized conditions. The results indicated that the addition of PE-MPs to the rhizosphere soil reduced the abundance of several key microbial biomarkers. This effect can be attributed to the formation of a "plastic circle" around the PE-MPs in the rhizosphere, which creates a microenvironment significantly different from the surrounding soil. Such changes in habitat are likely unfavorable for the survival of certain microbial groups, leading to a decrease in their population (Shang et al., 2024).

To investigate the correlation and potential competition or cooperation between key biomarkers in the rhizosphere soil, we constructed symbiotic microbial networks for these biomarkers under four conditions: no fertilization, fertilization, no fertilization with PE-MPs intervention, and fertilization with PE-MPs intervention. The results revealed that under the no fertilization condition, biomarkers in the rhizosphere were negatively correlated, such as Ligilactobacillus with Capronia, Amesia, and Kohlmeyeriopsis. In contrast, under fertilized conditions, biomarkers exhibited positive correlations, such as Paenibacillus with Filobasidium, Siepmannia, Myrothecium, and Ceratobasidium (Fig. 7c). The observed patterns can be explained by the differences in nutrient availability. In unfertilized soil, nutrients are relatively scarce, and plant root secretions serve as a limited carbon source. As a result, microbial groups compete for these resources, leading to negative correlations. Conversely, fertilization provides abundant nutrients (C, N, and P), promoting microbial growth and fostering a mutually beneficial symbiotic relationship between the microbes (Sun et al., 2021).

3.5 *Pisum sativum L*.-soil-microbe relationships

To investigate the correlation between soil parameters, *Pisum sativum L*. growth, and soil microbial communities, we conducted a Mantel test to analyze the relationships between the abundance of bacterial and fungal biomarkers, soil parameters, and *Pisum sativum L*. growth (Fig. 8). Pearson correlation analysis revealed that the abundance of bacterial biomarkers was significantly positively correlated with SAA, bulk density, PPH, RFA, RV, DRW, DSW, SOC, AP, TN, NO_3^--N, MBC, MBN, MBP, NGA, and ALP. Similarly, the abundance of fungal biomarkers was significantly positively correlated with RL, NO_3^--N, and ALP, and positively correlated with SBD, SAA, RAD, RFA, RV, DRW, DSW, SOC, AP, TN, NH_4^+-N, MBP, BG, LAP, and ALP. We further examined the direct and indirect effects of different PE-MPs particle sizes and concentrations and fertilization treatments on *Pisum sativum L*.-soil-microbe interactions using structural equation modeling (SEM) (Fig. 9). The SEM results showed that PE-MPs had negative effects on soil physicochemical properties, bacterial biomarkers, and *Pisum sativum L*. growth indicators, while positively influencing soil nutrients, fungal biomarkers, microbial biomass, and enzyme activities. Fertilization treatments, on the other hand, had positive effects on soil physicochemical properties, nutrients, microbial biomass, enzyme activities, bacterial and fungal biomarkers, and *Pisum sativum L*. growth indicators. Additionally, both PE-MPs and fertilization treatments were found to indirectly influence soil C, N, and P-related enzyme activities (0.50 and 0.15) and *Pisum sativum L*. growth indicators (− 0.64, $p < 0.05$ and − 0.42) through bacterial and fungal biomarkers.

Importantly, we found that CENA518 and Pseudopithomyces, as key biomarkers in the *Pisum sativum L*. rhizosphere under PE-MPs treatment, were not only enriched but also positively correlated with *Pisum sativum L*. root growth indicators, including RL, RAD, RFA, RV, and DRW. In contrast, Paenibacillus, Ceratobasidium, Microdiplodia, Siepmannia, Tulostoma, Myrothecium, Acrocalymma, and Filobasidium, identified as key biomarkers under fertilization treatment, showed negative correlations with these same root growth parameters. Collectively, these findings suggest that PE-MPs and fertilization treatments can directly influence *Pisum sativum L*. growth and indirectly affect soil C, N, and P-related enzyme activities, as well as *Pisum sativum L*. growth indicators, through their impact on microbial biomarker abundance.

4 Discussion

Existing research on microplastics (MPs) has predominantly concentrated on soil-microbe interactions, whereas limited investigations of their systemic impacts on tripartite plant-soil-microorganism networks—a critical gap in understanding agroecosystem responses (Li et al., 2025). Additionally, the influence of fertilization has often been overlooked in studies examining the effects of MPs on these systems. Our findings demonstrate that PE-MPs significantly impaired the growth of both the aboveground and root systems of *Pisum sativum L*. under unfertilized conditions, while fertilization alleviated the inhibitory effects of PE-MPs on *Pisum sativum L*. growth. Notably, specific PE-MPs treatments even enhanced growth, with these effects being closely related to the particle size and concentration of the PE-MPs (Fig. 2 and S1). This may be due to the mechanical blocking effect of PE-MPs on root growth (M. Yang et al., 2021), which inhibits root expansion and nutrient uptake from the soil. Smaller particles as well as higher concentrations of PE-MPs tend to be adsorbed onto surface of the plant root, blocking cell wall pores, thus hindering the normal absorption and transport of water and nutrients by the roots, and ultimately stunting plant growth (Hernández-Arenas et al., 2021; Liao et al., 2019; Lozano et al., 2020). These findings are consistent with our results under unfertilized conditions. However, other studies have highlighted the importance of MPs' shape (beads, fibers, and fragments), size, and chemical composition (e.g., high-density polyethylene, PEHD; polyester fiber, PES; polyester terephthalate, PET; polypropylene, PP; polystyrene, PS; polyamide, PA) of the MPs in their effect on plants. MPs with shapes and properties that differ significantly from natural soil particles tend to have a more pronounced impact on plants (de Souza Machado et al., 2019). Notably, PEHD and PE have been shown to promote root elongation, increase total root length, and reduce average root diameter, which can help plants absorb water and nutrients more effectively, ultimately enhancing root and aboveground plant biomass (de Souza Machado et al., 2019; Li et al., 2025). These findings align with our results under

fertilization conditions. Thus, the impact of PE-MPs on plant growth is closely linked to fertilization treatment. On one hand, the application of N, P, and K fertilizers promotes root growth (Jo et al., 2024). On the other hand, fertilization appears to modulate the effects of PE-MPs (Li et al., 2021), potentially accelerating the degradation of PE-MPs (Zhang et al., 2020) and mitigating their inhibitory impact on plant growth (Zhuang et al., 2024).

The addition of PE-MPs to the soil can lead to changes in soil bulk density, SAA, pH, nutrients, and the activity of enzymes involved in the C, N, and P cycles, all of which impact plant growth (de Souza Machado et al., 2018; Li et al., 2025; J. Wang et al., 2025; Zhuang et al., 2024). This study found that soil bulk density decreased with an increase in PE-MPs particle size and concentration, while SAA and pH increased with decreasing particle size and increasing in PE-MPs concentration (Fig. S2). The reduction in soil bulk density following PE-MPs addition is likely due to the lower density of PE-MPs compared to many natural soil minerals. When large-sized or high-concentration PE-MPs are added, they occupy space without significantly increasing mass, thus decreasing soil bulk density (de Souza Machado et al., 2018; Rillig et al., 2017). Smaller PE-MP particles have a larger specific surface area and higher surface energy, which allows them to adsorb more organic matter and microorganisms. This facilitates the formation of organic cement, enhancing the stability of soil aggregates and promoting soil structure (de Souza Machado et al., 2018). Additionally, as PE-MP concentration increases, their distribution becomes denser, creating more adsorption sites that promote the aggregation of soil particles and increase the content of SAA (Liang et al., 2024). The effect of PE-MPs on soil pH is likely due to their adsorption capacity, which can capture free H^+, acidic substances, and alkaline compounds in the soil (Rong et al., 2021; F. Wang et al., 2020). Furthermore, when PE-MPs were applied to the soil, there was an increase in soil SOC, AP, and NO_3^--N content, while TN and NH_4^+-N content decreased (Fig. 4). This can be attributed to the influence of PE-MPs on the activity of enzymes involved in the C, N, and P cycles (Guo et al., 2024). Specifically, the application of PE-MPs resulted in a decrease in NAG, an enzyme involved in organic nitrogen mineralization, which in turn reduced the release of NH_4^+-N from hydrolyzed organic nitrogen in the soil (Wang et al., 2023). In contrast, the activity of BG, involved in the C cycle, increased, leading to the hydrolysis of β-glucosidic bonds and the release of glucose, thus increasing the available carbon content in the soil (Lian et al., 2024; Liu et al., 2017). Similarly, the increase in alkaline phosphatase activity, which is involved in the P cycle, facilitated the hydrolysis of phosphates and the release of inorganic phosphorus, thereby boosting the available phosphorus content (J. Wang et al., 2025; Zhuang et al., 2024). Moreover, the polymer units of PE-MPs contain approximately 80% carbon, which contributes to an increase in SOC storage after the addition of PE-MPs to the soil (Rillig, 2018). Previous studies have also shown that PE-MPs increase the content of water-stable aggregates (Fig. 3), which reduces NO_3^--N leaching and increases its content in the soil (Li et al., 2025).

Soil microorganisms play a crucial role in the material cycling processes in the environment. Higher microbial diversity typically leads to a more complex community structure, which contributes to greater ecosystem stability (Blagodatskaya and Kuzyakov, 2008). PE-MPs can influence soil microbial communities by altering the physical and chemical properties, nutrient transport, and plant growth (W. Yang et al., 2021). Furthermore, PE-MPs can act as a habitat for microorganisms, fostering the enrichment of species with specific functions within the "microplastic ball" (Li et al., 2023; Q. Wang et al., 2022). Research has shown that the impact of PE-MPs on soil microbial communities is complex. On one hand, PE-MPs reduce the alpha diversity of bacterial communities in the soil, although the effect is not strongly correlated with the concentration of PE-MPs (Huang et al., 2019). On the other hand, PE-MPs can promote bacterial differentiation and succession, facilitating bacterial enrichment in the soil (J. Wang et al., 2020). Some studies have also suggested that, in the short term, the effect of PE-MPs on microbial communities is relatively small (Blöcker et al., 2020). In our study, we observed that under unfertilized conditions, the impact of PE-MPs on bacterial and fungal communities varied depending on the particle size and concentration, highlighting the complexity of these interactions (Fig. 5a). This aligns with existing studies, which show that PE-MPs of different particle sizes, particularly small and medium-sized PE-MPs (0.5–1500 μm), have more pronounced effects on soil bacteria and fungi (Gao et al., 2024).

Under fertilized conditions, we found that PE-MPs increased the diversity and evenness (Shannon index) of bacteria but reduced the diversity and evenness of fungi (Fig. 5a). This may be due to fertilization altering the nutritional status of the microbial community, which in turn influences how PE-MPs affect these communities (Qiong et al., 2018). Moreover, we observed that under unfertilized conditions, PE-MPs increased the relative abundance of Ascomycota and Proteobacteria, while decreasing the abundance of Crenarchaeota and Basidiomycota (Fig. 5c), consistent with previous findings (Z.-C. Wang et al., 2024). Under fertilized conditions, the relative abundance of Acidobacteriota and Mortierellomycota decreased, whereas the relative abundance of Firmicutes and Ascomycota increased (Fig. 5c). These changes are likely attributed to the increased nutrient availability from fertilization, which can drive shifts in the relative abundance of these microbial phyla (Sun et al., 2021).

Microbial biomarkers are highly valuable in assessing soil health, investigating microbial community functions, and monitoring soil fertility and plant health (Tackmann et al., 2018; F. Wang et al., 2024). In this study, we employed Lefse analysis to identify microbial biomarkers in soil microbial communities under different treatment conditions. Specifically, in the fertilization-PE-MPs coupling treatment, Allorhizobium-Neorhizobium-Pararhizobium-Rhizobium and Pseudomonas genera were identified as key microbial markers (Fig. 7a). This finding can be explained by the fact that Allorhizobium-Neorhizobium-Pararhizobium-Rhizobium is a significant member of the Rhizobium family, known for its ability to fix nitrogen in symbiosis with plants (Gu et al., 2020). Fertilization likely alters the nitrogen balance in the soil, and this genus can adapt to the change by fixing nitrogen, leading to its increased abundance in the microbial community. Additionally, Pseudomonas is capable of forming biofilms on the surface of PE-MPs, allowing it to attach to the microplastics and utilize the polymers in PE-MPs as carbon sources, which promotes its enrichment in the presence of PE-MPs (Lee et al., 2020; Wilkes and Aristilde, 2017). Through Mantel test analysis, we found that bacterial biomarkers were significantly and positively correlated with SAA, whereas fungal biomarkers were positively correlated with RL, NO_3^--N, and ALP (Fig. 8). We then used partial least squares structural equation modeling (SEM) to explore further explored the direct and indirect effects of PE-MPs and fertilization treatments on *Pisum sativum L*. growth, soil microbial communities, and enzyme activity using (Fig. 9). SEM results revealed that both PE-MPs and fertilization treatments not only directly impacted *Pisum sativum L.* growth but also indirectly affected growth and soil enzyme activities by altering fungal and bacterial biomarkers. Importantly, microbial biomarkers were predominantly influenced by the particle size and concentration of PE-MPs, as well as by the fertilization treatments.

This study simulated environmental pollution scenarios by artificially introducing PE-MPs to investigate their effects on the plant-soil-microorganism system. However, this simulation differs from the natural presence of PE-MPs in the environment. In nature, PE-MPs undergo long-term degradation, migration, and aging processes, which introduce additional complexities that are difficult to replicate or restore in a short experimental timeframe. Furthermore, although this study primarily focused on the combined effects of PE-MPs and fertilization on the plant-soil-microorganism system from a phenomenological perspective, the underlying mechanisms of these effects remain unclear. Future research should therefore aim to explore these specific mechanisms in more detail to better understand the role of PE-MPs in ecosystems.

5 Conclusion

In this study, we explored the effects of fertilization on *Pisum sativum L.* growth characteristics, soil physicochemical properties, nutrient content, enzyme activity, and microbial communities in soils contaminated with PE-MPs of varying particle sizes and concentrations. Our results underscore the negative impact of PE-MPs on the *Pisum sativum L.*-soil-microbe agricultural ecosystem. Specifically, PE-MPs significantly inhibited *Pisum sativum L.* growth, reduced soil bulk density, TN, and NH_4^+-N, while increasing SAA, pH, SOC, AP, and NO_3^--N levels. These effects were closely linked to the particle size and concentration of PE-MPs. Further analysis revealed that, in addition to their direct impact on *Pisum sativum L.* growth characteristics, PE-MPs also indirectly influenced soil enzyme activity and *Pisum sativum L.* growth by

decreasing the diversity of bacterial and fungal communities in the soil. However, our study also demonstrated that fertilization can effectively mitigate the negative impacts of PE-MPs on the *Pisum sativum L.*-soil-microbe ecosystem. Notably, we identified specific biomarkers enriched in the rhizosphere of *Pisum sativum L.* under different treatments (unfertilized, fertilized, unfertilized-PE-MPs, and fertilized-PE-MPs), which may serve as valuable indicators for assessing soil health. These findings provide a new perspective on soil quality assessment under PE-MPs contamination. Nevertheless, the mechanisms underlying these effects in other soil types or under long-term cultivation conditions remain unclear. Future research should further explore the interaction between fertilization and PE-MPs in the plant-soil-microbe system and identify optimal fertilization strategies for PE-MPs-contaminated agricultural soils.

References

1. Bethanis J, Golia EE (2024) Micro- and nano-plastics in agricultural soils: A critical meta-analysis of their impact on plant growth, nutrition, metal accumulation in plant tissues and crop yield. Appl Soil Ecol 194:105202. https://doi.org/https://doi.org/10.1016/j.apsoil.2023.105202
2. Blagodatskaya E, Kuzyakov Y (2008) Mechanisms of real and apparent priming effects and their dependence on soil microbial biomass and community structure: critical review. Biol Fertil SOILS 45:115–131. https://doi.org/10.1007/s00374-008-0334-y
3. Blöcker L, Watson C, Wichern F (2020) Living in the plastic age - Different short-term microbial response to microplastics addition to arable soils with contrasting soil organic matter content and farm management legacy. Environ Pollut 267:115468. https://doi.org/https://doi.org/10.1016/j.envpol.2020.115468
4. Bosker T, Bouwman LJ, Brun NR, Behrens P, Vijver MG (2019) Microplastics accumulate on pores in seed capsule and delay germination and root growth of the terrestrial vascular plant Lepidium sativum. Chemosphere 226:774–781. https://doi.org/https://doi.org/10.1016/j.chemosphere.2019.03.163
5. Casella C, Vadivel D, Dondi D (2024) The Current Situation of the Legislative Gap on Microplastics (MPs) as New Pollutants for the Environment. Water Air Soil Pollut 235:778. https://doi.org/10.1007/s11270-024-07589-1
6. Chen J, Xu H, Seven J, Zilla T, Dippold MA, Kuzyakov Y (2024) Microbial phosphorus recycling in soil by intra- and extracellular mechanisms. ISME Commun 3:135. https://doi.org/10.1038/s43705-023-00340-7
7. Colzi I, Renna L, Bianchi E, Castellani MB, Coppi A, Pignattelli S, Loppi S, Gonnelli C (2022) Impact of microplastics on growth, photosynthesis and essential elements in Cucurbita pepo L. J Hazard Mater 423:127238. https://doi.org/https://doi.org/10.1016/j.jhazmat.2021.127238
8. de Souza Machado AA, Lau CW, Kloas W, Bergmann J, Bachelier JB, Faltin E, Becker R, Görlich AS, Rillig MC (2019) Microplastics Can Change Soil Properties and Affect Plant Performance. Environ Sci Technol 53:6044–6052. https://doi.org/10.1021/acs.est.9b01339
9. de Souza Machado AA, Lau CW, Till J, Kloas W, Lehmann A, Becker R, Rillig MC (2018) Impacts of Microplastics on the Soil Biophysical Environment. Environ Sci Technol 52:9656–9665. https://doi.org/10.1021/acs.est.8b02212
10. Feng X, Sun Y, Zhang S, Wang F (2021) Ecological Effects of Microplastics on Soil-Plant Systems. Acta Pedol. Sin
11. Gao B, Gao F, Zhang X, Li Y, Yao H (2024) Effects of different sizes of microplastic particles on soil respiration, enzyme activities, microbial communities, and seed germination. Sci Total Environ 933:173100. https://doi.org/https://doi.org/10.1016/j.scitotenv.2024.173100
12. Gu S, Wei Z, Shao Z, Friman V-P, Cao K, Yang T, Kramer J, Wang X, Li M, Mei X, Xu Y, Shen Q, Kümmerli R, Jousset A (2020) Competition for iron drives phytopathogen control by natural rhizosphere microbiomes. Nat Microbiol 5:1002–1010. https://doi.org/10.1038/s41564-020-0719-8
13. Guo W, Ye Z, Zhao Y, Lu Q, Shen B, Zhang X, Zhang W, Chen S-C, Li Y (2024) Effects of different microplastic types on soil physicochemical properties, enzyme activities, and bacterial communities. Ecotoxicol Environ Saf

286:117219. https://doi.org/https://doi.org/10.1016/j.ecoenv.2024.117219

14. Hernández-Arenas R, Beltrán-Sanahuja A, Navarro-Quirant P, Sanz-Lazaro C (2021) The effect of sewage sludge containing microplastics on growth and fruit development of tomato plants. Environ Pollut 268:115779. https://doi.org/https://doi.org/10.1016/j.envpol.2020.115779
15. Hodson ME, Duffus-Hodson CA, Clark A, Prendergast-Miller MT, Thorpe KL (2017) Plastic Bag Derived-Microplastics as a Vector for Metal Exposure in Terrestrial Invertebrates. Environ Sci Technol 51:4714–4721. https://doi.org/10.1021/acs.est.7b00635
16. Hu X, Liu J, Liang A, Gu H, Liu Z, Jin J, Wang G (2025) Soil metagenomics reveals reduced tillage improves soil functional profiles of carbon, nitrogen, and phosphorus cycling in bulk and rhizosphere soils. Agric Ecosyst Environ 379:109371. https://doi.org/https://doi.org/10.1016/j.agee.2024.109371
17. Huang Y, Zhao Y, Wang J, Zhang M, Jia W, Qin X (2019) LDPE microplastic films alter microbial community composition and enzymatic activities in soil. Environ Pollut 254:112983. https://doi.org/https://doi.org/10.1016/j.envpol.2019.112983
18. Inubushi K, Yutaro K, Chiaki S, Makiba S, Yoshiharu S, U., and, Matsushima MY (2022) Effects of biodegradable plastics on soil properties and greenhouse gas production. Soil Sci Plant Nutr 68:183–188. https://doi.org/10.1080/00380768.2021.2022437
19. Iqbal S, Li Y, Xu J, Worthy FR, Gui H, Faraj TK, Jones DL, Bu D (2025) Smallest microplastics intensify maize yield decline, soil processes and consequent global warming potential. J Hazard Mater 486:136993. https://doi.org/https://doi.org/10.1016/j.jhazmat.2024.136993
20. Jo S-H, Kim J-H, Moon J-H, Yang S-Y, Baek J-K, Song Y-S, Shon J-Y, Chung N-J, Lee H-S (2024) Effects of mineral fertilization (NPK) on combined high temperature and ozone damage in rice. BMC Plant Biol 24:974. https://doi.org/10.1186/s12870-024-05695-0
21. Judy JD, Williams M, Gregg A, Oliver D, Kumar A, Kookana R, Kirby JK (2019) Microplastics in municipal mixed-waste organic outputs induce minimal short to long-term toxicity in key terrestrial biota. Environ Pollut 252:522–531. https://doi.org/https://doi.org/10.1016/j.envpol.2019.05.027
22. Lee HM, Kim HR, Jeon E, Yu HC, Lee S, Li J, Kim D-H (2020) Evaluation of the Biodegradation Efficiency of Four Various Types of Plastics by Pseudomonas aeruginosa Isolated from the Gut Extract of Superworms. Microorganisms 8. https://doi.org/10.3390/microorganisms8091341
23. Li G, Cai L, Liu Y (2023) Different effects of conventional and biodegradable microplastics on the amelioration process of cadmium-contaminated soil. Sci Total Environ 892:164589. https://doi.org/https://doi.org/10.1016/j.scitotenv.2023.164589
24. Li H-Z, Zhu D, Lindhardt JH, Lin S-M, Ke X, Cui L (2021) Long-Term Fertilization History Alters Effects of Microplastics on Soil Properties, Microbial Communities, and Functions in Diverse Farmland Ecosystem. Environ Sci Technol 55:4658–4668. https://doi.org/10.1021/acs.est.0c04849
25. Li L, Luo Y, Li R, Zhou Q, Peijnenburg WJGM, Yin N, Yang J, Tu C, Zhang Y (2020) Effective uptake of submicrometre plastics by crop plants via a crack-entry mode. Nat Sustain 3:929–937. https://doi.org/10.1038/s41893-020-0567-9
26. Li Y, Liu L, Meng X, Qiu J, Liu Y, Zhao F, Tan H (2025) Microplastics affect the nitrogen nutrition status of soybean by altering the nitrogen cycle in the rhizosphere soil. J Hazard Mater 490:137803. https://doi.org/https://doi.org/10.1016/j.jhazmat.2025.137803
27. Lian Y, Shi R, Liu J, Zeb A, Wang Q, Wang J, Yu M, Li J, Zheng Z, Ali N, Bao Y, Liu W (2024) Effects of polystyrene, polyethylene, and polypropylene microplastics on the soil-rhizosphere-plant system: Phytotoxicity, enzyme activity, and microbial community. J Hazard Mater 465:133417. https://doi.org/https://doi.org/10.1016/j.jhazmat.2023.133417

28. Liang R, He J, Sun F-H, Zhang R-F, Wang X-X (2024) Effects of Polyethylene Microplastics on Soil Nutrients and Enzyme Activities. Environ Sci 45:3679–3687. https://doi.org/10.13227/j.hjkx.202306183
29. Liao Y-C, Nazygul J, Li M, Wang X-L, Jiang L-J (2019) Effects of Microplastics on the Growth, Physiology, and Biochemical Characteristics of Wheat (Triticum aestivum). Environ Sci 40:4661–4667. https://doi.org/10.13227/j.hjkx.201903113
30. Liu H, Yang X, Liu G, Liang C, Xue S, Chen H, Ritsema CJ, Geissen V (2017) Response of soil dissolved organic matter to microplastic addition in Chinese loess soil. Chemosphere 185:907–917. https://doi.org/https://doi.org/10.1016/j.chemosphere.2017.07.064
31. Liu M, Lu S, Song Y, Lei L, Hu J, Lv W, Zhou W, Cao C, Shi H, Yang X, He D (2018) Microplastic and mesoplastic pollution in farmland soils in suburbs of Shanghai. China Environ Pollut 242:855–862. https://doi.org/https://doi.org/10.1016/j.envpol.2018.07.051
32. Liu S-S, Qin J-Q, Wu X-G (2024) Effect of Microplastics and Phenanthrene on Soil Chemical Properties, Enzymatic Activities, and Microbial Communities. Environ Sci 45:496–507. https://doi.org/10.13227/j.hjkx.202302197
33. Lozano YM, Lehnert T, Linck LT, Lehmann A, Rillig MC (2020) Microplastic shape, concentration and polymer type affect soil properties and plant biomass. https://doi.org/10.1101/2020.07.27.223768. bioRxiv
34. Meng F, Yang X, Riksen M, Geissen V (2022) Effect of different polymers of microplastics on soil organic carbon and nitrogen – A mesocosm experiment. Environ Res 204:111938. https://doi.org/https://doi.org/10.1016/j.envres.2021.111938
35. Mohammed M, Dakora FD (2024) Microbes in Agriculture: Prospects and Constraints to Their Wider Adoption and Utilization in Nutrient-Poor Environments. Microorganisms. https://doi.org/10.3390/microorganisms12112225
36. Ng E-L, Lwanga H, Eldridge E, Johnston SM, Hu P, Geissen H-W, Chen V, D (2018) An overview of microplastic and nanoplastic pollution in agroecosystems. Sci Total Environ 627:1377–1388. https://doi.org/https://doi.org/10.1016/j.scitotenv.2018.01.341
37. Nizzetto L, Futter M, Langaas S (2016) Are Agricultural Soils Dumps for Microplastics of Urban Origin? Environ Sci Technol 50:10777–10779. https://doi.org/10.1021/acs.est.6b04140
38. Norling M, Hurley R, Schell T, Futter MN, Rico A, Vighi M, Blanco A, Ledesma JLJ, Nizzetto L (2024) Retention efficiency for microplastic in a landscape estimated from empirically validated dynamic model predictions. J Hazard Mater 464:132993. https://doi.org/https://doi.org/10.1016/j.jhazmat.2023.132993
39. Qiong X, Qiqi W, Lei W, Andong C, Chuanjie W, Wenju Z, Minggang X (2018) Fertilization impacts on soil microbial communities and enzyme activities across China's croplands: a meta-analysis. J. Plant Nutr, Fertitizer
40. Rillig MC (2018) Microplastic Disguising As Soil Carbon Storage. Environ Sci Technol 52:6079–6080. https://doi.org/10.1021/acs.est.8b02338
41. Rillig MC, Ziersch L, Hempel S (2017) Microplastic transport in soil by earthworms. Sci Rep 7:1362. https://doi.org/10.1038/s41598-017-01594-7
42. Rong L, Zhao, Longfei, Zhao, Leicheng, Cheng Z, Yao Y, Yuan C, Wang L, Sun H (2021) LDPE microplastics affect soil microbial communities and nitrogen cycling. Sci Total Environ 773:145640. https://doi.org/https://doi.org/10.1016/j.scitotenv.2021.145640
43. Sapre S, Gontia-Mishra I, Tiwari S (2022) Plant Growth-Promoting Rhizobacteria Ameliorates Salinity Stress in Pea (Pisum sativum). J Plant Growth Regul 41:647–656. https://doi.org/10.1007/s00344-021-10329-y
44. Shah T, Ali A, Haider G, Asad M, Munsif F (2023) Microplastics alter soil enzyme activities and microbial community structure without negatively affecting plant growth in an agroecosystem. Chemosphere 322:138188. https://doi.org/https://doi.org/10.1016/j.chemosphere.2023.138188

45. Shang Y, Gu X, Yu H, Zheng H, Li W, Quan Z, Wang F (2024) Effects of microplastics on soil microbial community structure and symbiotic network analysis. J. Environ. Eng. Technol
46. Steinmetz Z, Wollmann C, Schaefer M, Buchmann C, David J, Tröger J, Muñoz K, Frör O, Schaumann GE (2016) Plastic mulching in agriculture. Trading short-term agronomic benefits for long-term soil degradation? Sci. Total Environ 550:690–705. https://doi.org/https://doi.org/10.1016/j.scitotenv.2016.01.153
47. Sulaman S, Nadeem M, Shabaan M, Orman S, Anwar-ul-Haq M, Zulfiqar U (2025) Exogenous Application of Nitrogen (N) and Potassium (K) Improves Drought Tolerance in Plants: A Review. J. Soil Sci. https://doi.org/10.1007/s42729-025-02433-9. Plant Nutr
48. Sun A, Jiao X-Y, Chen Q, Wu A-L, Zheng Y, Lin Y-X, He J-Z, Hu H-W (2021) Microbial communities in crop phyllosphere and root endosphere are more resistant than soil microbiota to fertilization. Soil Biol Biochem 153:108113. https://doi.org/https://doi.org/10.1016/j.soilbio.2020.108113
49. Sun X-D, Yuan X-Z, Jia Y, Feng L-J, Zhu F-P, Dong S-S, Liu J, Kong X, Tian H, Duan J-L, Ding Z, Wang S-G, Xing B (2020) Differentially charged nanoplastics demonstrate distinct accumulation in Arabidopsis thaliana. Nat Nanotechnol 15:755–760. https://doi.org/10.1038/s41565-020-0707-4
50. Tackmann J, Arora N, Schmidt TSB, Rodrigues JFM, von Mering C (2018) Ecologically informed microbial biomarkers and accurate classification of mixed and unmixed samples in an extensive cross-study of human body sites. Microbiome 6:192. https://doi.org/10.1186/s40168-018-0565-6
51. Tian S, Zhu B, Yin R, Wang M, Jiang Y, Zhang C, Li D, Chen X, Kardol P, Liu M (2022) Organic fertilization promotes crop productivity through changes in soil aggregation. Soil Biol Biochem 165:108533. https://doi.org/https://doi.org/10.1016/j.soilbio.2021.108533
52. Wan Y, Wu C, Xue Q, Hui X (2019) Effects of plastic contamination on water evaporation and desiccation cracking in soil. Sci Total Environ 654:576–582. https://doi.org/https://doi.org/10.1016/j.scitotenv.2018.11.123
53. Wang C, Kuzyakov Y (2024) Mechanisms and implications of bacterial–fungal competition for soil resources. ISME J 18:wrae073. https://doi.org/10.1093/ismejo/wrae073
54. Wang F, Zhang H, Liu H, Wu C, Wan Y, Zhu L, Yang J, Cai P, Chen J, Ge T (2024) Combating wheat yellow mosaic virus through microbial interactions and hormone pathway modulations. Microbiome 12:200. https://doi.org/10.1186/s40168-024-01911-z
55. Wang F, Zhang X, Zhang, Shuqi, Zhang S, Sun Y (2020) Interactions of microplastics and cadmium on plant growth and arbuscular mycorrhizal fungal communities in an agricultural soil. Chemosphere 254:126791. https://doi.org/https://doi.org/10.1016/j.chemosphere.2020.126791
56. Wang J, Huang M, Wang Q, Sun Y, Zhao Y, Huang Y (2020) LDPE microplastics significantly alter the temporal turnover of soil microbial communities. Sci Total Environ 726:138682. https://doi.org/https://doi.org/10.1016/j.scitotenv.2020.138682
57. Wang J, Liu X, Li Y, Powell T, Wang X, Wang G, Zhang P (2019) Microplastics as contaminants in the soil environment: A mini-review. Sci Total Environ 691:848–857. https://doi.org/https://doi.org/10.1016/j.scitotenv.2019.07.209
58. Wang J, Lv S, Zhang M, Chen G, Zhu T, Zhang S, Teng Y, Christie P, Luo Y (2016) Effects of plastic film residues on occurrence of phthalates and microbial activity in soils. Chemosphere 151:171–177. https://doi.org/https://doi.org/10.1016/j.chemosphere.2016.02.076
59. Wang J, Zhu Z, Sun L, Sun Y, Yang S, Qin Q, Xue Y (2025) The bridging role of soil organic carbon in regulating bacterial community by microplastic pollution: Evidence from different microplastic additions. J Hazard Mater 490:137761. https://doi.org/https://doi.org/10.1016/j.jhazmat.2025.137761

60. Wang Q, Feng X, Liu Y, Cui W, Sun Y, Zhang S, Wang F (2022) Effects of microplastics and carbon nanotubes on soil geochemical properties and bacterial communities. J Hazard Mater 433:128826. https://doi.org/https://doi.org/10.1016/j.jhazmat.2022.128826
61. Wang Q, Feng X, Liu Y, Li W, Cui W, Sun Y, Zhang S, Wang F, Xing B (2023) Response of peanut plant and soil N-fixing bacterial communities to conventional and biodegradable microplastics. J Hazard Mater 459:132142. https://doi.org/https://doi.org/10.1016/j.jhazmat.2023.132142
62. Wang S, Ye H, Yang C, Zhang Y, Pu J, Ren Y, Xie K, Wang L, Zeng D, He H, Ji H, Herrera-Estrella LR, Xu G, Chen A (2025) OsNLP3 and OsPHR2 orchestrate direct and mycorrhizal pathways for nitrate uptake by regulating NAR2.1–NRT2s complexes in rice. Proc. Natl. Acad. Sci. 122, e2416345122. https://doi.org/10.1073/pnas.2416345122
63. Wang X, Leng Y, Wang J, Huang X, Fu Y, Fan C, Gao W, Zhang W, Ning Z, Chen M (2024) Effects of Microplastics on Soil N2O Emission and Nitrogen Transformations from Tropical Agricultural Soils. Environ Sci 45:6139–6147. https://doi.org/10.13227/j.hjkx.202310172
64. Wang X, Xing Y, Lv M, Zhang T, Ya H, Jiang B (2022) Recent advances on the effects of microplastics on elements cycling in the environment. Sci Total Environ 849:157884. https://doi.org/https://doi.org/10.1016/j.scitotenv.2022.157884
65. Wang Z-C, Li Z, Li J-C, Qu Z-Y, Yang W-H, Li W-P (2024) Effect of Polyethylene Microplastics on the Microbial Community of Saline Soils. Environ Sci 45:3088–3097. https://doi.org/10.13227/j.hjkx.202305246
66. Wilkes RA, Aristilde L (2017) Degradation and metabolism of synthetic plastics and associated products by Pseudomonas sp.: capabilities and challenges. J Appl Microbiol 123:582–593. https://doi.org/10.1111/jam.13472
67. Wu X, Hou H, Liu Y, Yin S, Bian S, Liang S, Wan C, Yuan S, Xiao K, Liu B, Hu J, Yang J (2022) Microplastics affect rice (Oryza sativa L.) quality by interfering metabolite accumulation and energy expenditure pathways: A field study. J Hazard Mater 422:126834. https://doi.org/https://doi.org/10.1016/j.jhazmat.2021.126834
68. Xiong Z, Zhang Y, Chen X, Peng L, Zou L, Liu B, Li Q (2024) Mitigating the effects of polyethylene microplastics on Pisum sativum L. quality by applying microplastics-degrading bacteria: A field study. Environ Res 263:120201. https://doi.org/https://doi.org/10.1016/j.envres.2024.120201
69. Xu B, Fei L, Zachary C, Dan H, Zhijiang L, Yan H, Haizhen W, Zhenmei L, Philip C, Caixian B, Jay T, G., and, Xu J (2020) Microplastics in the soil environment: Occurrence, risks, interactions and fate – A review. Crit Rev Environ Sci Technol 50:2175–2222. https://doi.org/10.1080/10643389.2019.1694822
70. Yan Y, Chen Z, Zhu F, Zhu C, Wang C, Gu C (2021) Effect of Polyvinyl Chloride Microplastics on Bacterial Community and Nutrient Status in Two Agricultural Soils. Bull Environ Contam Toxicol 107:602–609. https://doi.org/10.1007/s00128-020-02900-2
71. Yan Y, Wang C, Zhang J, Sun Y, Xu X, Zhu N, Cai Y, Xu D, Wang X, Xin X, Chen J (2022) Response of soil microbial biomass C, N, and P and microbial quotient to agriculture and agricultural abandonment in a meadow steppe of northeast China. Soil Tillage Res 223:105475. https://doi.org/https://doi.org/10.1016/j.still.2022.105475
72. Yang M, Huang D-Y, Tian Y-B, Zhu Q-H, Zhang Q, Zhu H-H, Xu C (2021) Influences of different source microplastics with different particle sizes and application rates on soil properties and growth of Chinese cabbage (Brassica chinensis L). Ecotoxicol Environ Saf 222:112480. https://doi.org/https://doi.org/10.1016/j.ecoenv.2021.112480
73. Yang W, Cheng P, Adams CA, Zhang S, Sun Y, Yu H, Wang F (2021) Effects of microplastics on plant growth and arbuscular mycorrhizal fungal communities in a soil spiked with ZnO nanoparticles. Soil Biol Biochem 155:108179. https://doi.org/https://doi.org/10.1016/j.soilbio.2021.108179
74. Zeb A, Liu W, Meng L, Lian J, Wang Q, Lian Y, Chen C, Wu J (2022) Effects of polyester microfibers (PMFs) and cadmium on lettuce (Lactuca sativa) and the rhizospheric microbial communities: A study involving physio-

biochemical properties and metabolomic profiles. J Hazard Mater 424:127405. https://doi.org/https://doi.org/10.1016/j.jhazmat.2021.127405

75. Zhang M, Zhao Y, Qin X, Jia W, Chai L, Huang M, Huang Y (2019) Microplastics from mulching film is a distinct habitat for bacteria in farmland soil. Sci Total Environ 688:470–478. https://doi.org/https://doi.org/10.1016/j.scitotenv.2019.06.108
76. Zhang Q, Guo W, Wang B, Feng, Yuanyuan, Han L, Zhang C, Xie H, Liu X, Feng Y (2023) Influences of microplastics types and size on soil properties and cadmium adsorption in paddy soil after one rice season. Resour Environ Sustain 11:100102. https://doi.org/https://doi.org/10.1016/j.resenv.2022.100102
77. Zhang S, Wang J, Hao X (2020) Fertilization accelerates the decomposition of microplastics in mollisols. Sci Total Environ 722:137950. https://doi.org/https://doi.org/10.1016/j.scitotenv.2020.137950
78. Zhang Z, Cui Q, Chen L, Zhu X, Zhao S, Duan C, Zhang X, Song D, Fang L (2022) A critical review of microplastics in the soil-plant system: Distribution, uptake, phytotoxicity and prevention. J Hazard Mater 424:127750. https://doi.org/https://doi.org/10.1016/j.jhazmat.2021.127750
79. Zhao M, Li C, Zhang C, Han B, Wang X, Zhang J, Wang J, Cao B, Zhao Y, Chen Y, Zou G (2022) Typical microplastics in field and facility agriculture dynamically affect available cadmium in different soil types through physicochemical dynamics of carbon, iron and microbes. J Hazard Mater 440:129726. https://doi.org/https://doi.org/10.1016/j.jhazmat.2022.129726
80. Zhao S, Zhang Z, Chen L, Cui Q, Cui Y, Song D, Fang L (2022) Review on migration, transformation and ecological impacts of microplastics in soil. Appl Soil Ecol 176:104486. https://doi.org/https://doi.org/10.1016/j.apsoil.2022.104486
81. Zhou W, Xu J, Fu B, Wu Y, Zhang K, Han J, Kong J, Ma Y (2024) Microplastic accumulation and transport in agricultural soils with long-term sewage sludge amendments. J Hazard Mater 480:136263. https://doi.org/https://doi.org/10.1016/j.jhazmat.2024.136263
82. Zhuang Q-L, Yuan H-Y, Qi J-Q, Sun Z-R, Tao B-X, Zhang B-H (2024) Phosphorus fertiliser application mitigates the negative effects of microplastic on soil microbes and rice growth. J Hazard Mater 465:133278. https://doi.org/https://doi.org/10.1016/j.jhazmat.2023.133278

Figures

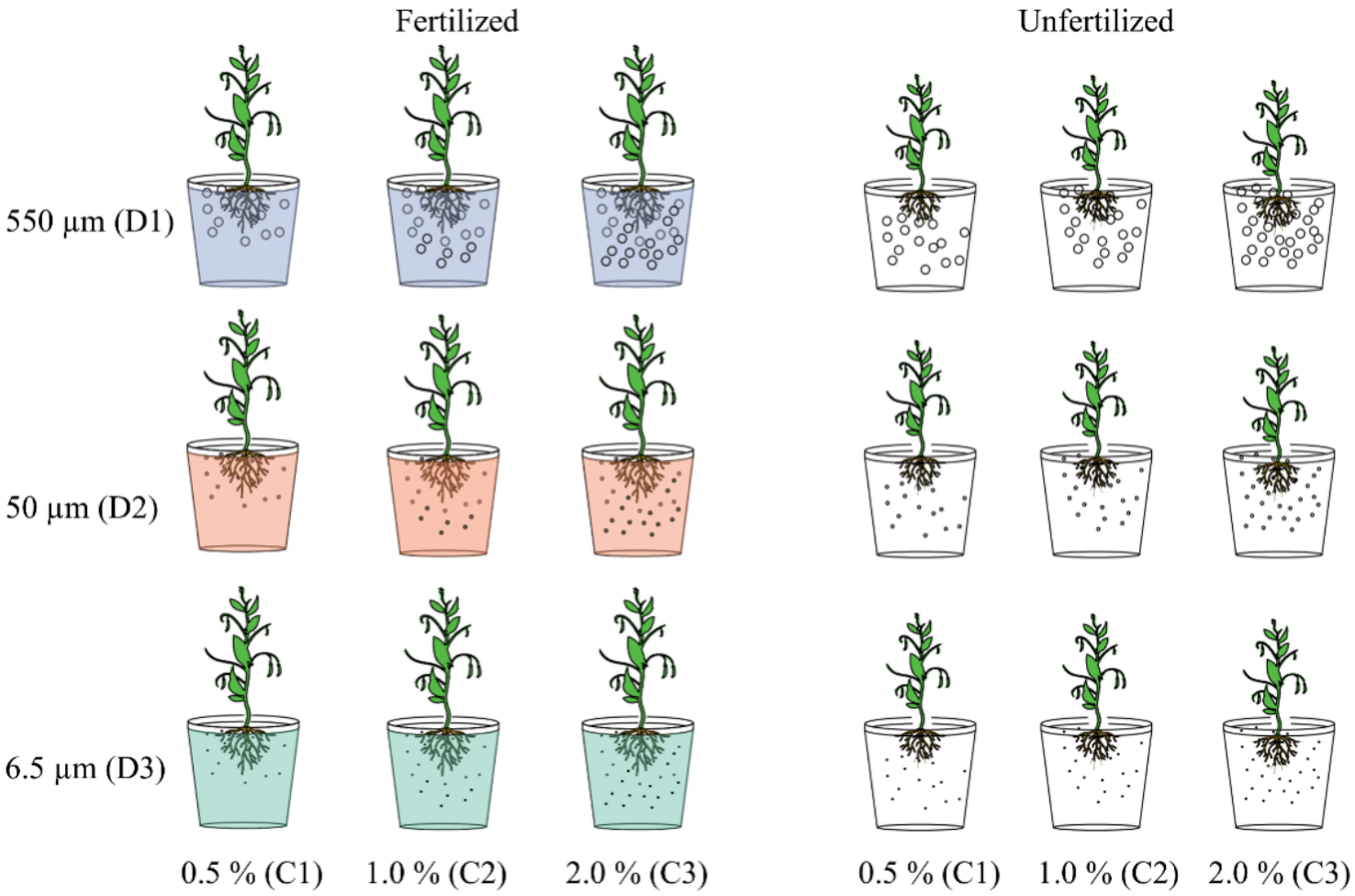


Figure 1

Schematic representation of the experiment. Polyethylene microplastics (PE-MPs) were added of 550 µm (D1), 50 µm (D2), 6.5 µm (D3) particle size and 0.5% (C1), 1.0% (C2), 2.0% (C3) concentration under the conditions of unfertilized and fertilized.

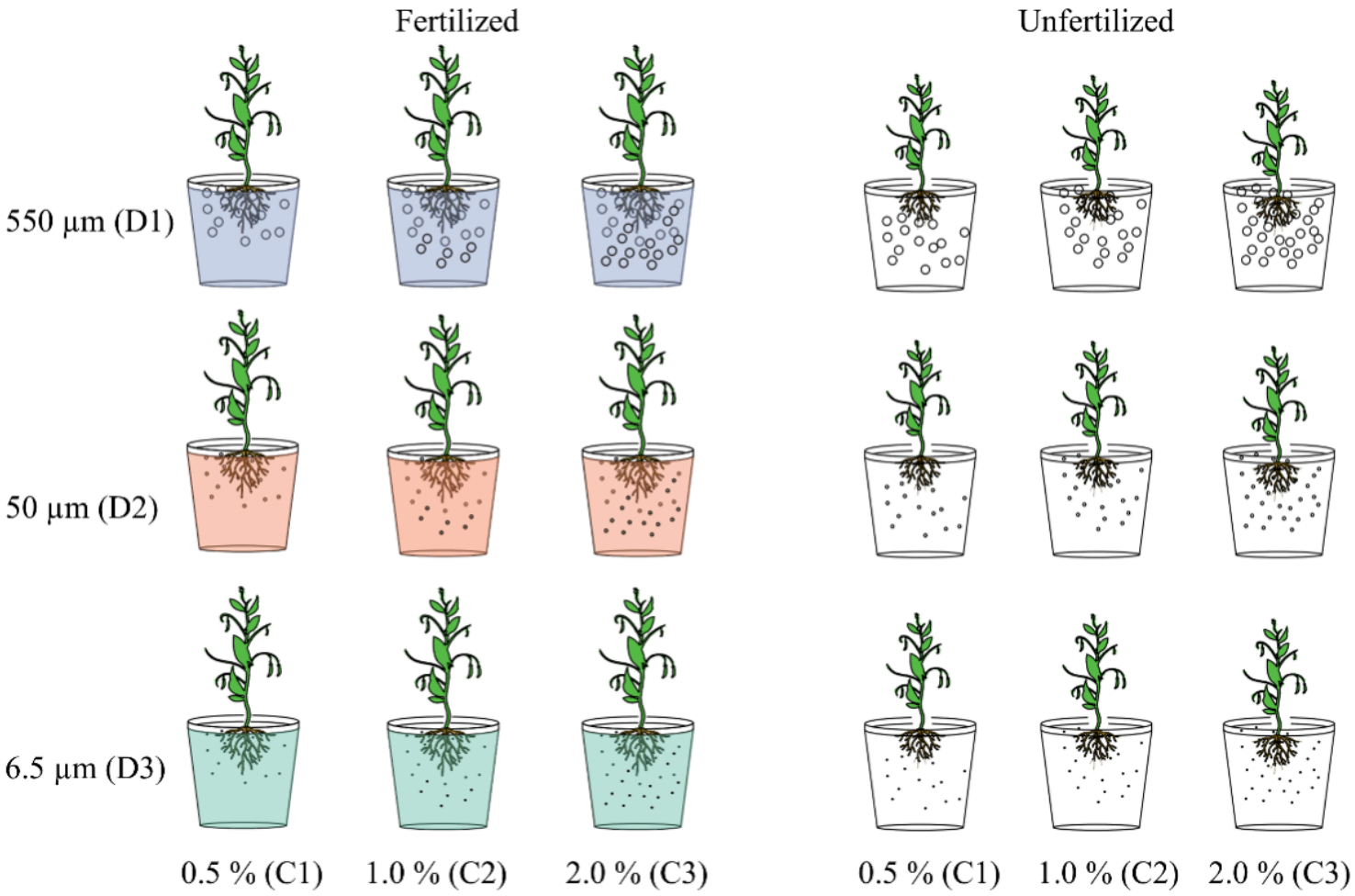


Figure 1

Schematic representation of the experiment. Polyethylene microplastics (PE-MPs) were added of 550 µm (D1), 50 µm (D2), 6.5 µm (D3) particle size and 0.5% (C1), 1.0% (C2), 2.0% (C3) concentration under the conditions of unfertilized and fertilized.

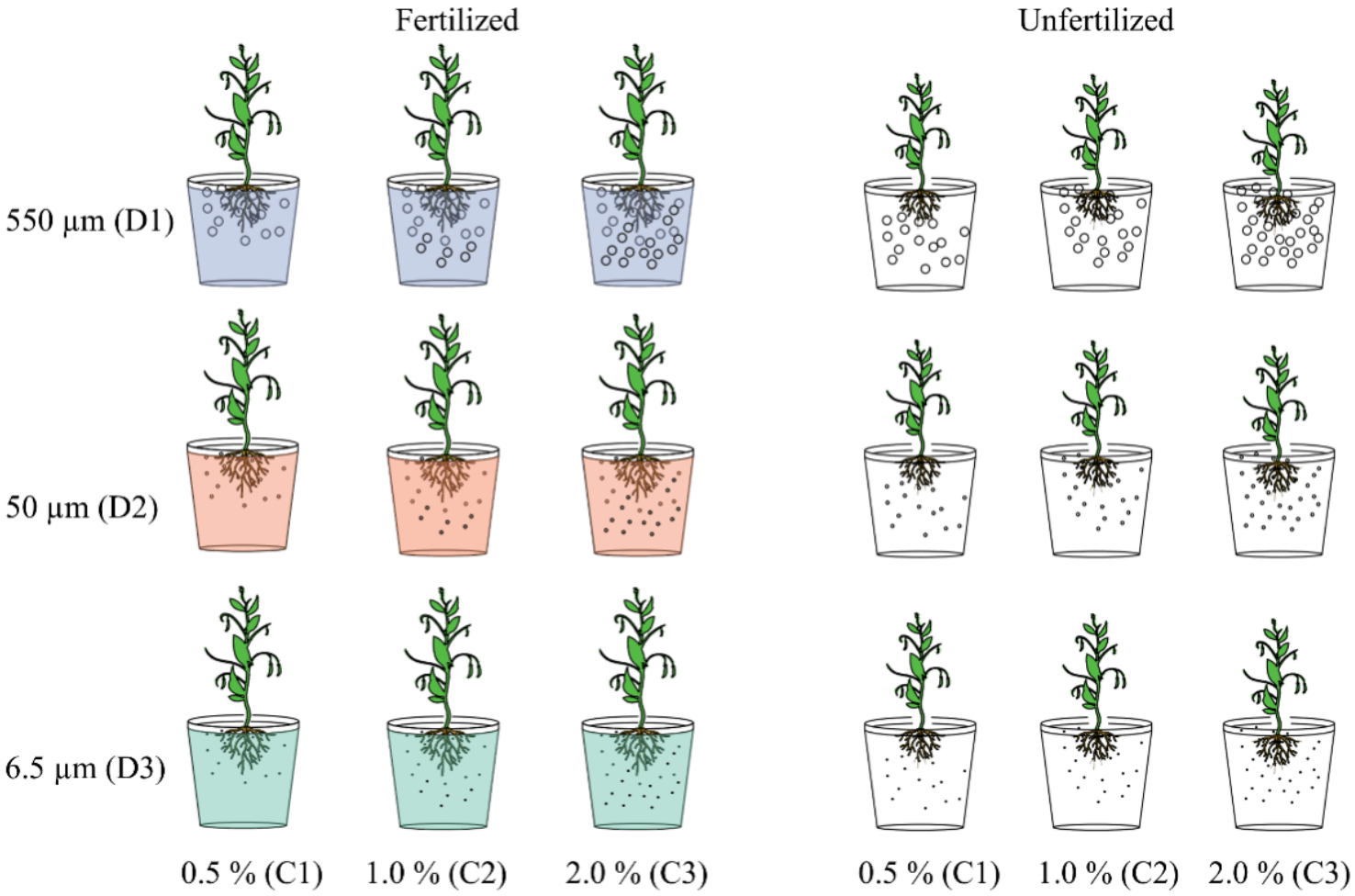


Figure 1

Schematic representation of the experiment. Polyethylene microplastics (PE-MPs) were added of 550 µm (D1), 50 µm (D2), 6.5 µm (D3) particle size and 0.5% (C1), 1.0% (C2), 2.0% (C3) concentration under the conditions of unfertilized and fertilized.

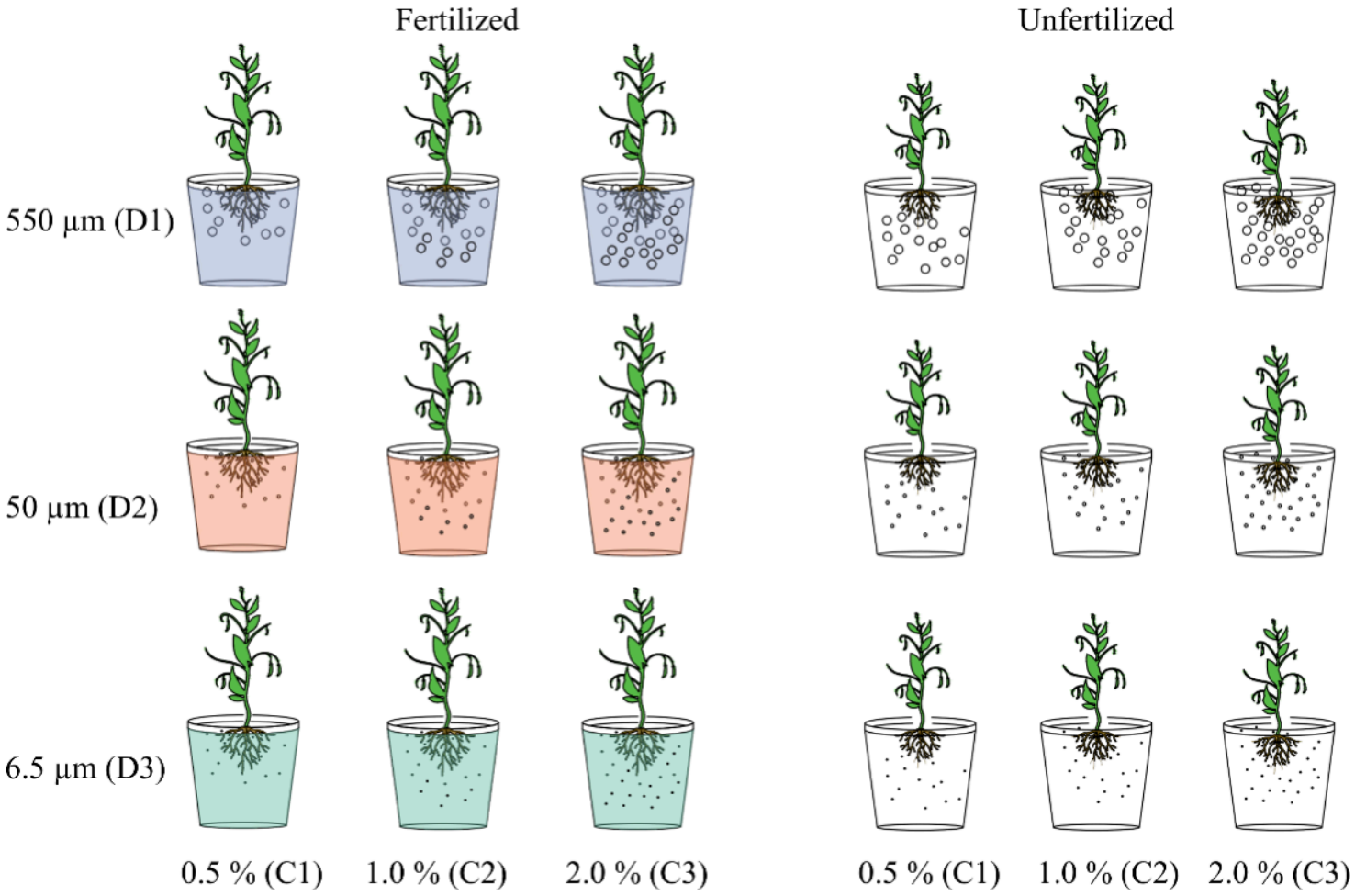


Figure 1

Schematic representation of the experiment. Polyethylene microplastics (PE-MPs) were added of 550 µm (D1), 50 µm (D2), 6.5 µm (D3) particle size and 0.5% (C1), 1.0% (C2), 2.0% (C3) concentration under the conditions of unfertilized and fertilized.

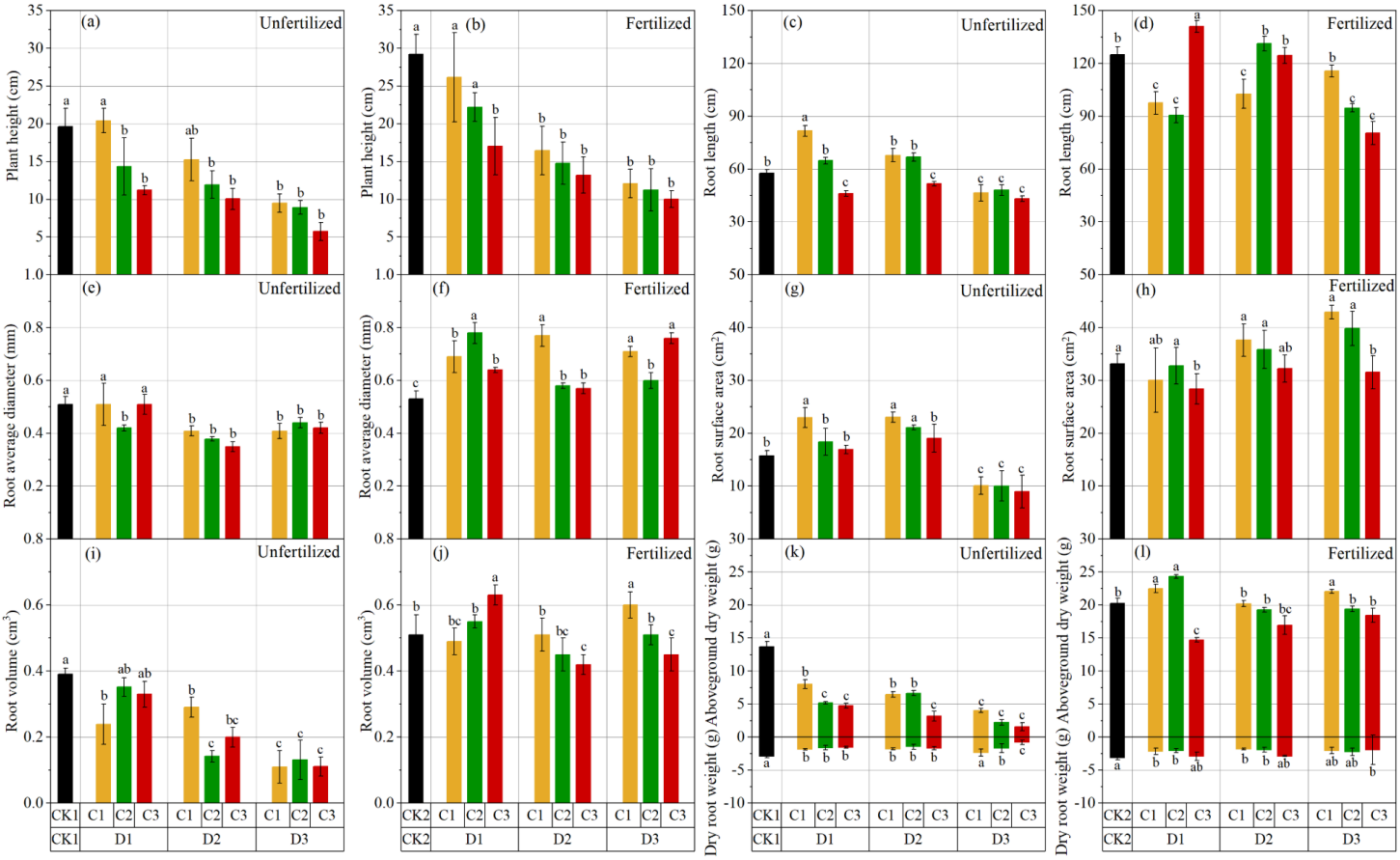


Figure 2

The effects of three particle size and concentrations of polyethylene microplastics (PE-MPs) on *Pisum sativum L.*growth under fertilized and unfertilized conditions. (a, b) Plant heigth, (c, d) Root length, (e, f) Root average diameter, (g, h) Root surface area, (i, j) Root volume, (k, l) aboveground dry weight and dry root weight. Data are means ± SD (n = 3). “CK1, CK2” represent the unfertilized and fertilized treatments without the intervention of PE-MPs, respectively. “D1, D2, D3” represent the PE-MPs treatments with particle sizes of 550 μm, 50 μm, and 6.5 μm, respectively. “C1, C2, C3” represent the concentrations of 0.5%, 1.0%, and 2.0% PE-MPs (w/w) relative to the soil weight. Different letters above the bar represent statistically significant difference among all the treatments at $P < 0.05$.

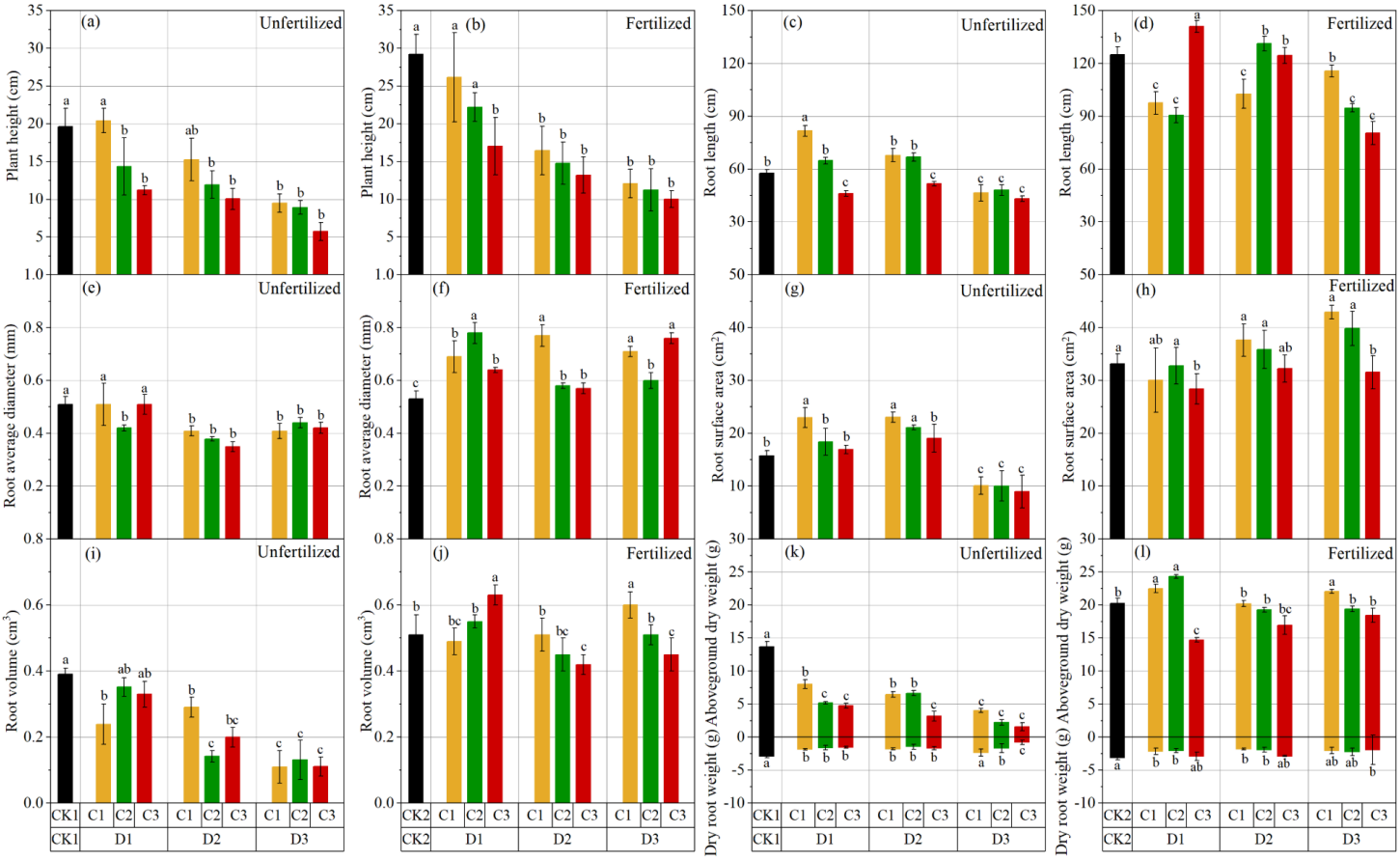


Figure 2

The effects of three particle size and concentrations of polyethylene microplastics (PE-MPs) on *Pisum sativum L.*growth under fertilized and unfertilized conditions. (a, b) Plant heigth, (c, d) Root length, (e, f) Root average diameter, (g, h) Root surface area, (i, j) Root volume, (k, l) aboveground dry weight and dry root weight. Data are means ± SD (n = 3). “CK1, CK2” represent the unfertilized and fertilized treatments without the intervention of PE-MPs, respectively. “D1, D2, D3” represent the PE-MPs treatments with particle sizes of 550 μm, 50 μm, and 6.5 μm, respectively. “C1, C2, C3” represent the concentrations of 0.5%, 1.0%, and 2.0% PE-MPs (w/w) relative to the soil weight. Different letters above the bar represent statistically significant difference among all the treatments at $P < 0.05$.

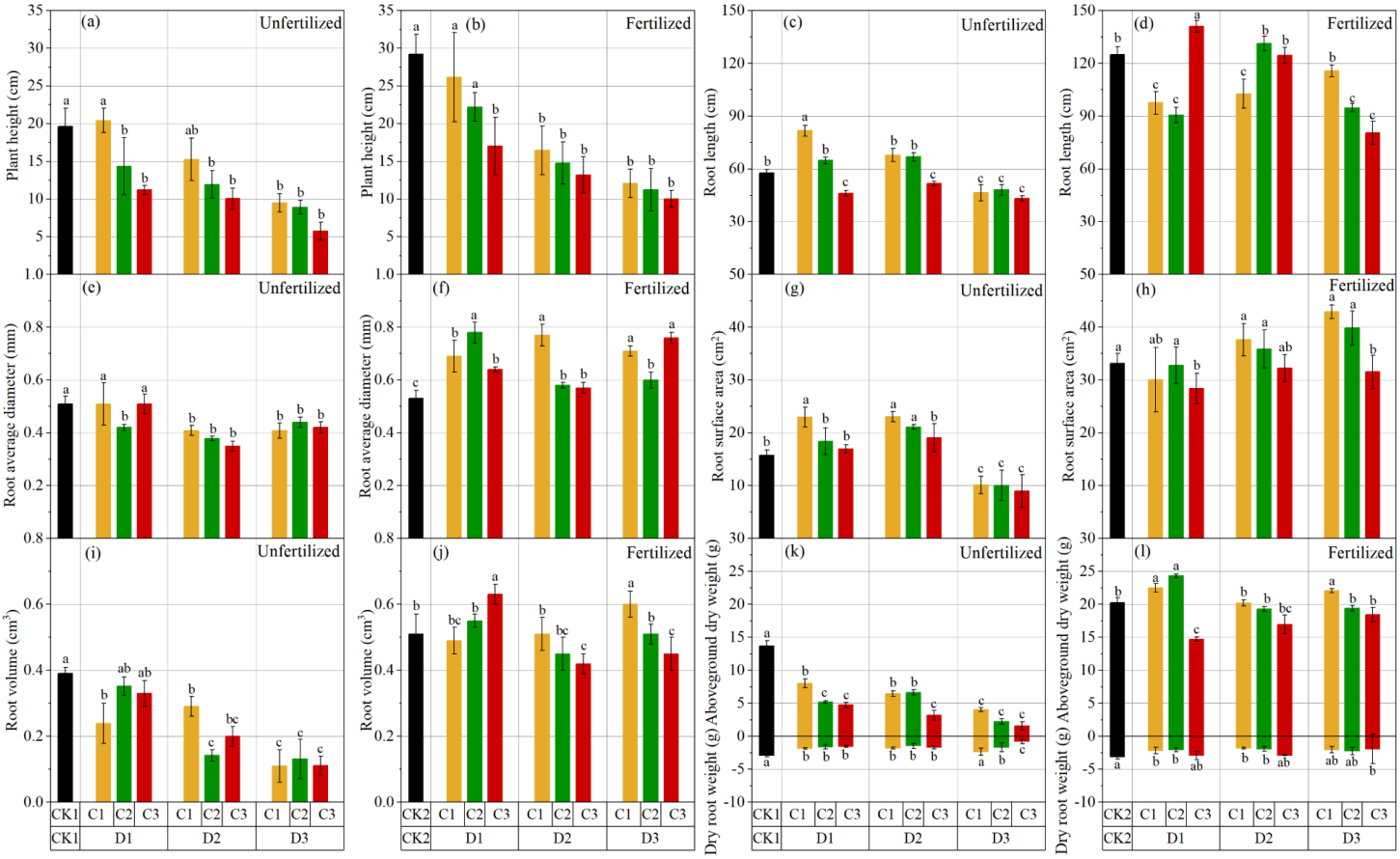


Figure 2

The effects of three particle size and concentrations of polyethylene microplastics (PE-MPs) on *Pisum sativum L.*growth under fertilized and unfertilized conditions. (a, b) Plant heigth, (c, d) Root length, (e, f) Root average diameter, (g, h) Root surface area, (i, j) Root volume, (k, l) aboveground dry weight and dry root weight. Data are means ± SD (n = 3). “CK1, CK2” represent the unfertilized and fertilized treatments without the intervention of PE-MPs, respectively. “D1, D2, D3” represent the PE-MPs treatments with particle sizes of 550 μm, 50 μm, and 6.5 μm, respectively. “C1, C2, C3” represent the concentrations of 0.5%, 1.0%, and 2.0% PE-MPs (w/w) relative to the soil weight. Different letters above the bar represent statistically significant difference among all the treatments at $P < 0.05$.

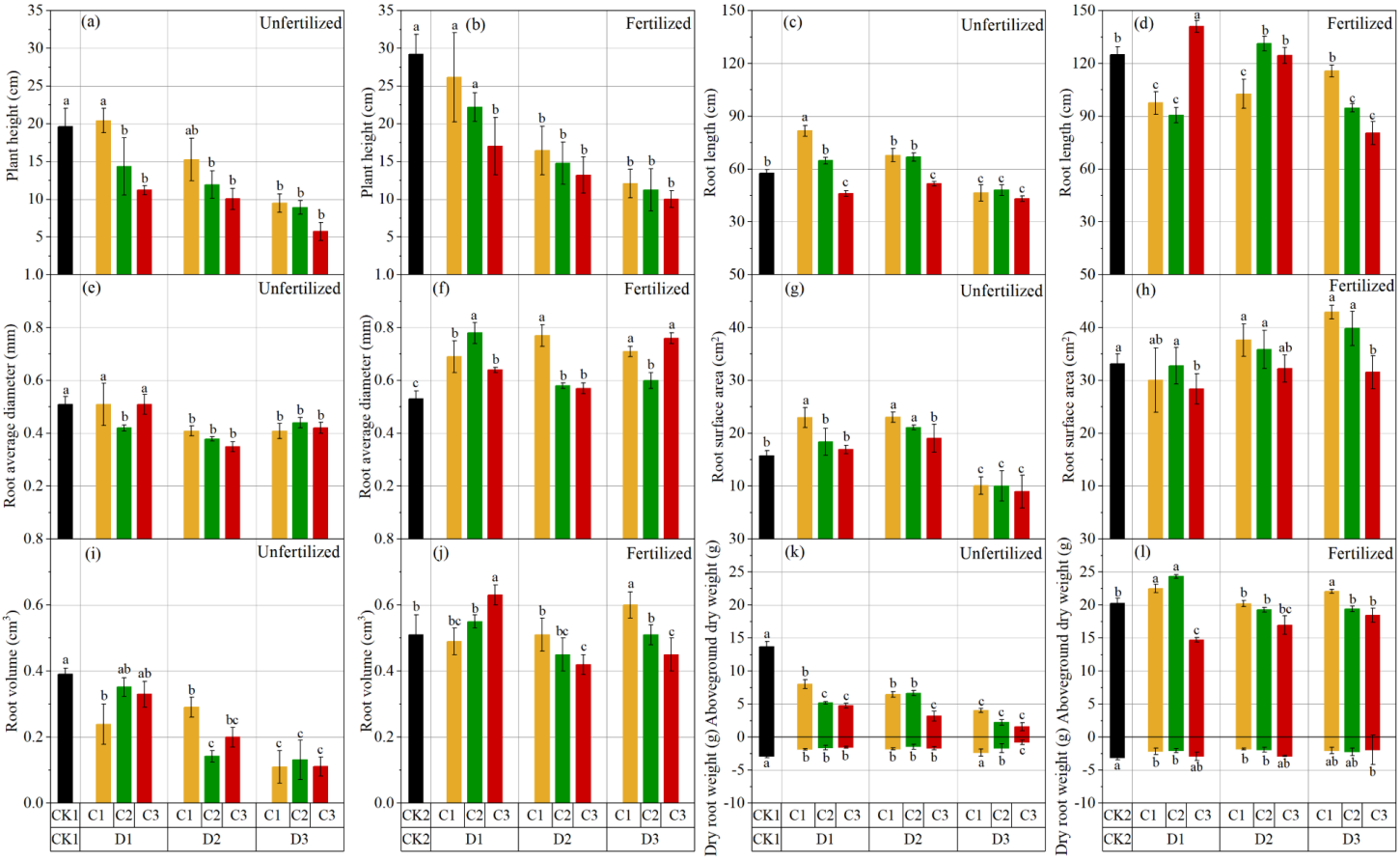


Figure 2

The effects of three particle size and concentrations of polyethylene microplastics (PE-MPs) on *Pisum sativum L.*growth under fertilized and unfertilized conditions. (a, b) Plant heigth, (c, d) Root length, (e, f) Root average diameter, (g, h) Root surface area, (i, j) Root volume, (k, l) aboveground dry weight and dry root weight. Data are means ± SD (n = 3). “CK1, CK2” represent the unfertilized and fertilized treatments without the intervention of PE-MPs, respectively. “D1, D2, D3” represent the PE-MPs treatments with particle sizes of 550 μm, 50 μm, and 6.5 μm, respectively. “C1, C2, C3” represent the concentrations of 0.5%, 1.0%, and 2.0% PE-MPs (w/w) relative to the soil weight. Different letters above the bar represent statistically significant difference among all the treatments at $P < 0.05$.

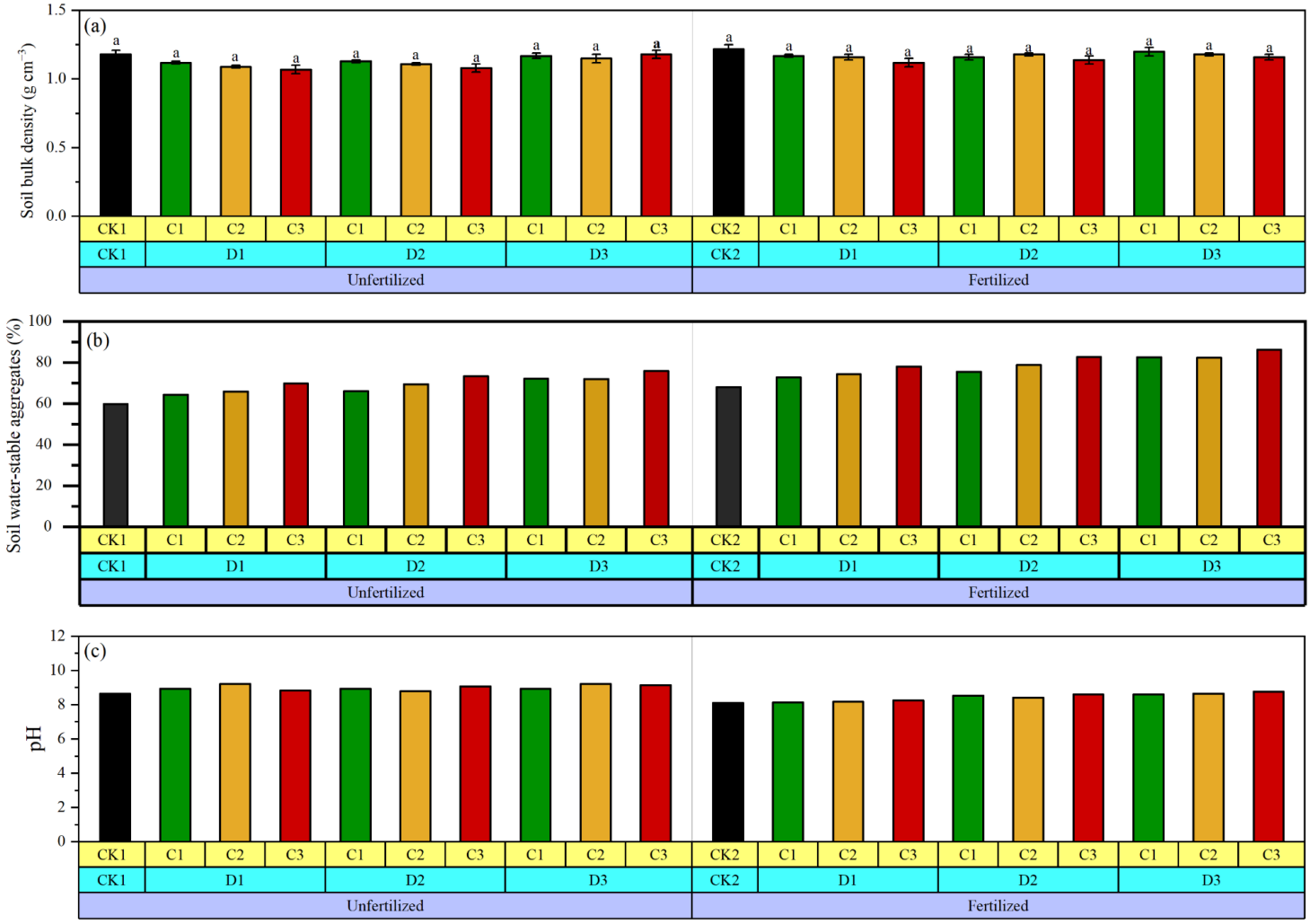


Figure 3

The effects of three particle size and concentrations of polyethylene microplastics (PE-MPs) on soil bulk density (a), soil water stable aggregates (b), and pH (c) under fertilized and unfertilized conditions. Data are means ± SD (n = 3). “CK1, CK2” represent the unfertilized and fertilized treatments without the intervention of PE-MPs, respectively. “D1, D2, D3” represent the PE-MPs treatments with particle sizes of 550 μm, 50 μm, and 6.5 μm, respectively. “C1, C2, C3” represent the concentrations of 0.5%, 1.0%, and 2.0% PE-MPs (w/w) relative to the soil weight. Different letters above the bar represent statistically significant difference among all the treatments at $P < 0.05$.

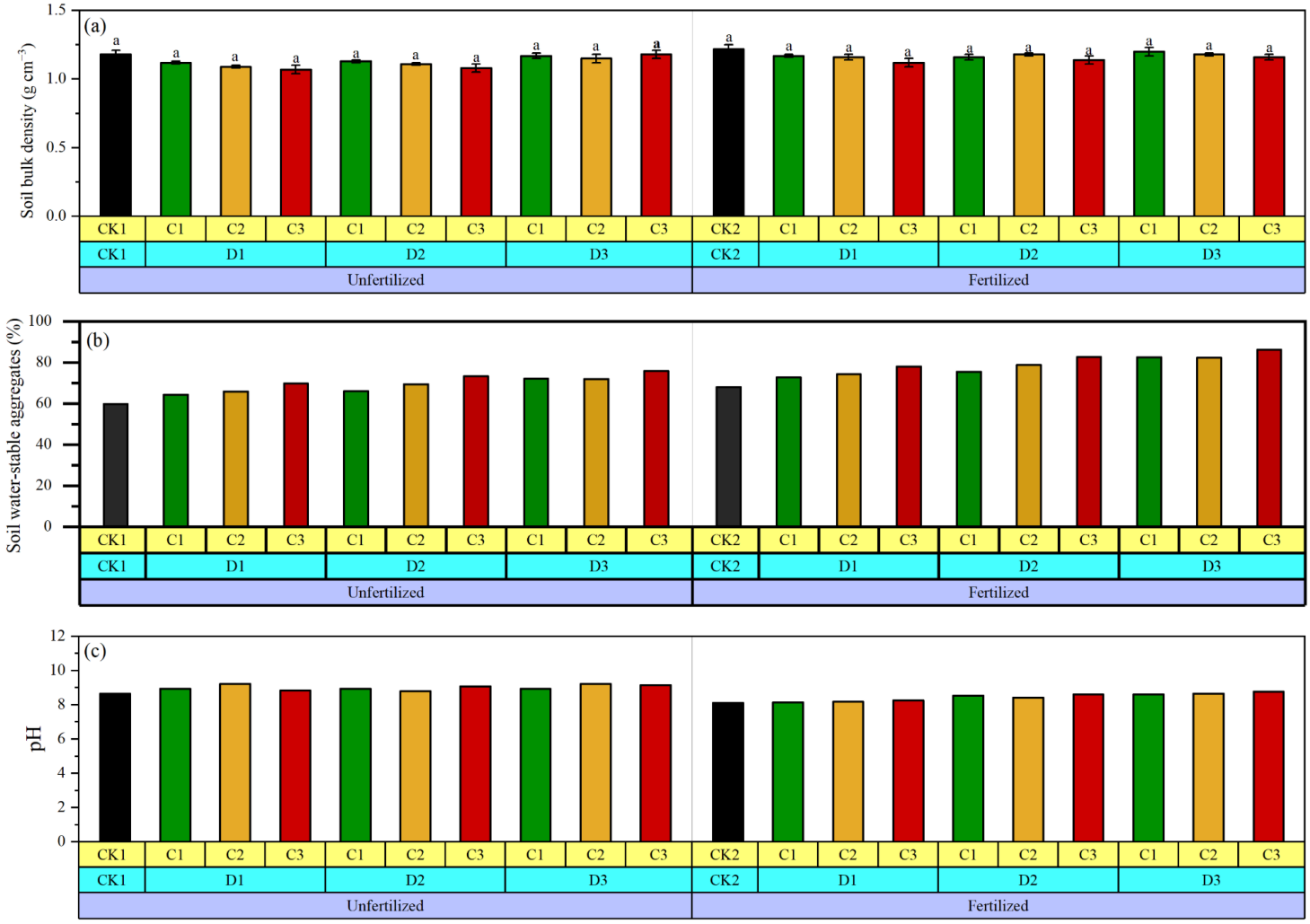


Figure 3

The effects of three particle size and concentrations of polyethylene microplastics (PE-MPs) on soil bulk density (a), soil water stable aggregates (b), and pH (c) under fertilized and unfertilized conditions. Data are means ± SD (n = 3). “CK1, CK2” represent the unfertilized and fertilized treatments without the intervention of PE-MPs, respectively. “D1, D2, D3” represent the PE-MPs treatments with particle sizes of 550 μm, 50 μm, and 6.5 μm, respectively. “C1, C2, C3” represent the concentrations of 0.5%, 1.0%, and 2.0% PE-MPs (w/w) relative to the soil weight. Different letters above the bar represent statistically significant difference among all the treatments at $P < 0.05$.

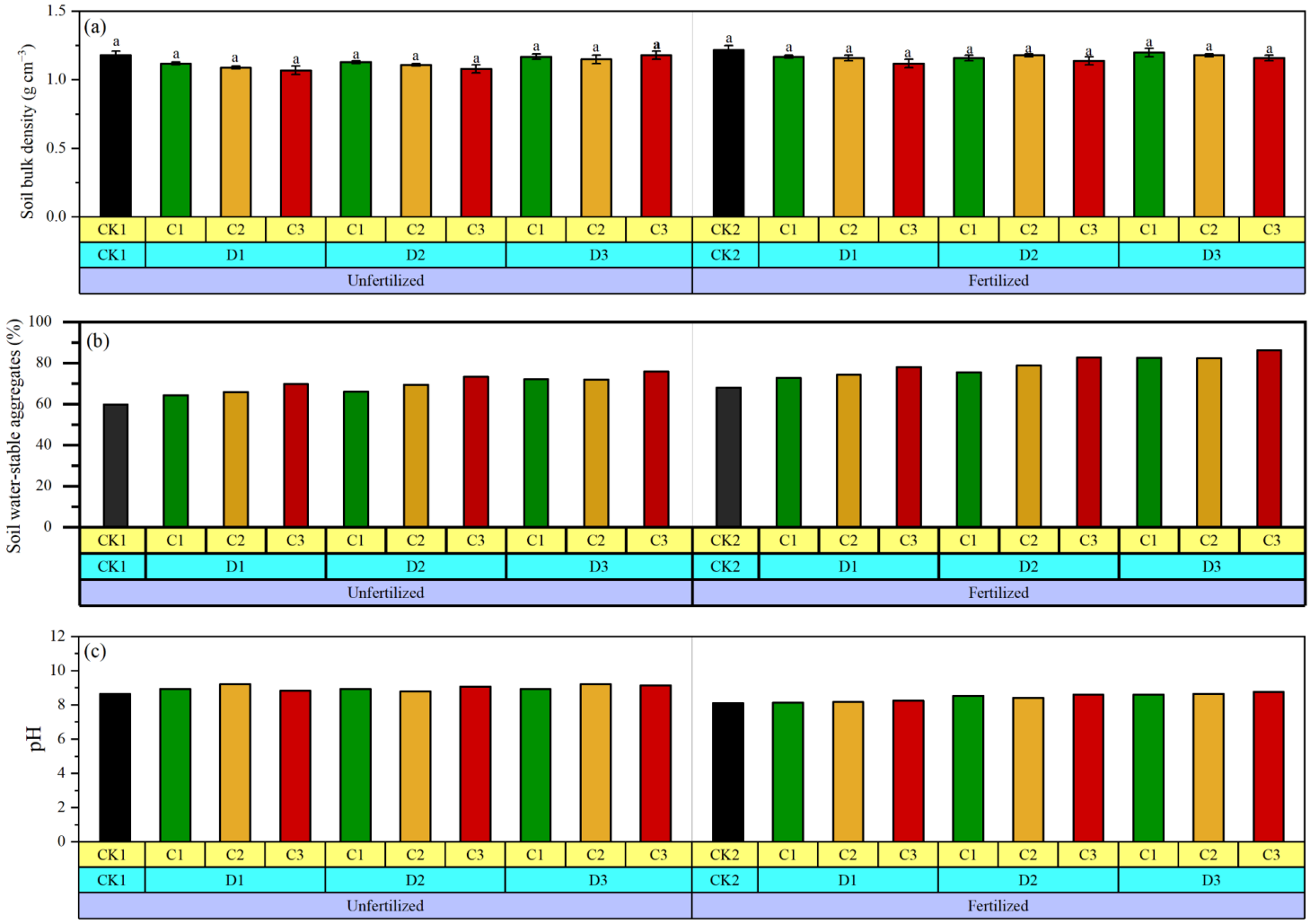


Figure 3

The effects of three particle size and concentrations of polyethylene microplastics (PE-MPs) on soil bulk density (a), soil water stable aggregates (b), and pH (c) under fertilized and unfertilized conditions. Data are means ± SD (n = 3). “CK1, CK2” represent the unfertilized and fertilized treatments without the intervention of PE-MPs, respectively. “D1, D2, D3” represent the PE-MPs treatments with particle sizes of 550 μm, 50 μm, and 6.5 μm, respectively. “C1, C2, C3” represent the concentrations of 0.5%, 1.0%, and 2.0% PE-MPs (w/w) relative to the soil weight. Different letters above the bar represent statistically significant difference among all the treatments at $P < 0.05$.

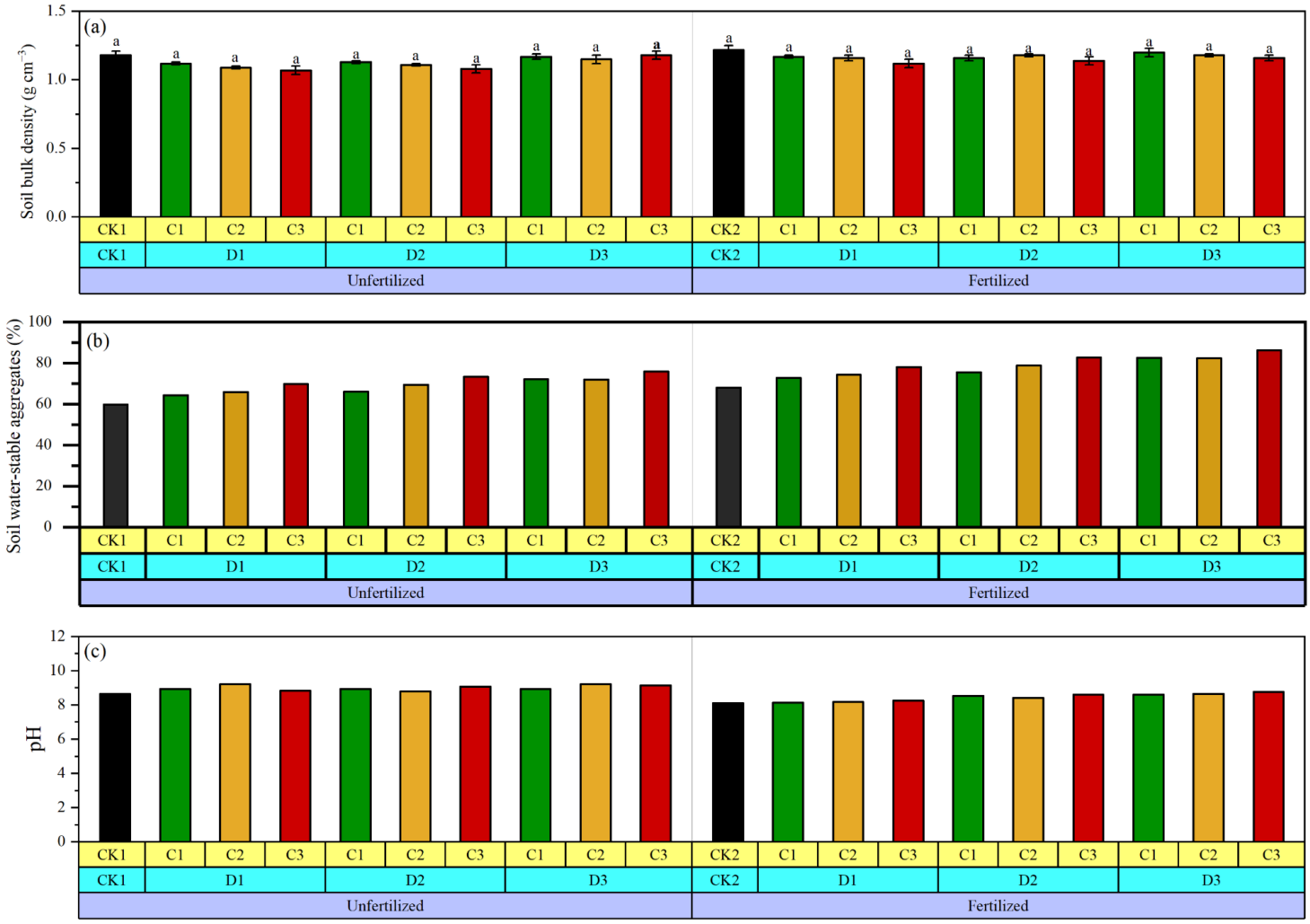


Figure 3

The effects of three particle size and concentrations of polyethylene microplastics (PE-MPs) on soil bulk density (a), soil water stable aggregates (b), and pH (c) under fertilized and unfertilized conditions. Data are means ± SD (n = 3). “CK1, CK2” represent the unfertilized and fertilized treatments without the intervention of PE-MPs, respectively. “D1, D2, D3” represent the PE-MPs treatments with particle sizes of 550 μm, 50 μm, and 6.5 μm, respectively. “C1, C2, C3” represent the concentrations of 0.5%, 1.0%, and 2.0% PE-MPs (w/w) relative to the soil weight. Different letters above the bar represent statistically significant difference among all the treatments at $P < 0.05$.

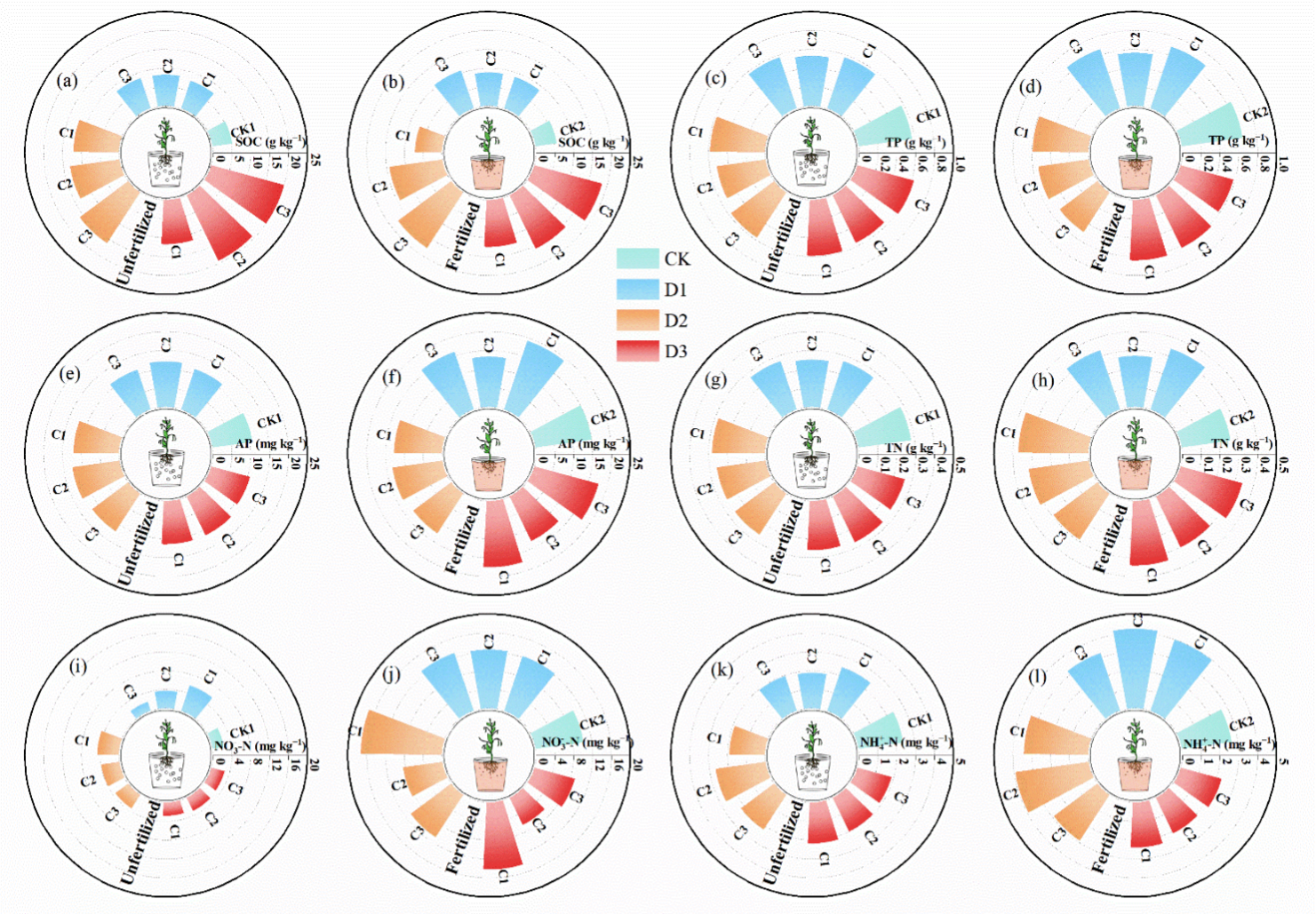


Figure 4

The effects of three particle size and concentrations of polyethylene microplastics (PE-MPs) on soil organic matter content (SOC), total phosphorus (TP), available phosphorus (AP), total nitrogen (TN), nitrate nitrogen (-N), and ammonium nitrogen (-N) under fertilized and unfertilized conditions. “CK1, CK2” represent the unfertilized and fertilized treatments without the intervention of PE-MPs, respectively. “D1, D2, D3” represent the PE-MPs treatments with particle sizes of 550 μm, 50 μm, and 6.5 μm, respectively. “C1, C2, C3” represent the concentrations of 0.5%, 1.0%, and 2.0% PE-MPs (w/w) relative to the soil weight.

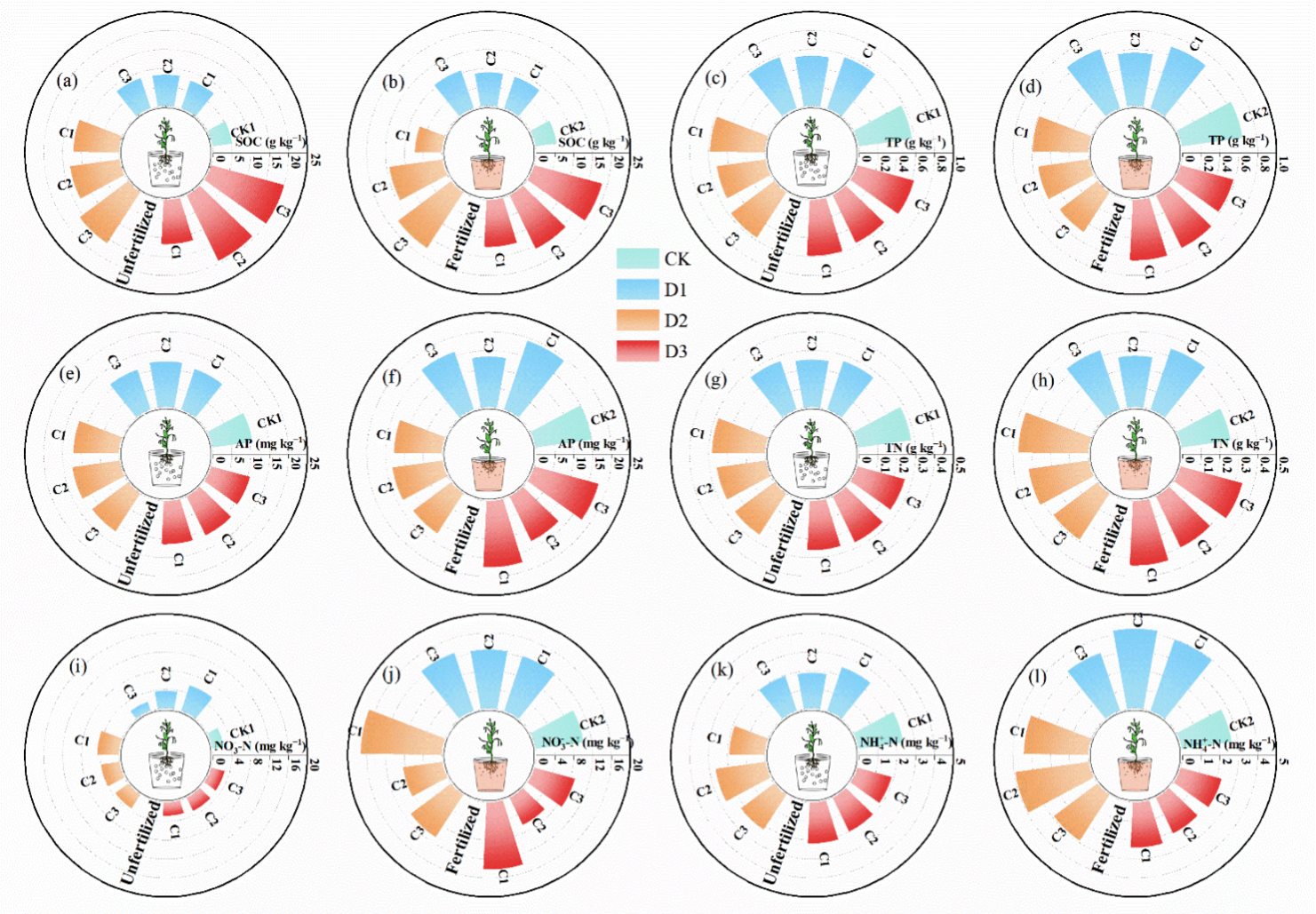


Figure 4

The effects of three particle size and concentrations of polyethylene microplastics (PE-MPs) on soil organic matter content (SOC), total phosphorus (TP), available phosphorus (AP), total nitrogen (TN), nitrate nitrogen (-N), and ammonium nitrogen (-N) under fertilized and unfertilized conditions. “CK1, CK2” represent the unfertilized and fertilized treatments without the intervention of PE-MPs, respectively. “D1, D2, D3” represent the PE-MPs treatments with particle sizes of 550 μm, 50 μm, and 6.5 μm, respectively. “C1, C2, C3” represent the concentrations of 0.5%, 1.0%, and 2.0% PE-MPs (w/w) relative to the soil weight.

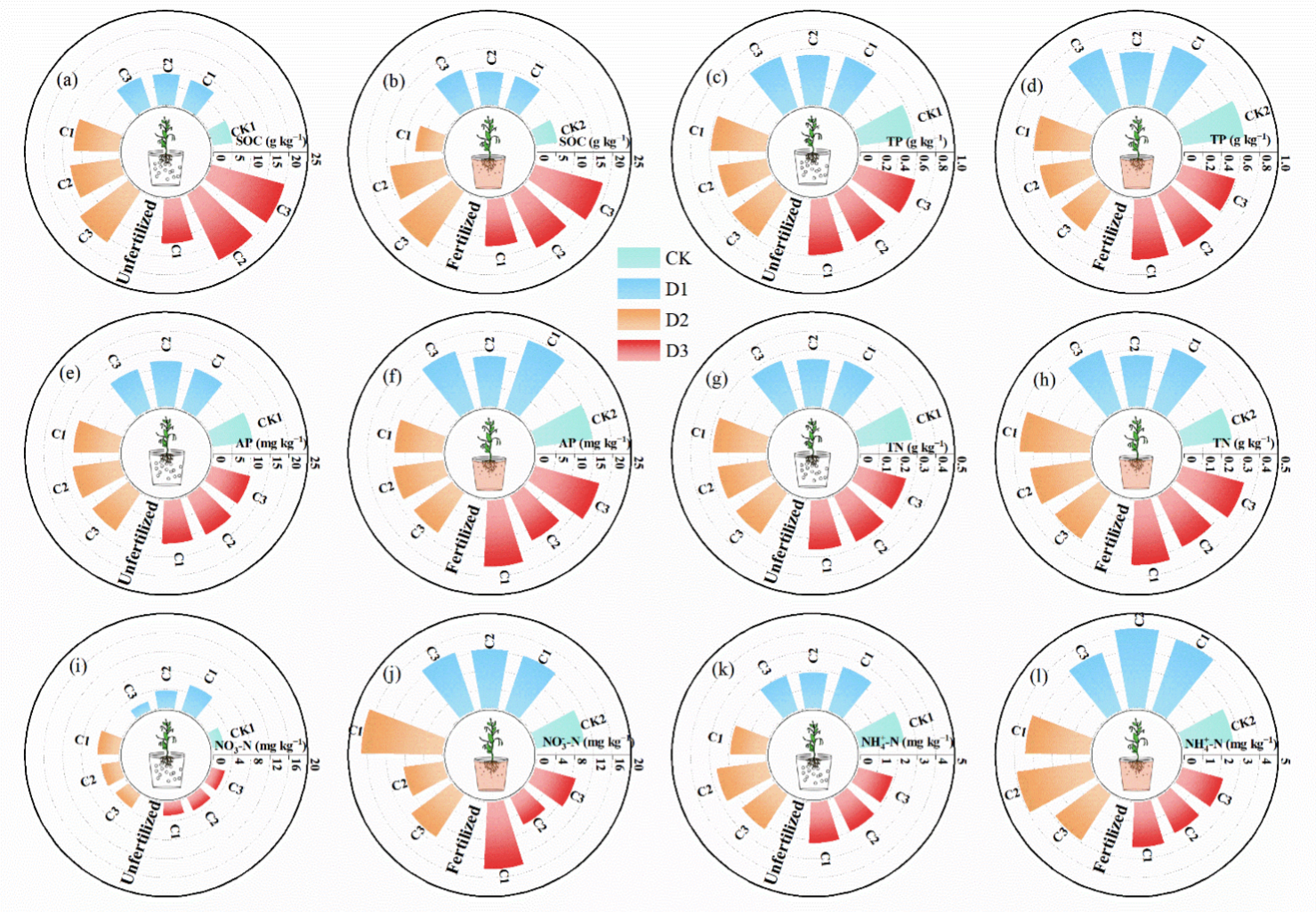


Figure 4

The effects of three particle size and concentrations of polyethylene microplastics (PE-MPs) on soil organic matter content (SOC), total phosphorus (TP), available phosphorus (AP), total nitrogen (TN), nitrate nitrogen (-N), and ammonium nitrogen (-N) under fertilized and unfertilized conditions. “CK1, CK2” represent the unfertilized and fertilized treatments without the intervention of PE-MPs, respectively. “D1, D2, D3” represent the PE-MPs treatments with particle sizes of 550 μm, 50 μm, and 6.5 μm, respectively. “C1, C2, C3” represent the concentrations of 0.5%, 1.0%, and 2.0% PE-MPs (w/w) relative to the soil weight.

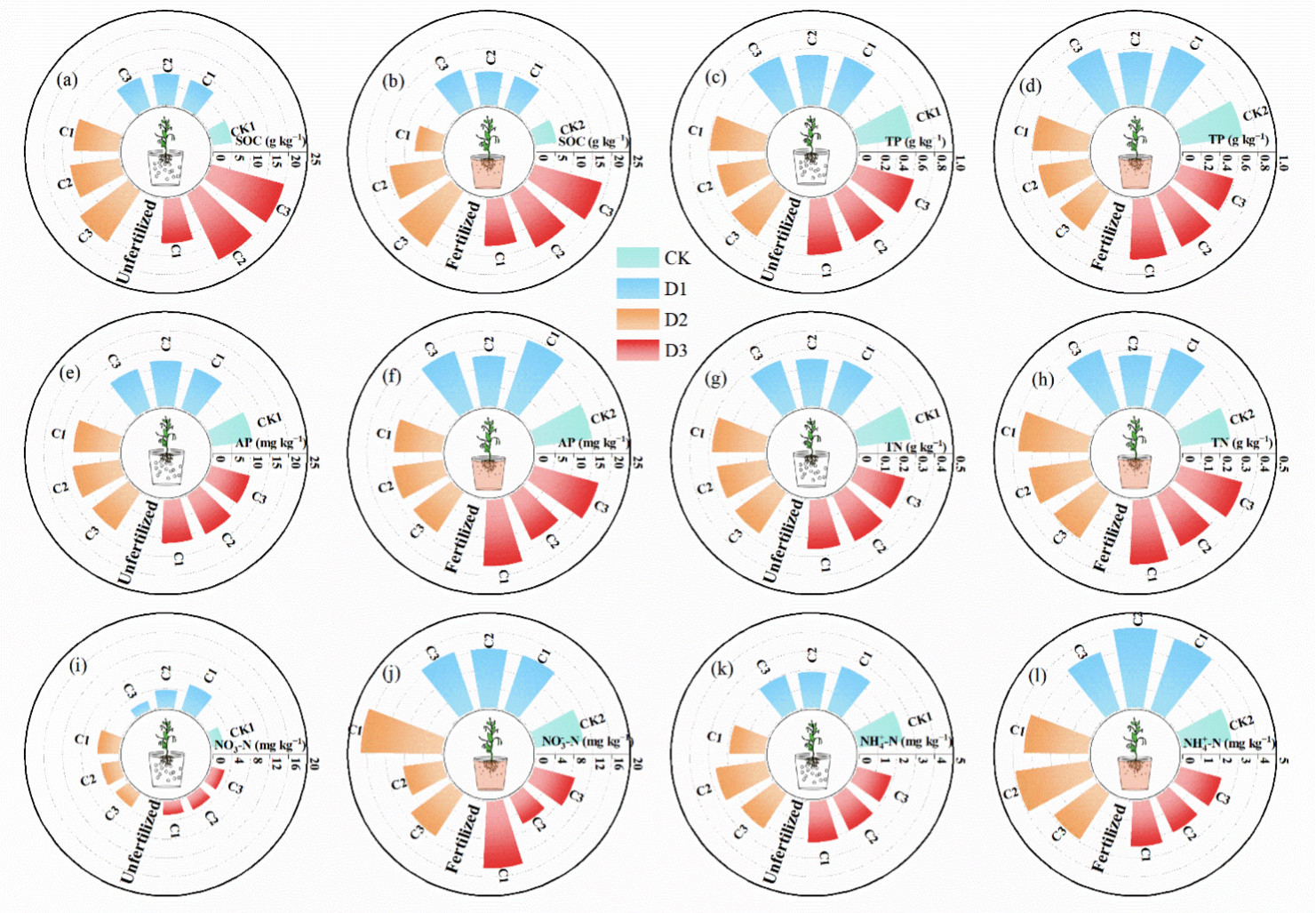


Figure 4

The effects of three particle size and concentrations of polyethylene microplastics (PE-MPs) on soil organic matter content (SOC), total phosphorus (TP), available phosphorus (AP), total nitrogen (TN), nitrate nitrogen (-N), and ammonium nitrogen (-N) under fertilized and unfertilized conditions. “CK1, CK2” represent the unfertilized and fertilized treatments without the intervention of PE-MPs, respectively. “D1, D2, D3” represent the PE-MPs treatments with particle sizes of 550 μm, 50 μm, and 6.5 μm, respectively. “C1, C2, C3” represent the concentrations of 0.5%, 1.0%, and 2.0% PE-MPs (w/w) relative to the soil weight.

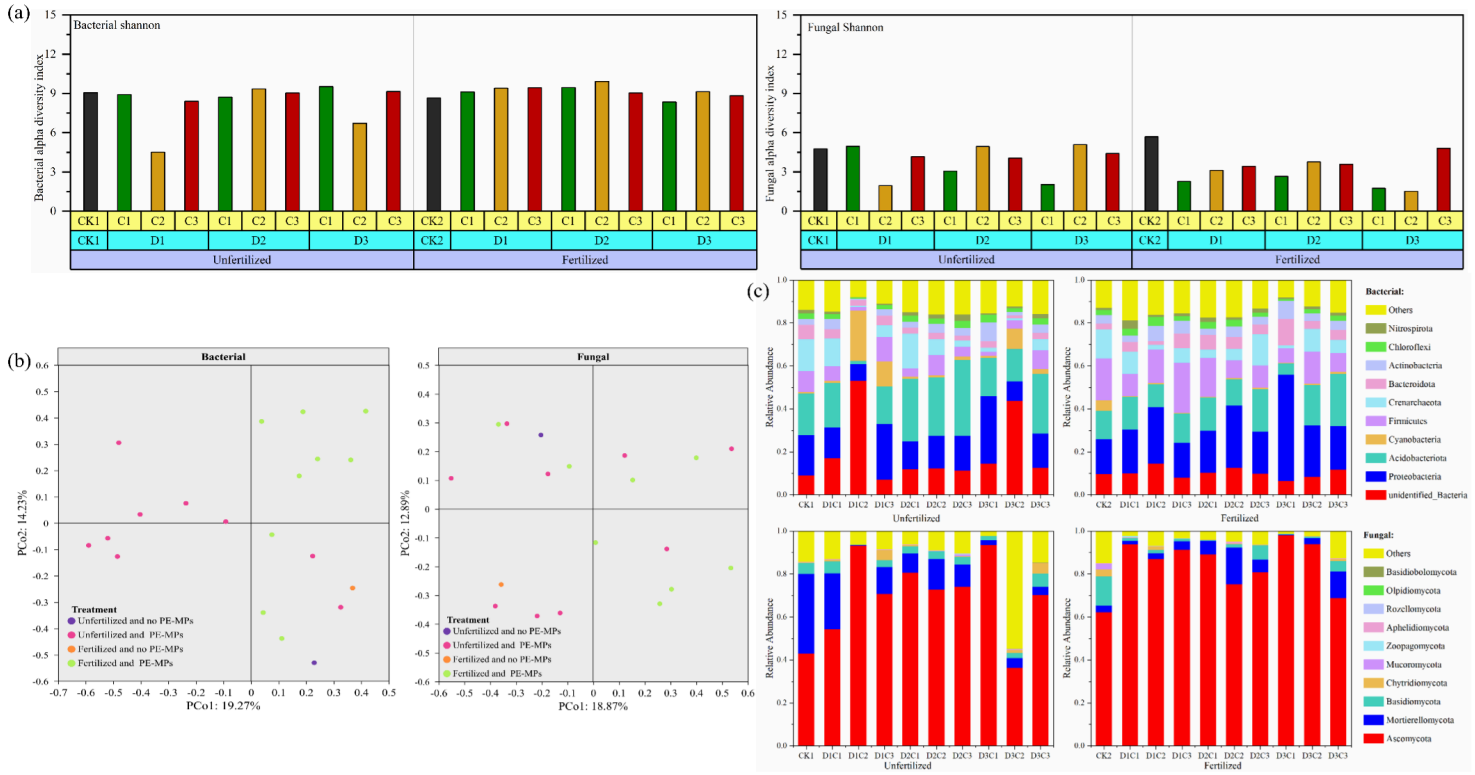


Figure 5

Differences in diversity and structure of bacterial and fungal communities in *Pisum sativum L.* rhizosphere soil with polyethylene microplastics (PE-MPs) of different particle sizes and concentrations under unfertilized and fertilized conditions. (a) Shannon index of bacterial and fungal community. (b) Principal coordinates analysis (PCoA) of bacterial and fungal communities. (c) Relative abundance of the major phyla in the bacterial and fungal community (top 10). “CK1, CK2” represent the unfertilized and fertilized treatments without the intervention of PE-MPs, respectively. “D1, D2, D3” represent the PE-MPs treatments with particle sizes of 550 μm, 50 μm, and 6.5 μm, respectively. “C1, C2, C3” represent the concentrations of 0.5%, 1.0%, and 2.0% PE-MPs (w/w) relative to the soil weight.

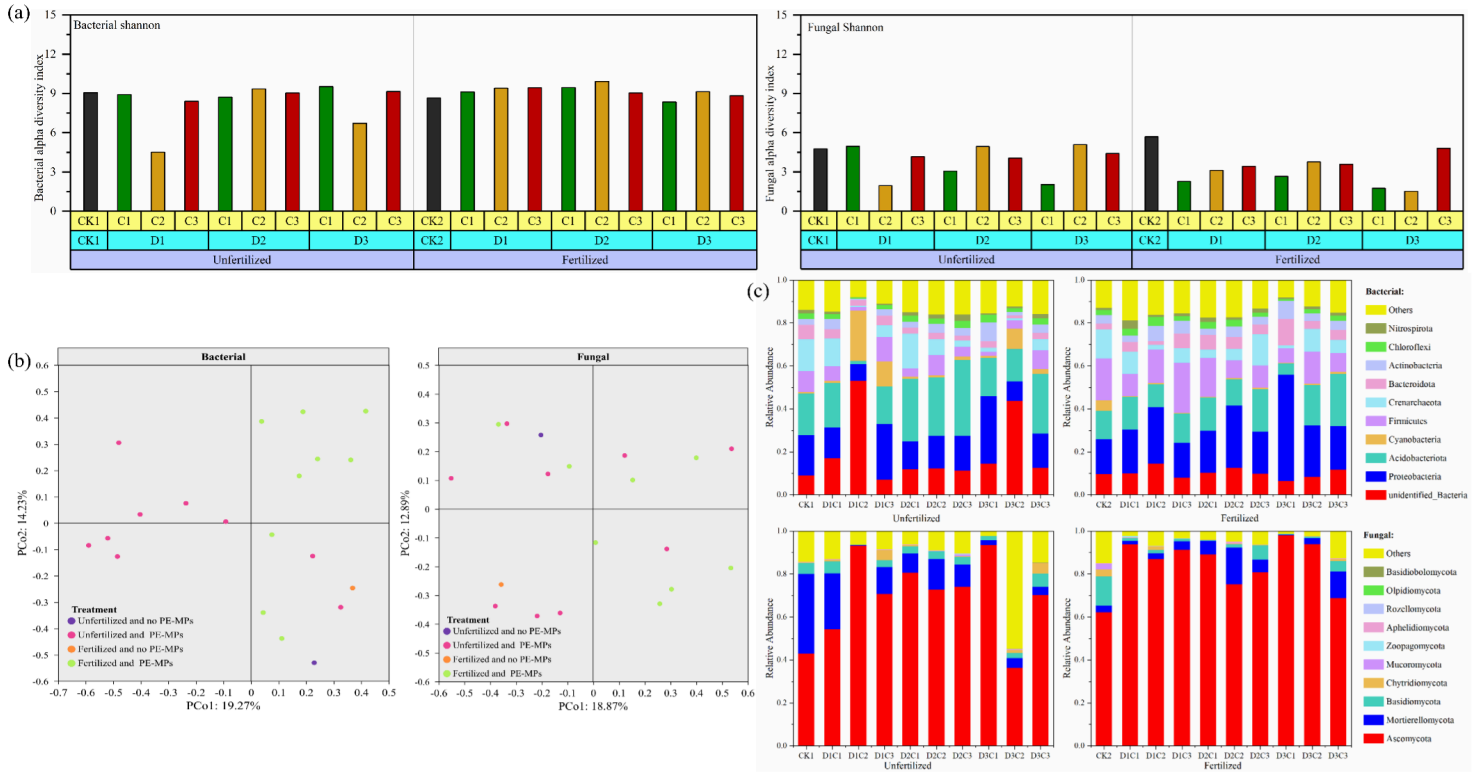


Figure 5

Differences in diversity and structure of bacterial and fungal communities in *Pisum sativum L.* rhizosphere soil with polyethylene microplastics (PE-MPs) of different particle sizes and concentrations under unfertilized and fertilized conditions. (a) Shannon index of bacterial and fungal community. (b) Principal coordinates analysis (PCoA) of bacterial and fungal communities. (c) Relative abundance of the major phyla in the bacterial and fungal community (top 10). “CK1, CK2” represent the unfertilized and fertilized treatments without the intervention of PE-MPs, respectively. “D1, D2, D3” represent the PE-MPs treatments with particle sizes of 550 μm, 50 μm, and 6.5 μm, respectively. “C1, C2, C3” represent the concentrations of 0.5%, 1.0%, and 2.0% PE-MPs (w/w) relative to the soil weight.

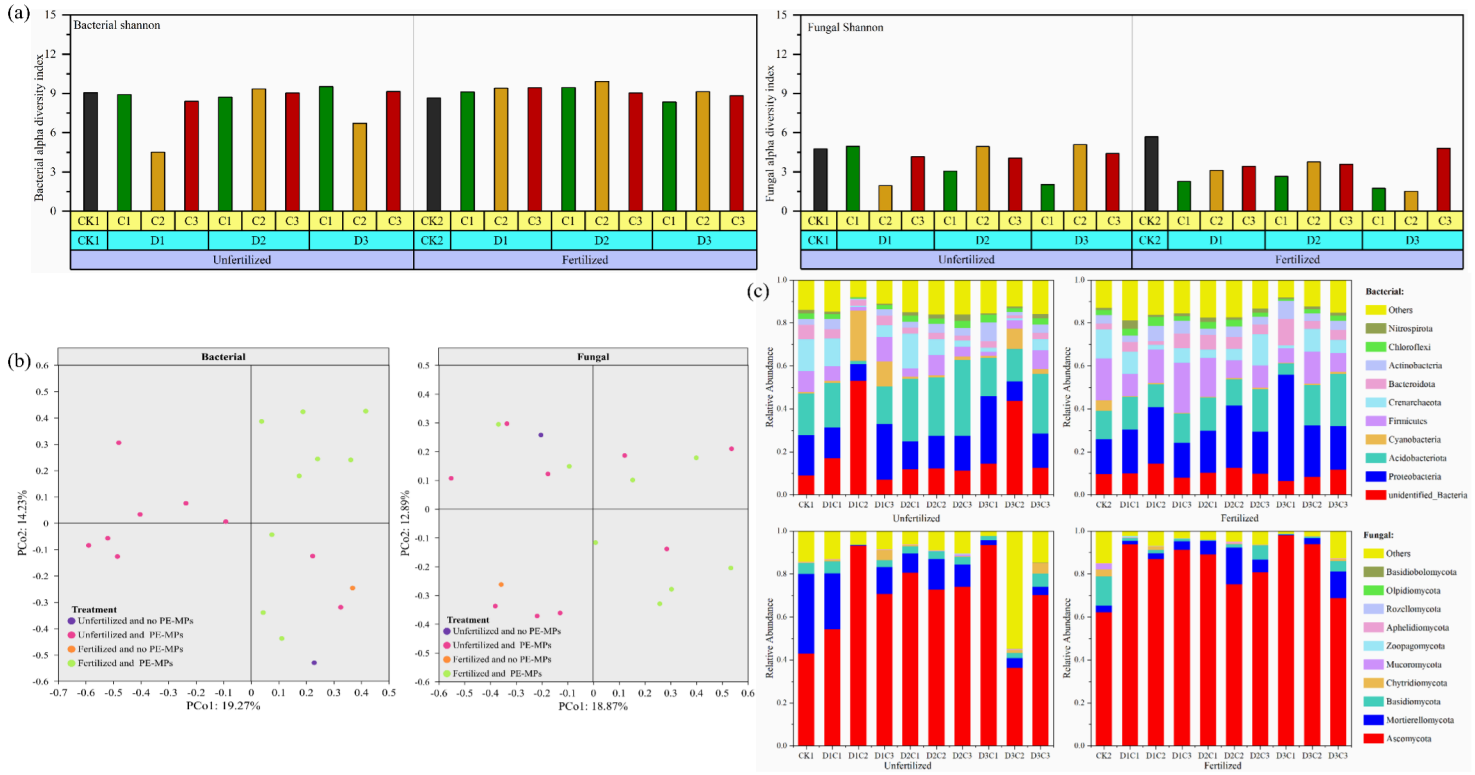


Figure 5

Differences in diversity and structure of bacterial and fungal communities in *Pisum sativum L.* rhizosphere soil with polyethylene microplastics (PE-MPs) of different particle sizes and concentrations under unfertilized and fertilized conditions. (a) Shannon index of bacterial and fungal community. (b) Principal coordinates analysis (PCoA) of bacterial and fungal communities. (c) Relative abundance of the major phyla in the bacterial and fungal community (top 10). “CK1, CK2” represent the unfertilized and fertilized treatments without the intervention of PE-MPs, respectively. “D1, D2, D3” represent the PE-MPs treatments with particle sizes of 550 μm, 50 μm, and 6.5 μm, respectively. “C1, C2, C3” represent the concentrations of 0.5%, 1.0%, and 2.0% PE-MPs (w/w) relative to the soil weight.

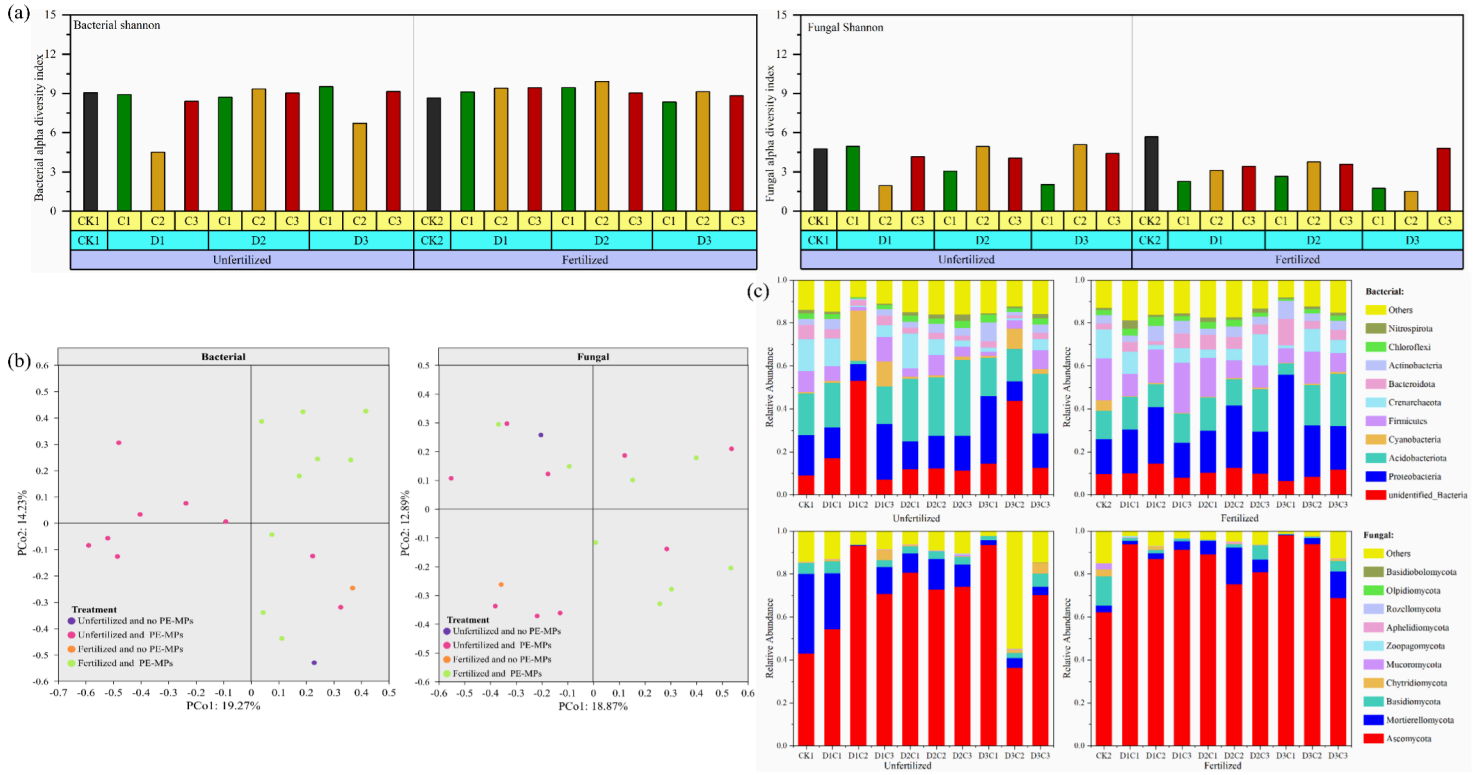


Figure 5

Differences in diversity and structure of bacterial and fungal communities in *Pisum sativum L.* rhizosphere soil with polyethylene microplastics (PE-MPs) of different particle sizes and concentrations under unfertilized and fertilized conditions. (a) Shannon index of bacterial and fungal community. (b) Principal coordinates analysis (PCoA) of bacterial and fungal communities. (c) Relative abundance of the major phyla in the bacterial and fungal community (top 10). “CK1, CK2” represent the unfertilized and fertilized treatments without the intervention of PE-MPs, respectively. “D1, D2, D3” represent the PE-MPs treatments with particle sizes of 550 μm, 50 μm, and 6.5 μm, respectively. “C1, C2, C3” represent the concentrations of 0.5%, 1.0%, and 2.0% PE-MPs (w/w) relative to the soil weight.

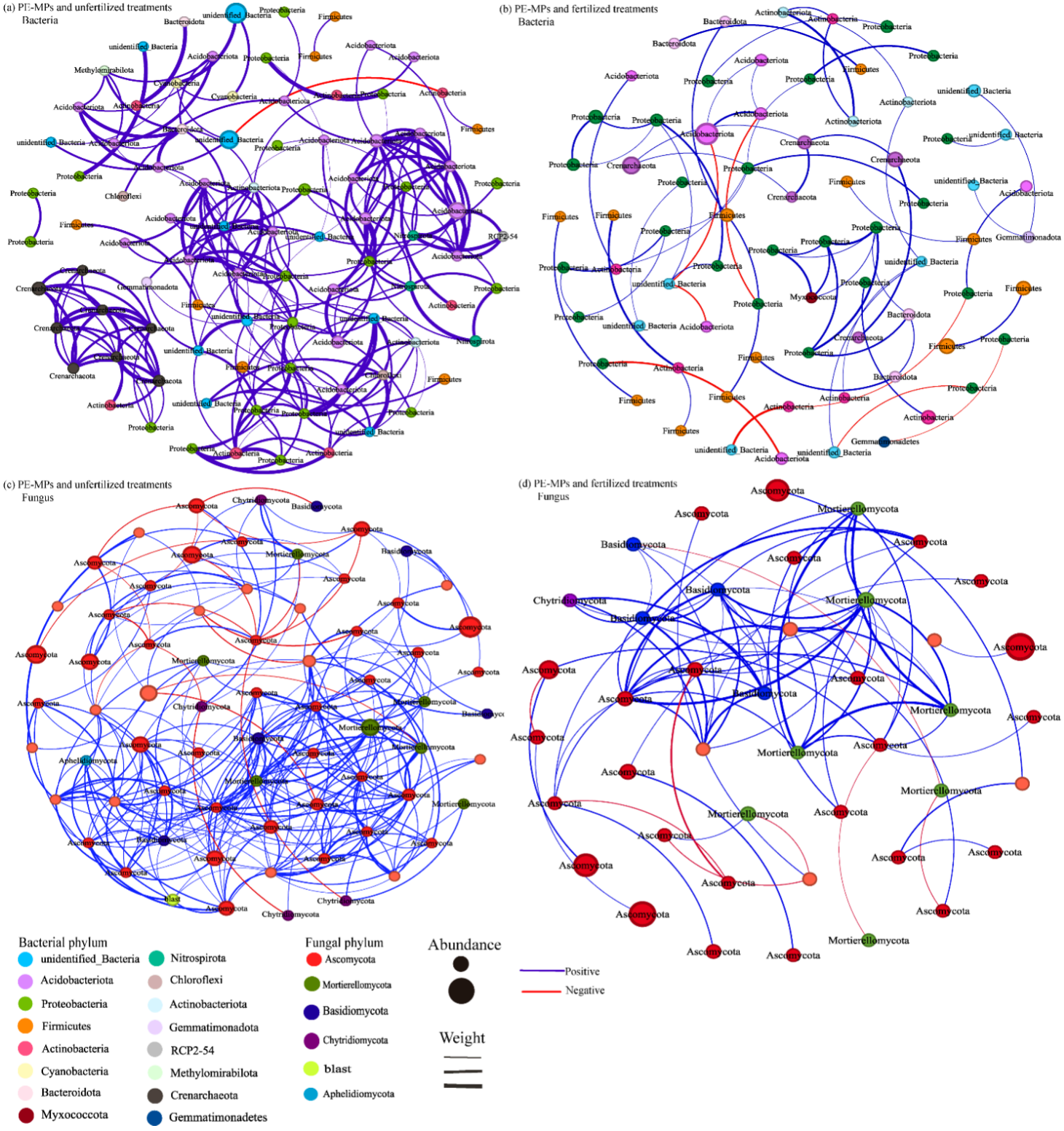


Figure 6

Co-occurrence networks of bacteria (a and b) and fungus (c and d) communities. Each node size indicates the relative abundance of OTUs in bacteria and fungus communities in the treatments. A red edge indicates a negative relationship, while a blue edge indicates a positive relationship between two individual nodes.

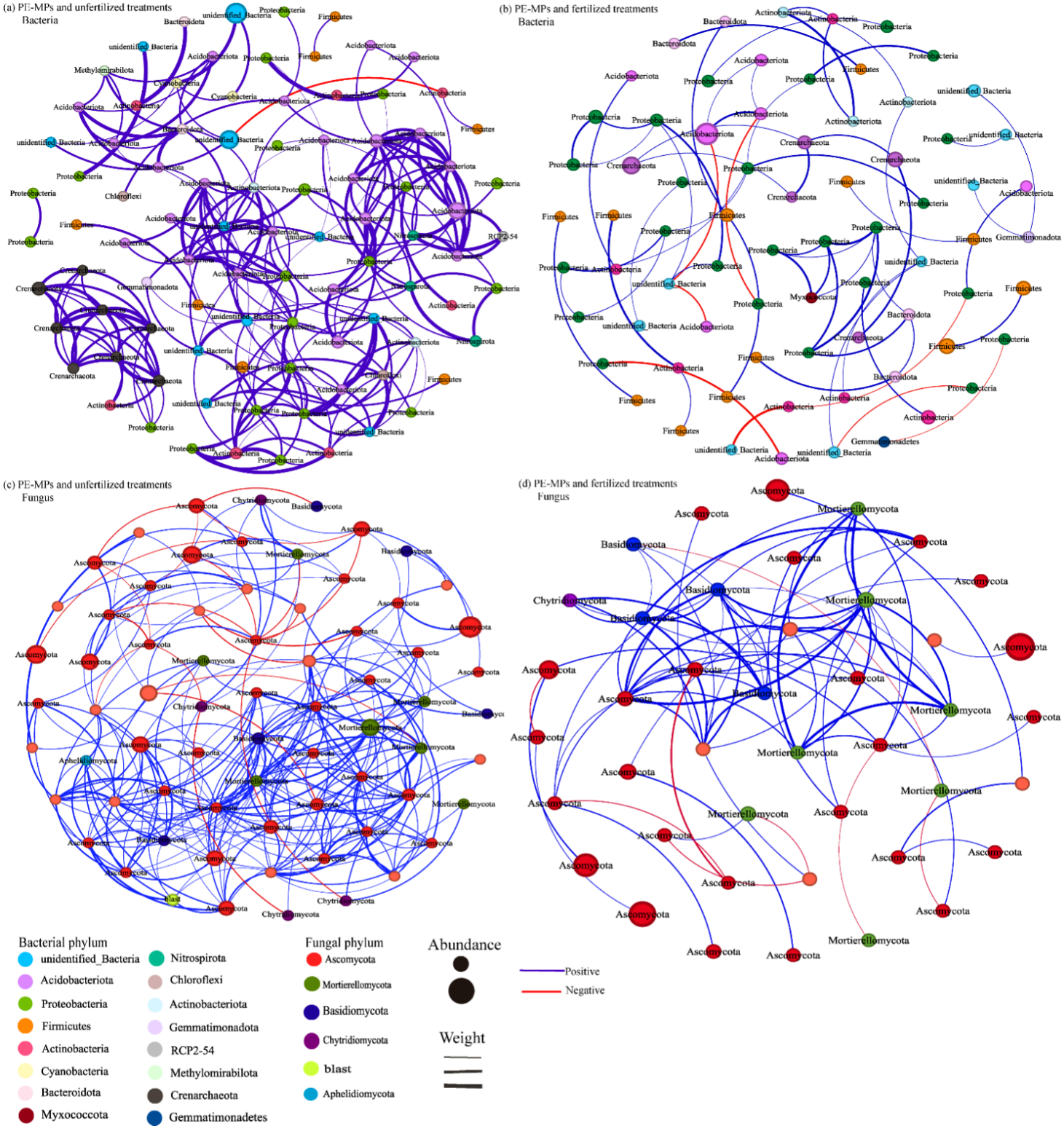


Figure 6

Co-occurrence networks of bacteria (a and b) and fungus (c and d) communities. Each node size indicates the relative abundance of OTUs in bacteria and fungus communities in the treatments. A red edge indicates a negative relationship, while a blue edge indicates a positive relationship between two individual nodes.

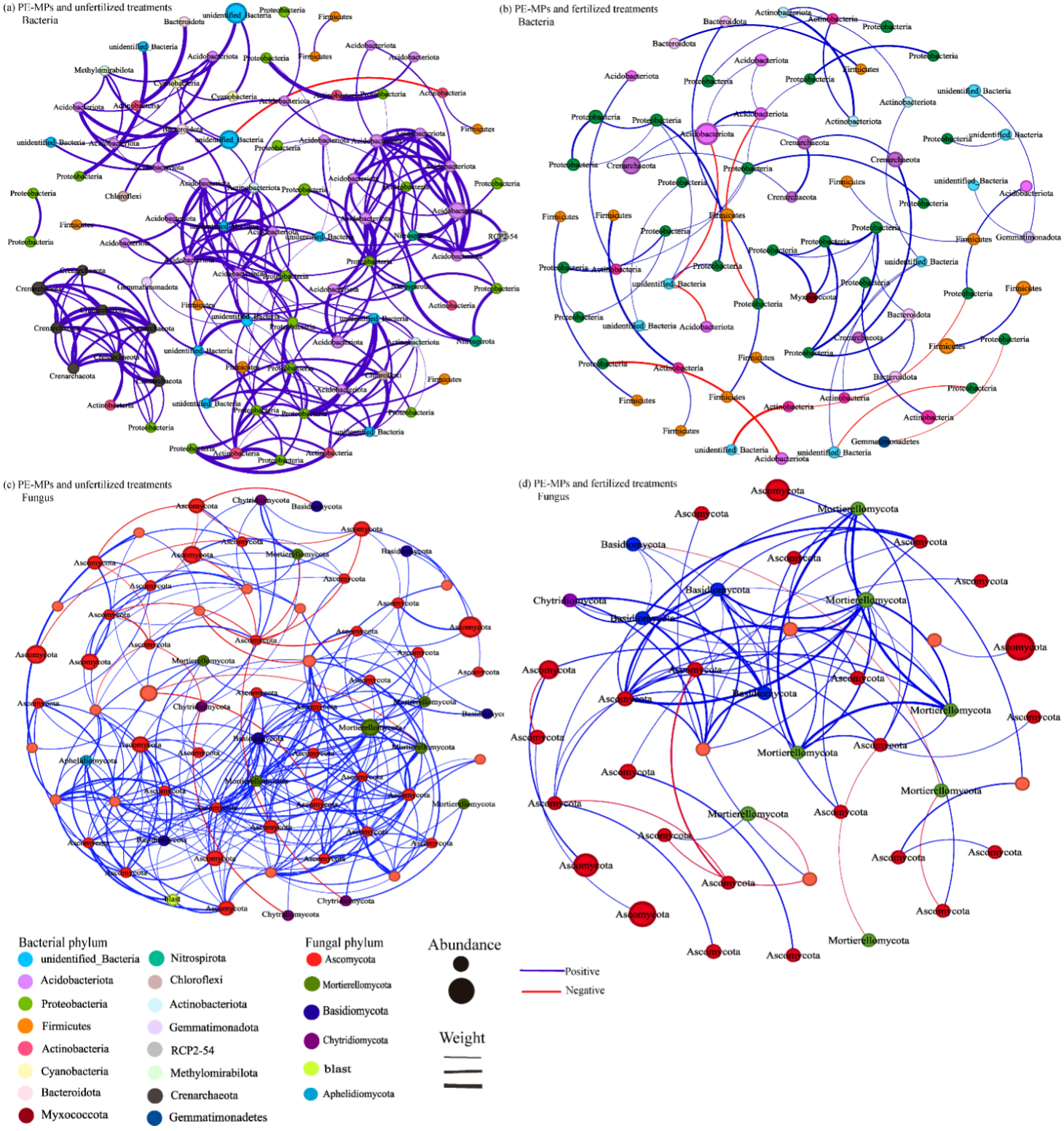


Figure 6

Co-occurrence networks of bacteria (a and b) and fungus (c and d) communities. Each node size indicates the relative abundance of OTUs in bacteria and fungus communities in the treatments. A red edge indicates a negative relationship, while a blue edge indicates a positive relationship between two individual nodes.

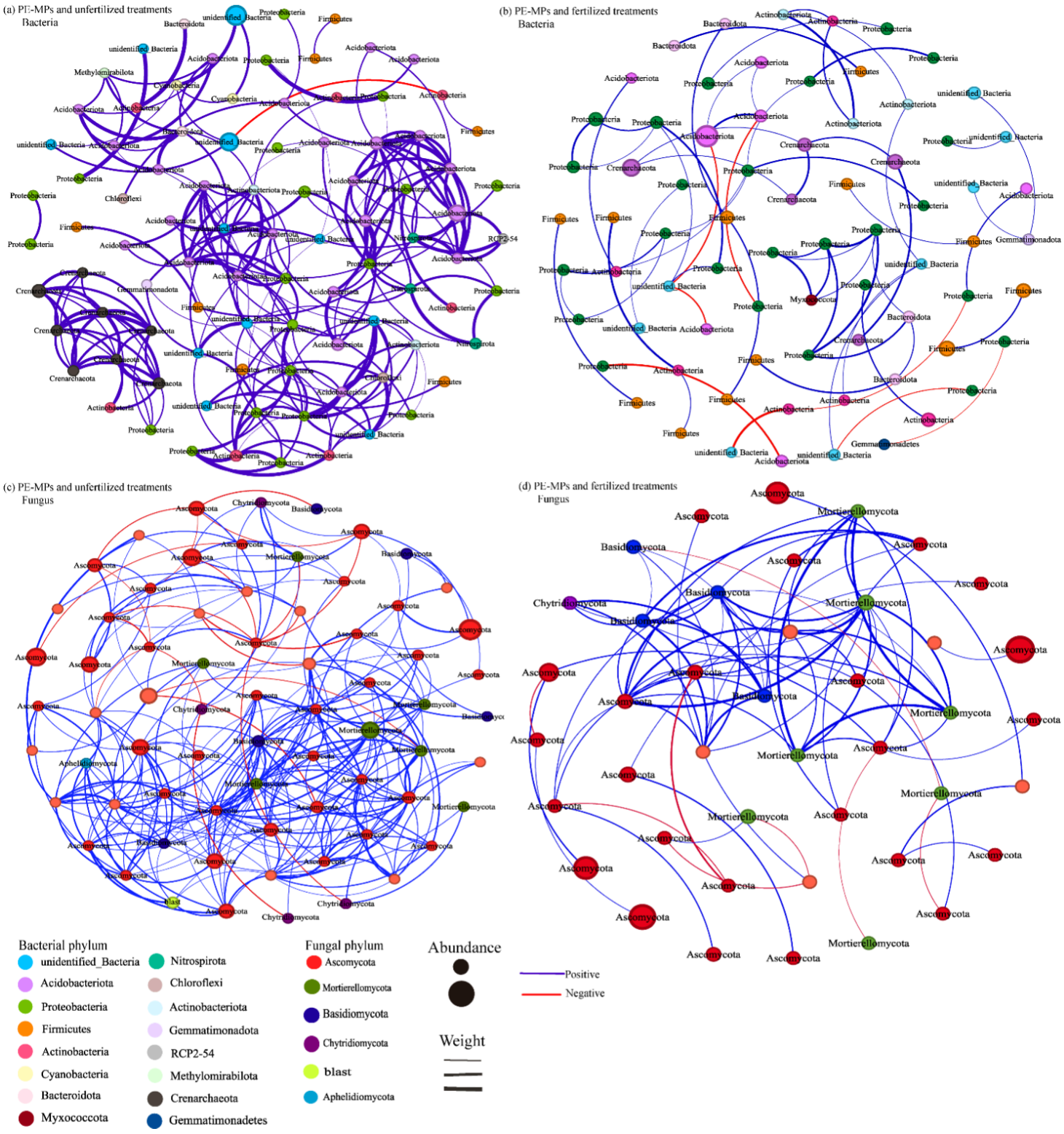


Figure 6

Co-occurrence networks of bacteria (a and b) and fungus (c and d) communities. Each node size indicates the relative abundance of OTUs in bacteria and fungus communities in the treatments. A red edge indicates a negative relationship, while a blue edge indicates a positive relationship between two individual nodes.

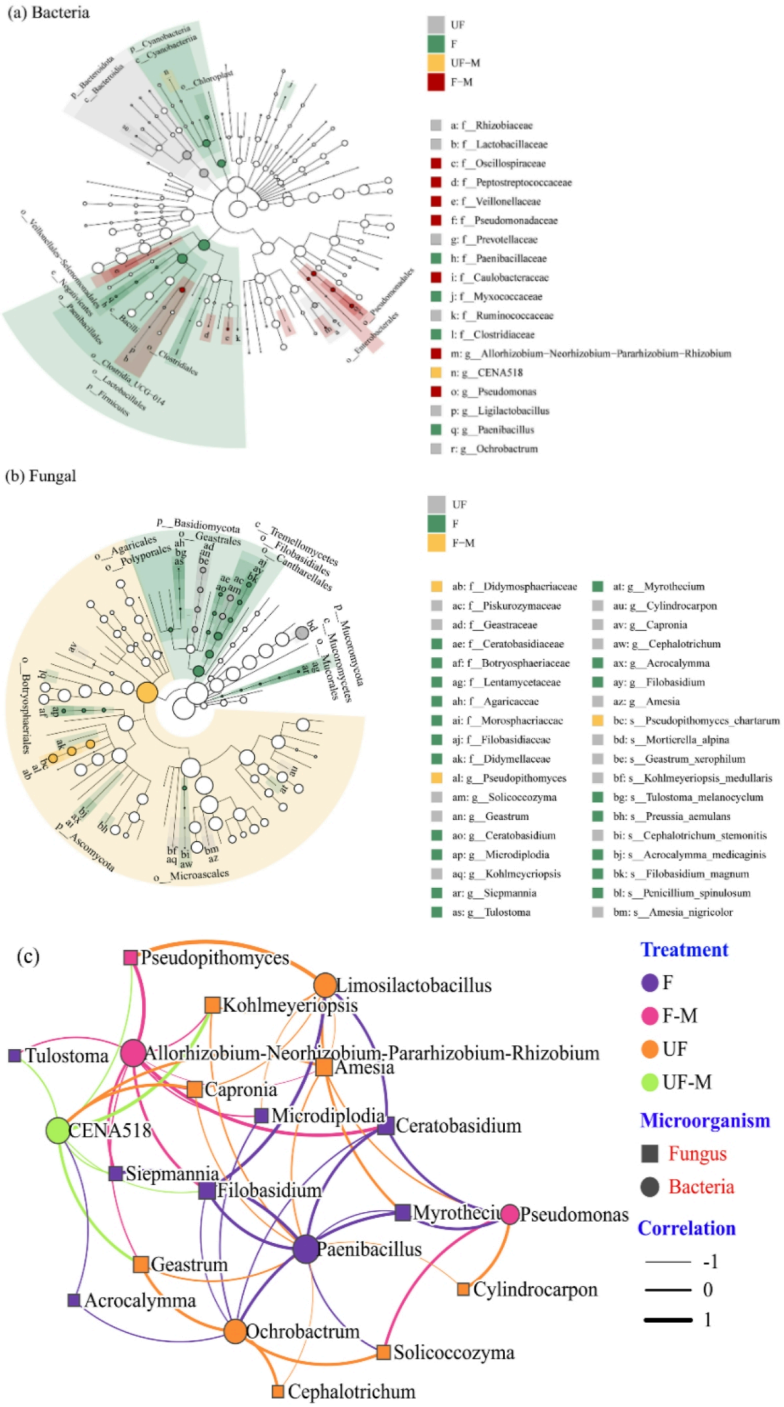


Figure 7

Bacterial and fungal biomarkers in three particle size and concentrations of polyethylene microplastics (PE-MPs), unfertilized and fertilized conditions in *Pisum sativum L.* rhizosphere soil and their correlation networks. (a) and (b) represents the linear discriminant analysis effect size (Lefse) analysis showing the significantly different bacterial and fungal taxa (biomarkers) among the different fertilized and PE-MPs treatment (LDA > 3 and $p < 0.05$). (c) represents the correlation networks of biomarkers in PE-MPs, unfertilized and fertilized conditions rhizospheres. “UF” represents the

unfertilized treatment. “F” represents the fertilized treatments. “UF-M” represents the PE-MPs and unfertilized treatments. “F-M” represents the PE-MPs and fertilized treatments.

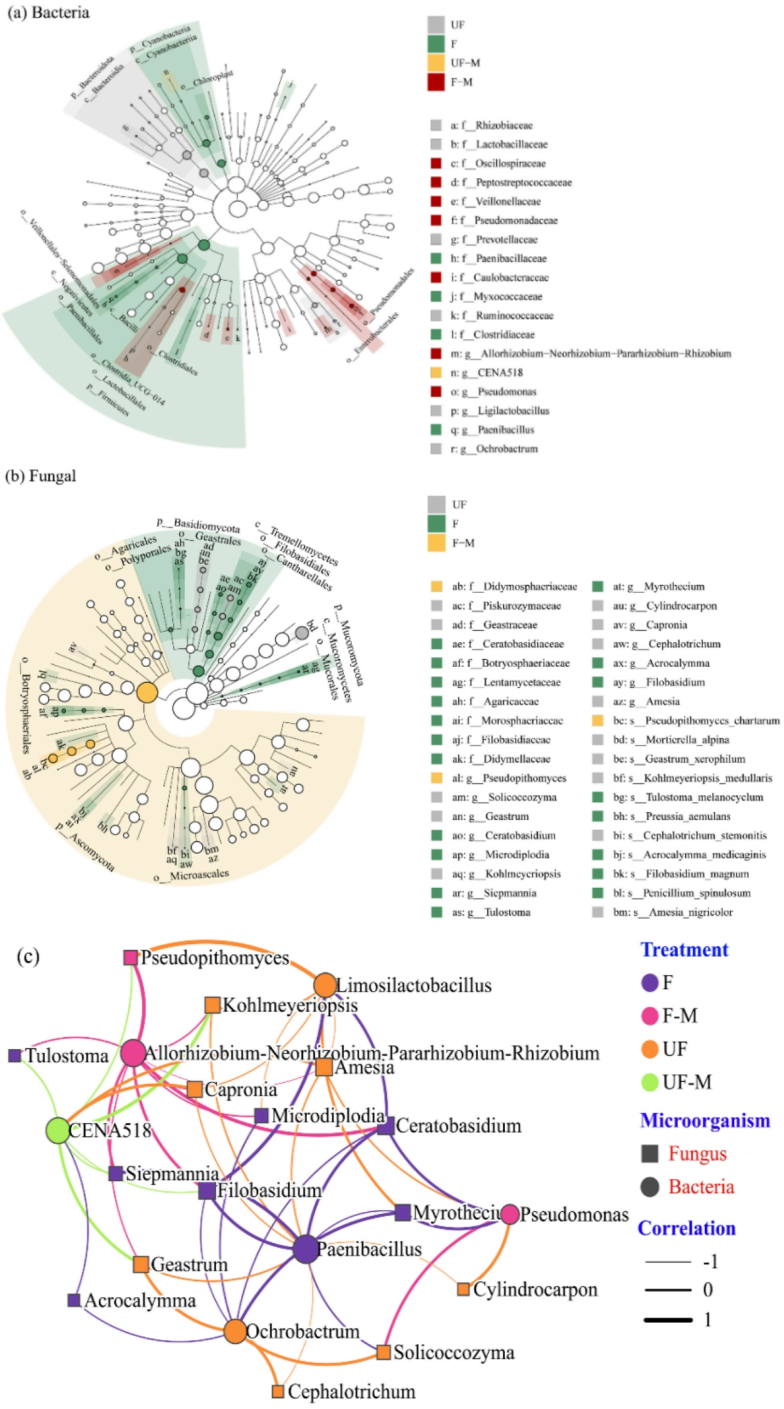


Figure 7

Bacterial and fungal biomarkers in three particle size and concentrations of polyethylene microplastics (PE-MPs), unfertilized and fertilized conditions in *Pisum sativum L.* rhizosphere soil and their correlation networks. (a) and (b) represents the linear discriminant analysis effect size (Lefse) analysis showing the significantly different bacterial and

fungal taxa (biomarkers) among the different fertilized and PE-MPs treatment (LDA > 3 and $p < 0.05$). (c) represents the correlation networks of biomarkers in PE-MPs, unfertilized and fertilized conditions rhizospheres. “UF” represents the unfertilized treatment. “F” represents the fertilized treatments. “UF-M” represents the PE-MPs and unfertilized treatments. “F-M” represents the PE-MPs and fertilized treatments.

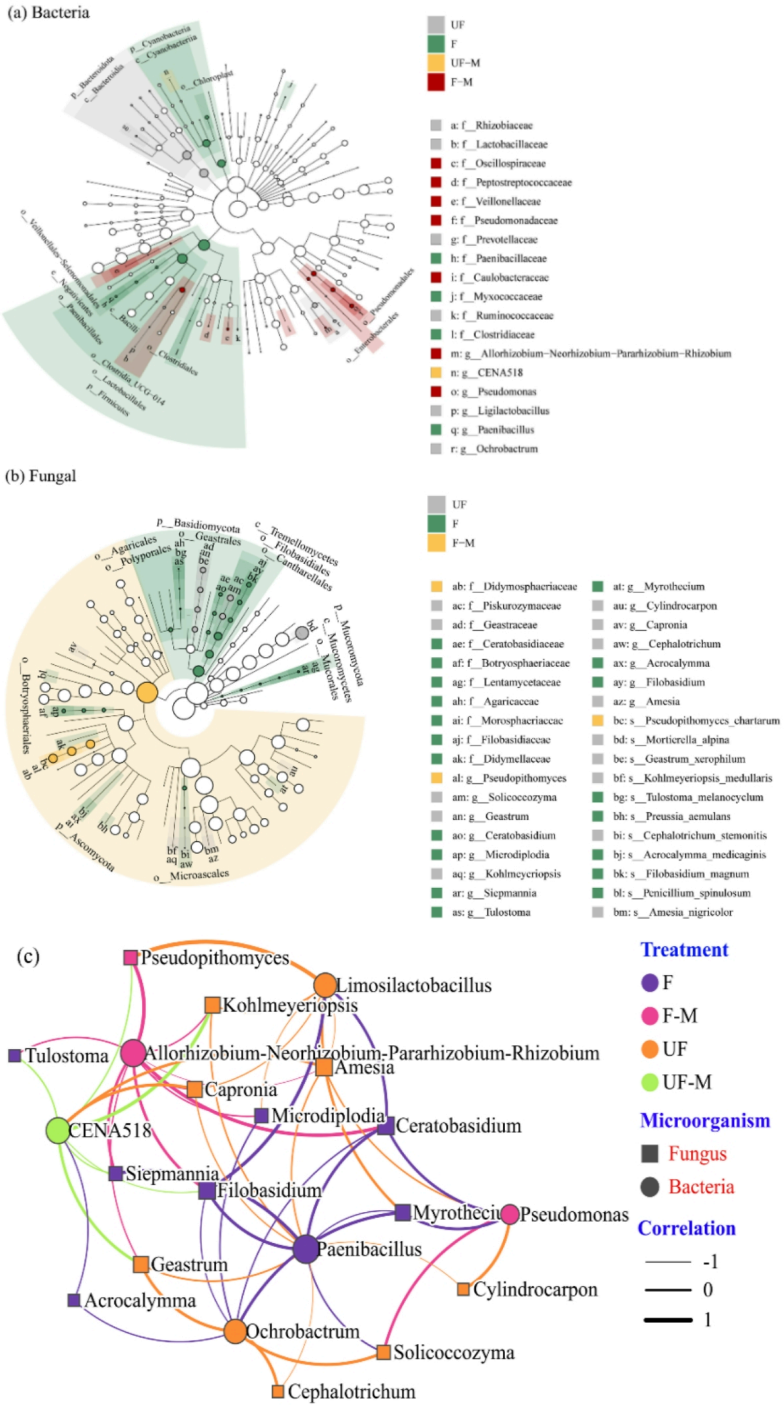


Figure 7

Bacterial and fungal biomarkers in three particle size and concentrations of polyethylene microplastics (PE-MPs), unfertilized and fertilized conditions in *Pisum sativum L.* rhizosphere soil and their correlation networks. (a) and (b) represents the linear discriminant analysis effect size (Lefse) analysis showing the significantly different bacterial and fungal taxa (biomarkers) among the different fertilized and PE-MPs treatment (LDA > 3 and $p < 0.05$). (c) represents the correlation networks of biomarkers in PE-MPs, unfertilized and fertilized conditions rhizospheres. “UF” represents the unfertilized treatment. “F” represents the fertilized treatments. “UF-M” represents the PE-MPs and unfertilized treatments. “F-M” represents the PE-MPs and fertilized treatments.

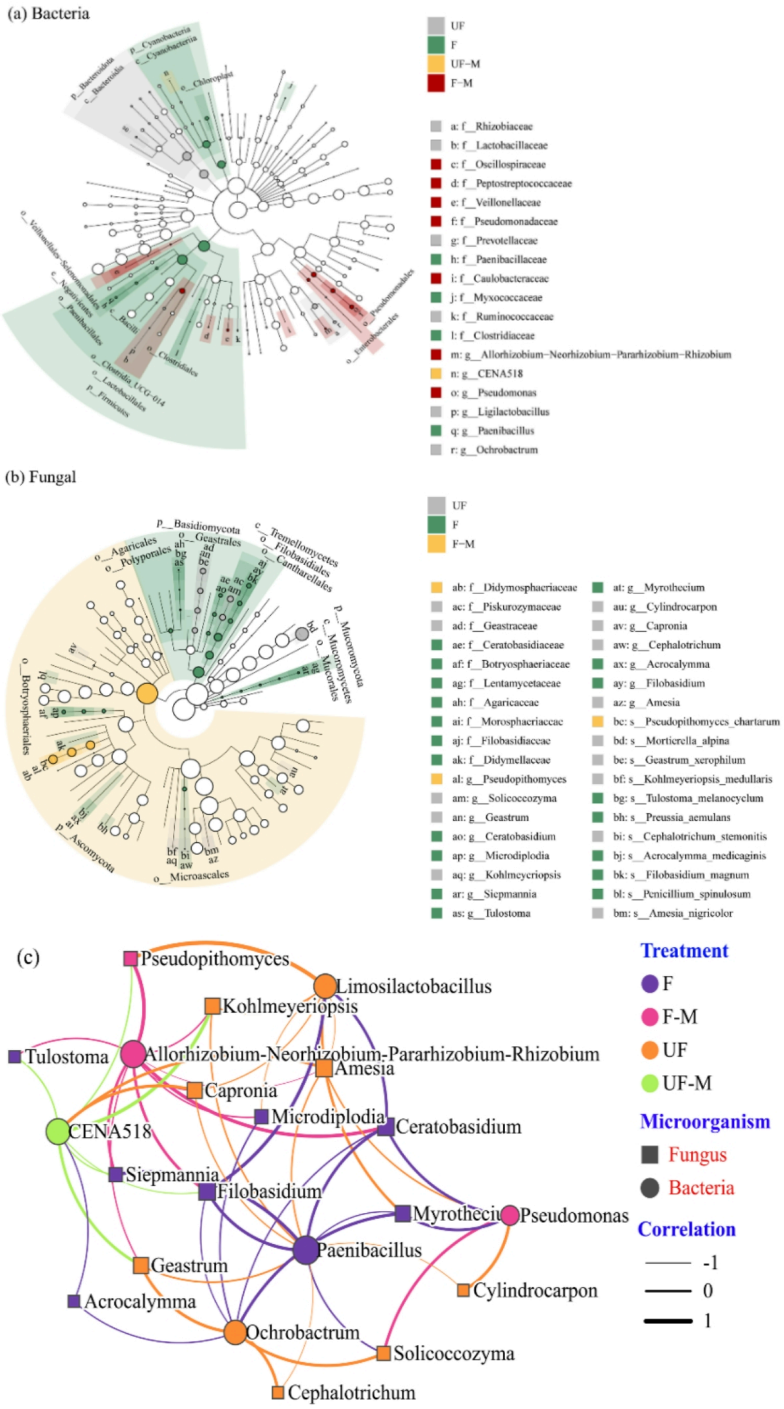


Figure 7

Bacterial and fungal biomarkers in three particle size and concentrations of polyethylene microplastics (PE-MPs), unfertilized and fertilized conditions in *Pisum sativum L.* rhizosphere soil and their correlation networks. (a) and (b) represents the linear discriminant analysis effect size (Lefse) analysis showing the significantly different bacterial and fungal taxa (biomarkers) among the different fertilized and PE-MPs treatment (LDA > 3 and $p < 0.05$). (c) represents the correlation networks of biomarkers in PE-MPs, unfertilized and fertilized conditions rhizospheres. “UF” represents the unfertilized treatment. “F” represents the fertilized treatments. “UF-M” represents the PE-MPs and unfertilized treatments. “F-M” represents the PE-MPs and fertilized treatments.

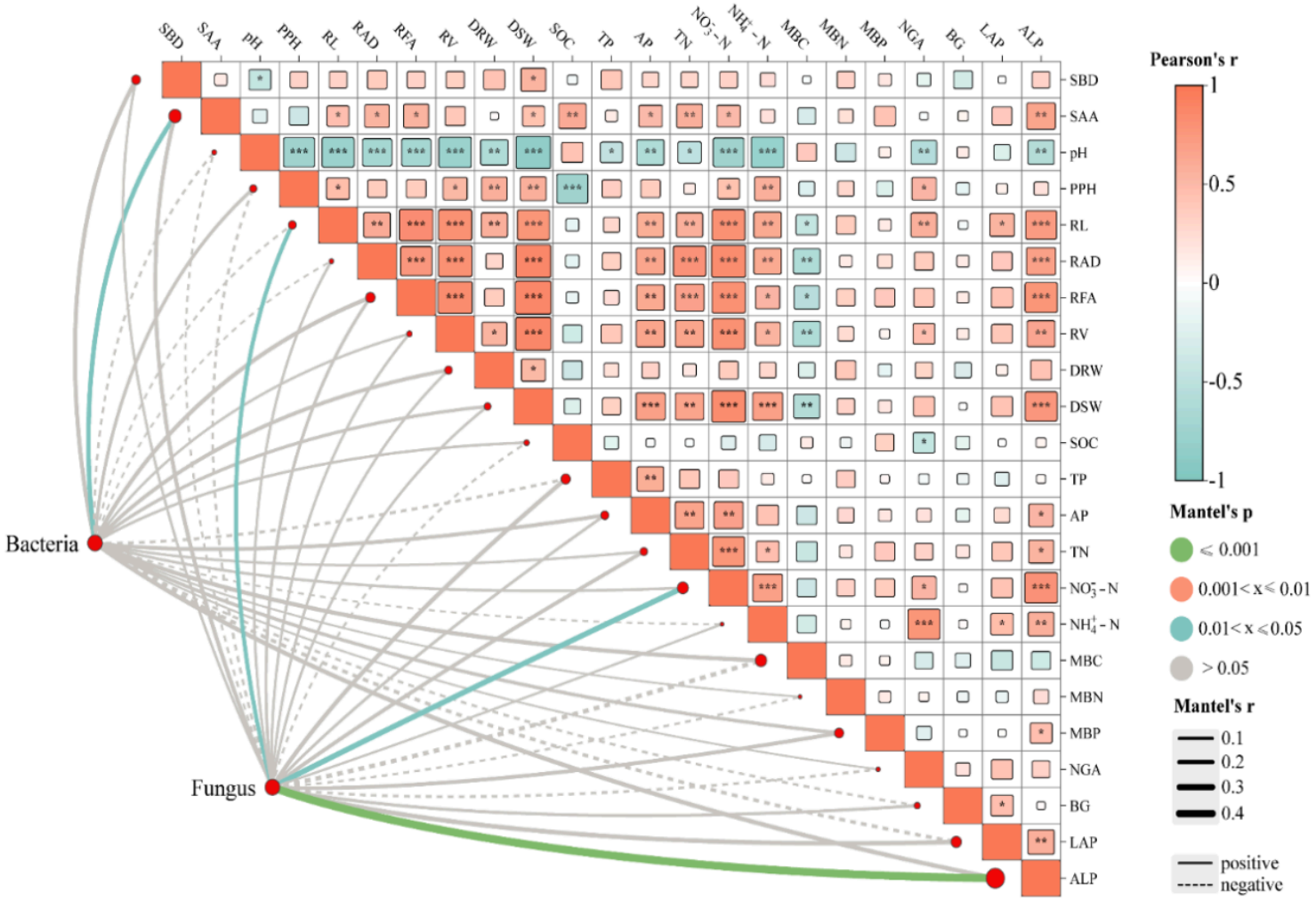


Figure 8

Pairwise comparisons of soil physicochemical properties, microbial biomass, enzyme activity, and *Pisum sativum L.* growth indicators were shown in the lower left corner, with a color gradient denoting Pearson’s correlation coefficient. Bacterial and fungal biomarkers were related to soil physicochemical properties, microbial biomass, enzyme activity, and *Pisum sativum L.* growth indexes by Mantel test. Edge color denotes the statistical significance and edge width corresponds to the Mantel’s r statistic for the corresponding distance correlations. (*: $p < 0.05$, **: $p < 0.01$, ***: $p < 0.001$). The SBD, SAA, and pH represent soil bulk density, water-stable aggregate content and pH value, respectively. The SOC, TP, TN, NO_3^-, and NH_4^+ represent soil organic matter content, total phosphorus, available phosphorus, total nitrogen, nitrate nitrogen, and ammonium nitrogen, respectively. The MBC, MBN, and MBP represent microbial biomass carbon, nitrogen, and phosphorus, respectively. The PPH, RL, RAD, RFA, RV, DRW, and DSW represent lant height, root

length, root average diameter, root surface area, root volume, aboveground dry weight, and dry root weight, respectively. The NGA, BG, LAP, and ALP represent N-acety-β-D-glucosidase, β-1, 4-glucosidase, leucine aminopeptidase, and alkaline phosphatase, respectively. The ANRP, CA, Pm, Lb, Pb, and Ob represent Allorhizobium-Neorhizobium-Pararhizobium-Rhizobium, CENA518, Pseudomonas, Ligilactobacillu, Paenibacillus, and Ochrobactrum, respectively. The Pp, Sc, Gt, Cb, Md, Ky, Sm, Tt, Mt, Cc, Cn, Ct, Ay, Fs, and As represent Pseudopithomyces, Solicoccozyma, Geastrum, Ceratobasidium, Myrothecium, Kohlmeyeriopsis, Siepmannia, Tulostoma, Myrothecium, Cylindrocarpon, Capronia, Cephalotrichum, Acrocalymma, Filobasidium, and Amesia, respectively.

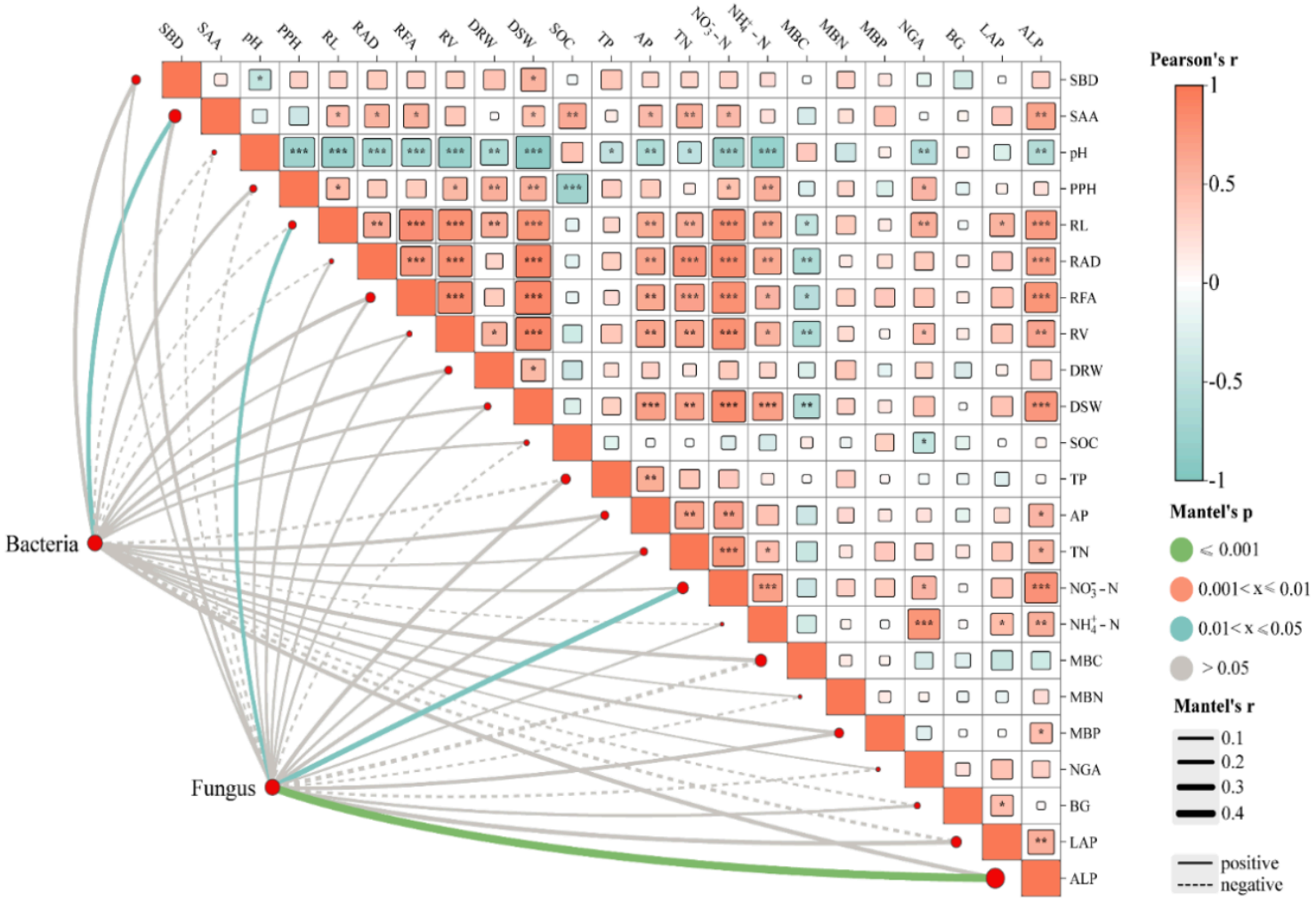


Figure 8

Pairwise comparisons of soil physicochemical properties, microbial biomass, enzyme activity, and *Pisum sativum L.* growth indicators were shown in the lower left corner, with a color gradient denoting Pearson's correlation coefficient. Bacterial and fungal biomarkers were related to soil physicochemical properties, microbial biomass, enzyme activity, and *Pisum sativum L.* growth indexes by Mantel test. Edge color denotes the statistical significance and edge width corresponds to the Mantel's r statistic for the corresponding distance correlations. (*: $p < 0.05$, **: $p < 0.01$, ***: $p < 0.001$). The SBD, SAA, and pH represent soil bulk density, water-stable aggregate content and pH value, respectively. The SOC, TP, TN, NO_3^-, and NH_4^+ represent soil organic matter content, total phosphorus, available phosphorus, total nitrogen, nitrate nitrogen, and ammonium nitrogen, respectively. The MBC, MBN, and MBP represent microbial biomass carbon, nitrogen, and phosphorus, respectively. The PPH, RL, RAD, RFA, RV, DRW, and DSW represent lant height, root length, root average diameter, root surface area, root volume, aboveground dry weight, and dry root weight, respectively. The NGA, BG, LAP, and ALP represent N-acety-β-D-glucosidase, β-1, 4-glucosidase, leucine aminopeptidase, and alkaline

phosphatase, respectively. The ANRP, CA, Pm, Lb, Pb, and Ob represent Allorhizobium-Neorhizobium-Pararhizobium-Rhizobium, CENA518, Pseudomonas, Ligilactobacillu, Paenibacillus, and Ochrobactrum, respectively. The Pp, Sc, Gt, Cb, Md, Ky, Sm, Tt, Mt, Cc, Cn, Ct, Ay, Fs, and As represent Pseudopithomyces, Solicoccozyma, Geastrum, Ceratobasidium, Myrothecium, Kohlmeyeriopsis, Siepmannia, Tulostoma, Myrothecium, Cylindrocarpon, Capronia, Cephalotrichum, Acrocalymma, Filobasidium, and Amesia, respectively.

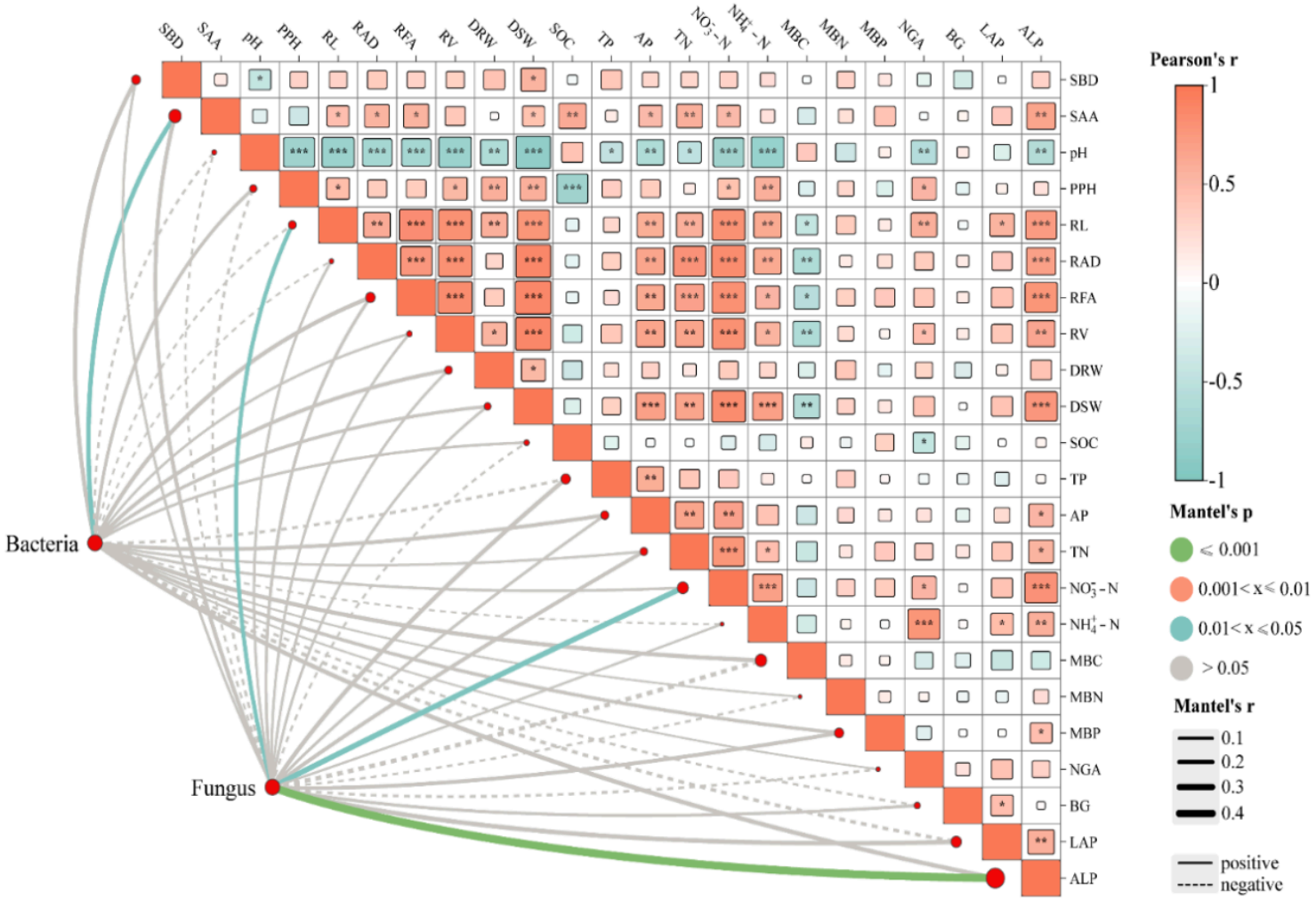


Figure 8

Pairwise comparisons of soil physicochemical properties, microbial biomass, enzyme activity, and *Pisum sativum L.* growth indicators were shown in the lower left corner, with a color gradient denoting Pearson's correlation coefficient. Bacterial and fungal biomarkers were related to soil physicochemical properties, microbial biomass, enzyme activity, and *Pisum sativum L.* growth indexes by Mantel test. Edge color denotes the statistical significance and edge width corresponds to the Mantel's r statistic for the corresponding distance correlations. (*: $p < 0.05$, **: $p < 0.01$, ***: $p < 0.001$). The SBD, SAA, and pH represent soil bulk density, water-stable aggregate content and pH value, respectively. The SOC, TP, TN, NO_3^-, and NH_4^+ represent soil organic matter content, total phosphorus, available phosphorus, total nitrogen, nitrate nitrogen, and ammonium nitrogen, respectively. The MBC, MBN, and MBP represent microbial biomass carbon, nitrogen, and phosphorus, respectively. The PPH, RL, RAD, RFA, RV, DRW, and DSW represent lant height, root length, root average diameter, root surface area, root volume, aboveground dry weight, and dry root weight, respectively. The NGA, BG, LAP, and ALP represent N-acety-β-D-glucosidase, β-1, 4-glucosidase, leucine aminopeptidase, and alkaline phosphatase, respectively. The ANRP, CA, Pm, Lb, Pb, and Ob represent Allorhizobium-Neorhizobium-Pararhizobium-Rhizobium, CENA518, Pseudomonas, Ligilactobacillu, Paenibacillus, and Ochrobactrum, respectively. The Pp, Sc, Gt, Cb,

Md, Ky, Sm, Tt, Mt, Cc, Cn, Ct, Ay, Fs, and As represent Pseudopithomyces, Solicoccozyma, Geastrum, Ceratobasidium, Myrothecium, Kohlmeyeriopsis, Siepmannia, Tulostoma, Myrothecium, Cylindrocarpon, Capronia, Cephalotrichum, Acrocalymma, Filobasidium, and Amesia, respectively.

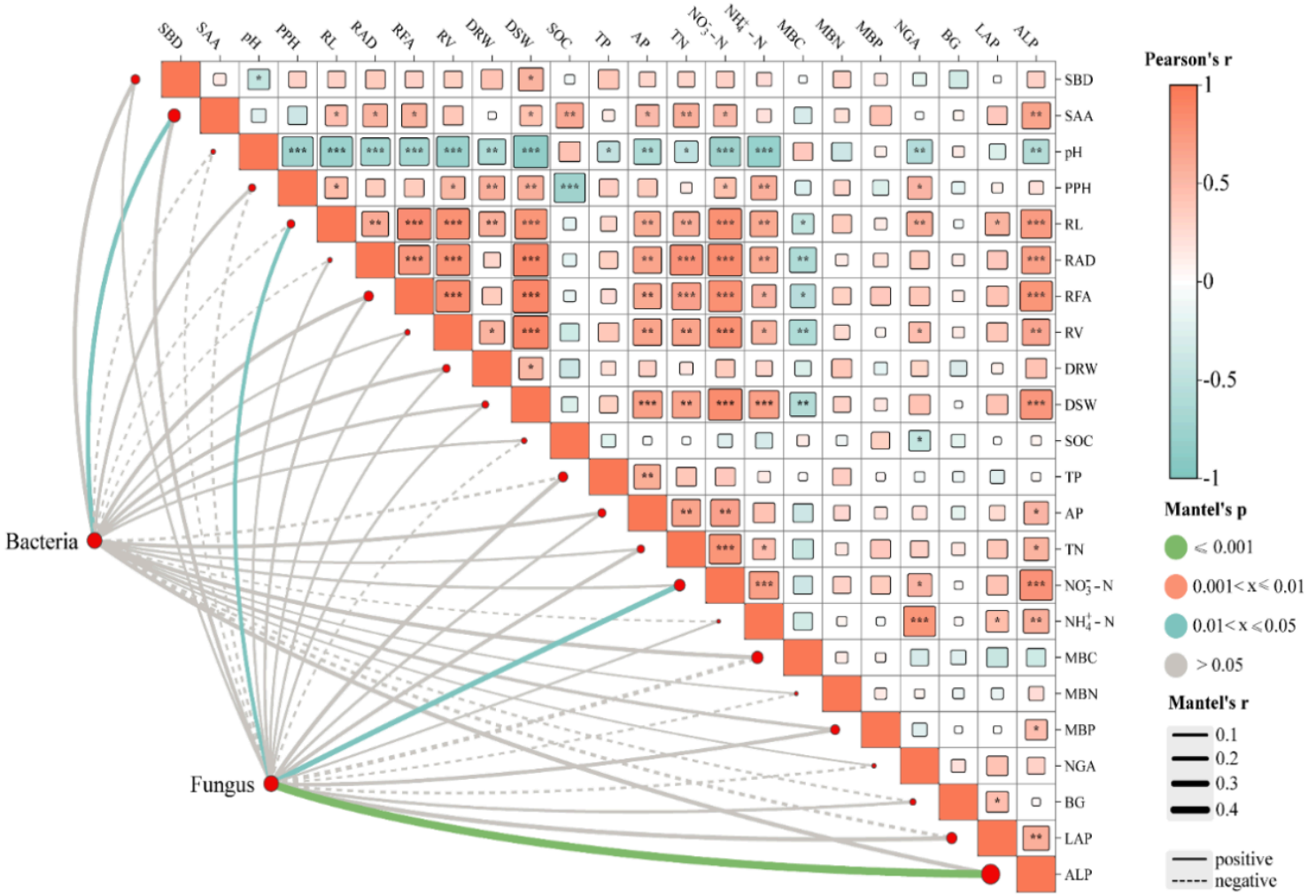


Figure 8

Pairwise comparisons of soil physicochemical properties, microbial biomass, enzyme activity, and *Pisum sativum L.* growth indicators were shown in the lower left corner, with a color gradient denoting Pearson's correlation coefficient. Bacterial and fungal biomarkers were related to soil physicochemical properties, microbial biomass, enzyme activity, and *Pisum sativum L.* growth indexes by Mantel test. Edge color denotes the statistical significance and edge width corresponds to the Mantel's r statistic for the corresponding distance correlations. (*: $p < 0.05$, **: $p < 0.01$, ***: $p < 0.001$). The SBD, SAA, and pH represent soil bulk density, water-stable aggregate content and pH value, respectively. The SOC, TP, TN, NO_3^-, and NH_4^+ represent soil organic matter content, total phosphorus, available phosphorus, total nitrogen, nitrate nitrogen, and ammonium nitrogen, respectively. The MBC, MBN, and MBP represent microbial biomass carbon, nitrogen, and phosphorus, respectively. The PPH, RL, RAD, RFA, RV, DRW, and DSW represent lant height, root length, root average diameter, root surface area, root volume, aboveground dry weight, and dry root weight, respectively. The NGA, BG, LAP, and ALP represent N-acety-β-D-glucosidase, β-1, 4-glucosidase, leucine aminopeptidase, and alkaline phosphatase, respectively. The ANRP, CA, Pm, Lb, Pb, and Ob represent Allorhizobium-Neorhizobium-Pararhizobium-Rhizobium, CENA518, Pseudomonas, Ligilactobacillu, Paenibacillus, and Ochrobactrum, respectively. The Pp, Sc, Gt, Cb, Md, Ky, Sm, Tt, Mt, Cc, Cn, Ct, Ay, Fs, and As represent Pseudopithomyces, Solicoccozyma, Geastrum, Ceratobasidium,

Myrothecium, Kohlmeyeriopsis, Siepmannia, Tulostoma, Myrothecium, Cylindrocarpon, Capronia, Cephalotrichum, Acrocalymma, Filobasidium, and Amesia, respectively.

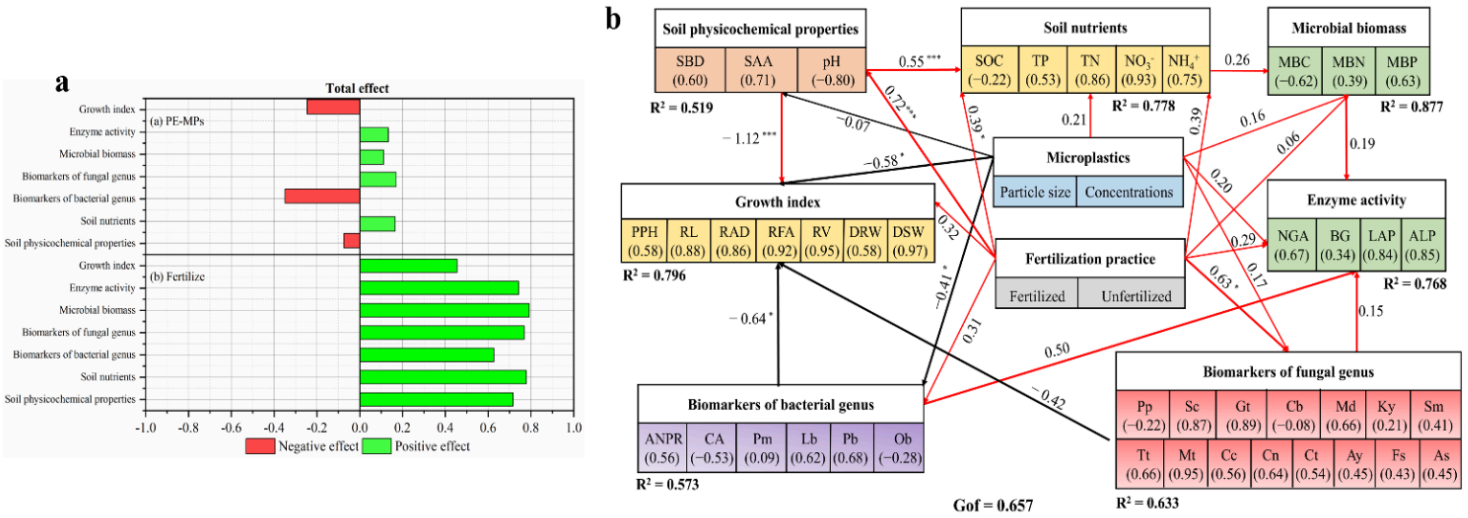


Figure 9

The effects of the bacterial and fungal biomarkers, soil physicochemical properties, soil nutrients, microbial biomass, and enzyme activity in *Pisum sativum L.* growth indicators. **a** Standardized total effect of the bacterial and fungal biomarkers, soil physicochemical properties, soil nutrients, microbial biomass, and enzyme activity, and *Pisum sativum L.* growth indicators. **b** The structural equation model showing the relationship between the bacterial and fungal biomarkers, soil physicochemical properties, soil nutrients, microbial biomass, and enzyme activity in *Pisum sativum L.* growth indicators. Red solid arrows suggest significant positive causality, whereas black solid arrows indicate significant negative causality. The number adjacent to each arrow represents the standardized path coefficient, and the width of the arrow reflects the magnitude of this coefficient. Asterisks indicate statistical significance (* $P < 0.05$, ** $P < 0.01$, *** $P < 0.001$). The R^2 value represents the coefficient of determination, indicating the proportion of variance explained by the model. The SBD, SAA, and pH represent soil bulk density, water-stable aggregate content and pH value, respectively. The SOC, TP, TN, NO_3^-, and NH_4^+ represent soil organic matter content, total phosphorus, available phosphorus, total nitrogen, nitrate nitrogen, and ammonium nitrogen, respectively. The MBC, MBN, and MBP represent microbial biomass carbon, nitrogen, and phosphorus, respectively. The PPH, RL, RAD, RFA, RV, DRW, and DSW represent lant height, root length, root average diameter, root surface area, root volume, aboveground dry weight, and dry root weight, respectively. The NGA, BG, LAP, and ALP represent N-acety-β-D-glucosidase, β-1, 4-glucosidase, leucine aminopeptidase, and alkaline phosphatase, respectively. The ANRP, CA, Pm, Lb, Pb, and Ob represent Allorhizobium-Neorhizobium-Pararhizobium-Rhizobium, CENA518, Pseudomonas, Ligilactobacillu, Paenibacillus, and Ochrobactrum, respectively. The Pp, Sc, Gt, Cb, Md, Ky, Sm, Tt, Mt, Cc, Cn, Ct, Ay, Fs, and As represent Pseudopithomyces, Solicoccozyma, Geastrum, Ceratobasidium, Myrothecium, Kohlmeyeriopsis, Siepmannia, Tulostoma, Myrothecium, Cylindrocarpon, Capronia, Cephalotrichum, Acrocalymma, Filobasidium, and Amesia, respectively.

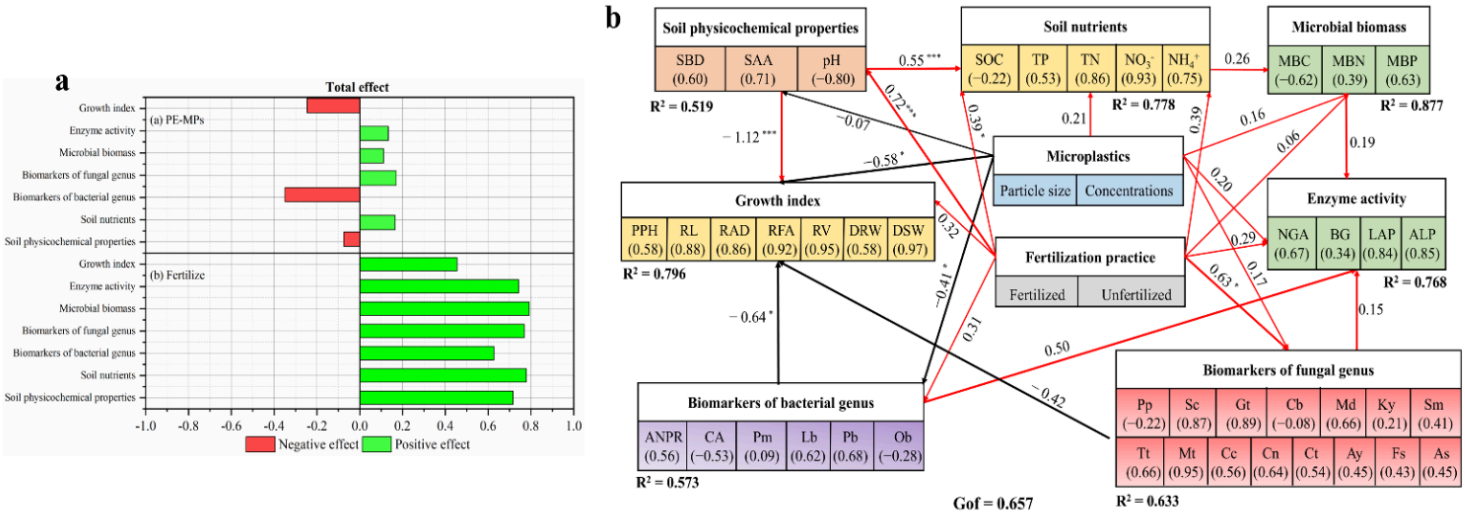


Figure 9

The effects of the bacterial and fungal biomarkers, soil physicochemical properties, soil nutrients, microbial biomass, and enzyme activity in *Pisum sativum L.* growth indicators. **a** Standardized total effect of the bacterial and fungal biomarkers, soil physicochemical properties, soil nutrients, microbial biomass, and enzyme activity, and *Pisum sativum L.* growth indicators. **b** The structural equation model showing the relationship between the bacterial and fungal biomarkers, soil physicochemical properties, soil nutrients, microbial biomass, and enzyme activity in *Pisum sativum L.* growth indicators. Red solid arrows suggest significant positive causality, whereas black solid arrows indicate significant negative causality. The number adjacent to each arrow represents the standardized path coefficient, and the width of the arrow reflects the magnitude of this coefficient. Asterisks indicate statistical significance (* $P < 0.05$, ** $P < 0.01$, *** $P < 0.001$). The R^2 value represents the coefficient of determination, indicating the proportion of variance explained by the model. The SBD, SAA, and pH represent soil bulk density, water-stable aggregate content and pH value, respectively. The SOC, TP, TN, NO_3^-, and NH_4^+ represent soil organic matter content, total phosphorus, available phosphorus, total nitrogen, nitrate nitrogen, and ammonium nitrogen, respectively. The MBC, MBN, and MBP represent microbial biomass carbon, nitrogen, and phosphorus, respectively. The PPH, RL, RAD, RFA, RV, DRW, and DSW represent lant height, root length, root average diameter, root surface area, root volume, aboveground dry weight, and dry root weight, respectively. The NGA, BG, LAP, and ALP represent N-acety-β-D-glucosidase, β-1, 4-glucosidase, leucine aminopeptidase, and alkaline phosphatase, respectively. The ANRP, CA, Pm, Lb, Pb, and Ob represent Allorhizobium-Neorhizobium-Pararhizobium-Rhizobium, CENA518, Pseudomonas, Ligilactobacillu, Paenibacillus, and Ochrobactrum, respectively. The Pp, Sc, Gt, Cb, Md, Ky, Sm, Tt, Mt, Cc, Cn, Ct, Ay, Fs, and As represent Pseudopithomyces, Solicoccozyma, Geastrum, Ceratobasidium, Myrothecium, Kohlmeyeriopsis, Siepmannia, Tulostoma, Myrothecium, Cylindrocarpon, Capronia, Cephalotrichum, Acrocalymma, Filobasidium, and Amesia, respectively.

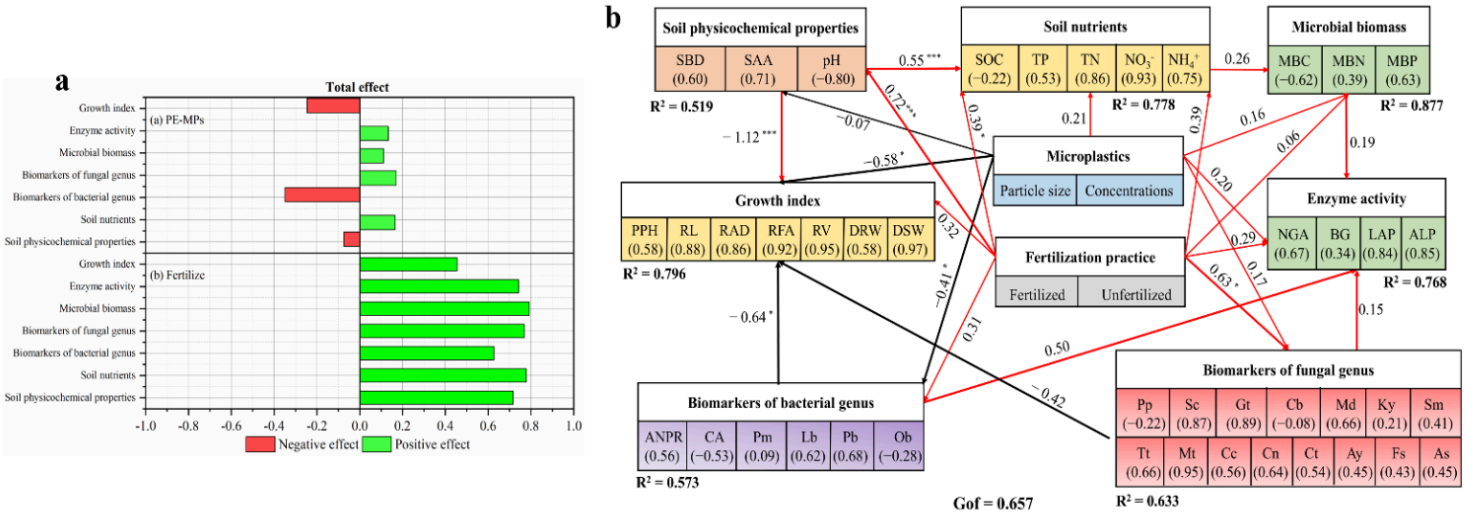


Figure 9

The effects of the bacterial and fungal biomarkers, soil physicochemical properties, soil nutrients, microbial biomass, and enzyme activity in *Pisum sativum L.* growth indicators. **a** Standardized total effect of the bacterial and fungal biomarkers, soil physicochemical properties, soil nutrients, microbial biomass, and enzyme activity, and *Pisum sativum L.* growth indicators. **b** The structural equation model showing the relationship between the bacterial and fungal biomarkers, soil physicochemical properties, soil nutrients, microbial biomass, and enzyme activity in *Pisum sativum L.* growth indicators. Red solid arrows suggest significant positive causality, whereas black solid arrows indicate significant negative causality. The number adjacent to each arrow represents the standardized path coefficient, and the width of the arrow reflects the magnitude of this coefficient. Asterisks indicate statistical significance (* $P < 0.05$, ** $P < 0.01$, *** $P < 0.001$). The R^2 value represents the coefficient of determination, indicating the proportion of variance explained by the model. The SBD, SAA, and pH represent soil bulk density, water-stable aggregate content and pH value, respectively. The SOC, TP, TN, NO_3^-, and NH_4^+ represent soil organic matter content, total phosphorus, available phosphorus, total nitrogen, nitrate nitrogen, and ammonium nitrogen, respectively. The MBC, MBN, and MBP represent microbial biomass carbon, nitrogen, and phosphorus, respectively. The PPH, RL, RAD, RFA, RV, DRW, and DSW represent lant height, root length, root average diameter, root surface area, root volume, aboveground dry weight, and dry root weight, respectively. The NGA, BG, LAP, and ALP represent N-acety-β-D-glucosidase, β-1, 4-glucosidase, leucine aminopeptidase, and alkaline phosphatase, respectively. The ANRP, CA, Pm, Lb, Pb, and Ob represent Allorhizobium-Neorhizobium-Pararhizobium-Rhizobium, CENA518, Pseudomonas, Ligilactobacillu, Paenibacillus, and Ochrobactrum, respectively. The Pp, Sc, Gt, Cb, Md, Ky, Sm, Tt, Mt, Cc, Cn, Ct, Ay, Fs, and As represent Pseudopithomyces, Solicoccozyma, Geastrum, Ceratobasidium, Myrothecium, Kohlmeyeriopsis, Siepmannia, Tulostoma, Myrothecium, Cylindrocarpon, Capronia, Cephalotrichum, Acrocalymma, Filobasidium, and Amesia, respectively.

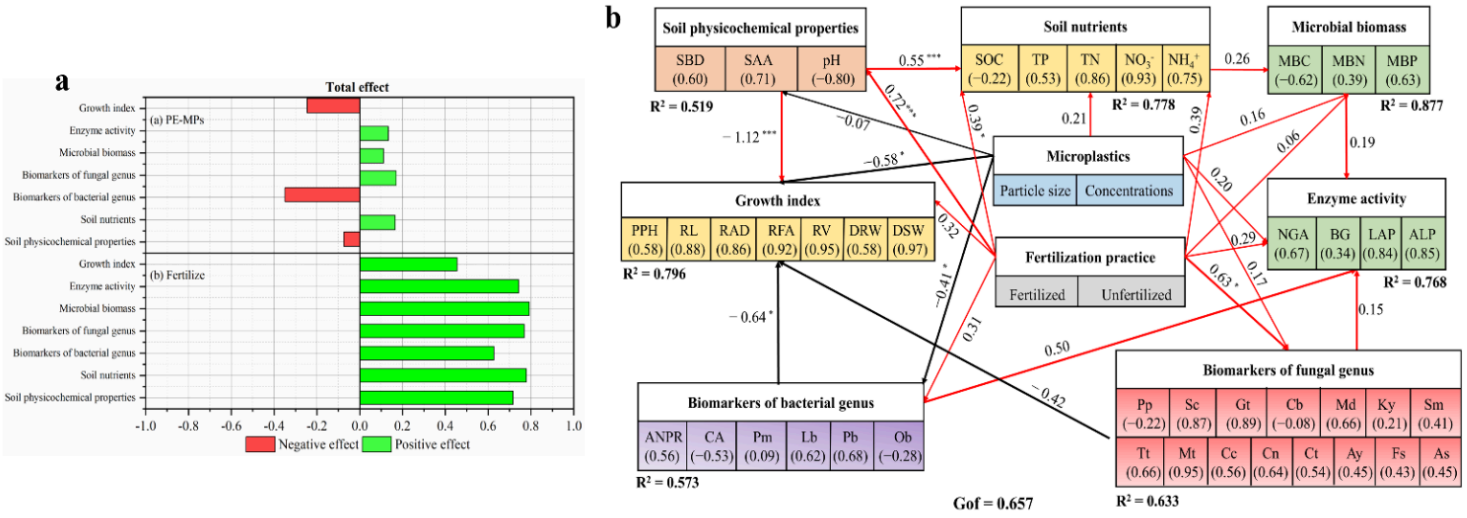


Figure 9

The effects of the bacterial and fungal biomarkers, soil physicochemical properties, soil nutrients, microbial biomass, and enzyme activity in *Pisum sativum L.* growth indicators. **a** Standardized total effect of the bacterial and fungal biomarkers, soil physicochemical properties, soil nutrients, microbial biomass, and enzyme activity, and *Pisum sativum L.* growth indicators. **b** The structural equation model showing the relationship between the bacterial and fungal biomarkers, soil physicochemical properties, soil nutrients, microbial biomass, and enzyme activity in *Pisum sativum L.* growth indicators. Red solid arrows suggest significant positive causality, whereas black solid arrows indicate significant negative causality. The number adjacent to each arrow represents the standardized path coefficient, and the width of the arrow reflects the magnitude of this coefficient. Asterisks indicate statistical significance (* $P < 0.05$, ** $P < 0.01$, *** $P < 0.001$). The R^2 value represents the coefficient of determination, indicating the proportion of variance explained by the model. The SBD, SAA, and pH represent soil bulk density, water-stable aggregate content and pH value, respectively. The SOC, TP, TN, NO_3^-, and NH_4^+ represent soil organic matter content, total phosphorus, available phosphorus, total nitrogen, nitrate nitrogen, and ammonium nitrogen, respectively. The MBC, MBN, and MBP represent microbial biomass carbon, nitrogen, and phosphorus, respectively. The PPH, RL, RAD, RFA, RV, DRW, and DSW represent lant height, root length, root average diameter, root surface area, root volume, aboveground dry weight, and dry root weight, respectively. The NGA, BG, LAP, and ALP represent N-acety-β-D-glucosidase, β-1, 4-glucosidase, leucine aminopeptidase, and alkaline phosphatase, respectively. The ANRP, CA, Pm, Lb, Pb, and Ob represent Allorhizobium-Neorhizobium-Pararhizobium-Rhizobium, CENA518, Pseudomonas, Ligilactobacillu, Paenibacillus, and Ochrobactrum, respectively. The Pp, Sc, Gt, Cb, Md, Ky, Sm, Tt, Mt, Cc, Cn, Ct, Ay, Fs, and As represent Pseudopithomyces, Solicoccozyma, Geastrum, Ceratobasidium, Myrothecium, Kohlmeyeriopsis, Siepmannia, Tulostoma, Myrothecium, Cylindrocarpon, Capronia, Cephalotrichum, Acrocalymma, Filobasidium, and Amesia, respectively.